**Technical Report Documentation Page**

| 1. Report No. | 2. Government Accession No. | 3. Recipient's Catalog No. |
|---|---|---|
| SWUTC/14/600451-00025-1 | | |

| 4. Title and Subtitle | 5. Report Date |
|---|---|
| CONTROLLING CONDUCTIVITY OF ASPHALT CONCRETE WITH GRAPHITE | August 2014 |
| | 6. Performing Organization Code |

| 7. Author(s) | 8. Performing Organization Report No. |
|---|---|
| Philip Park, Younho Rew, and Aishwarya Baranikumar | Report 600451-00025-1 |

| 9. Performing Organization Name and Address | 10. Work Unit No. (TRAIS) |
|---|---|
| Texas A&M Transportation Institute<br>College Station, Texas 77843-3135 | 11. Contract or Grant No.<br>DTRT12-G-UTC06 |

| 12. Sponsoring Agency Name and Address | 13. Type of Report and Period Covered |
|---|---|
| Southwest Region University Transportation Center<br>Texas A&M Transportation Institute<br>College Station, Texas 77843-3135 | 14. Sponsoring Agency Code |

15. Supplementary Notes

Supported by a grant from the U.S. Department of Transportation, University Transportation Centers Program.

16. Abstract

Electrically conductive asphalt concrete has a huge potential for various multifunctional applications such as self-healing, self-sensing, and deicing. In order to utilize the full spectrum of applications of electrically conductive asphalt composites, precise control of the asphalt mixture resistivity is needed. Most of the previous research using conductive fibers as the primary conductive additives observed a sudden transition from the insulated to conductive phase, commonly known as the percolation threshold, which obstructs more precise conductivity control. Aiming to control the electrical conductivity of asphalt concrete with a smooth transition from the insulated to conductive phase, the researchers have selected graphite powders as an alternative conductive additive in this study. Nine types of graphite having different particle shape, size, and origin were mixed with asphalt binders, and their effects on imparting conductivity were investigated. Based on the results, the research team selected two types of graphite and evaluated the effects on the electrical conductivity of asphalt concrete. The team also examined the effects of aggregate gradation, binder content, and binder type.

The results showed that the electrical conductivity of asphalt mastic is sensitive to the graphite type. The natural flake graphite is effective to mitigate the percolation threshold, and a sufficiently high conductivity can be achieved by replacing a part of the fillers with graphite (the conductivity ranged from $10^{-6}$ to $10^{-2}$/Ω•cm). The results also showed that the binder type does not make a significant change in the mixture conductivity, but the aggregate gradation brings approximately two order differences in the volume resistivity. Mechanical performance of the conductive asphalt is also an important factor for practical field applications. The indirect tension test results showed that the addition of graphite improves the indirect tensile strength up to 41 percent. The electrical and mechanical data obtained from this study provide essential information on the selection of graphite type and asphalt mixture design to achieve the proper electrical conductivity required for the probable multifunctional applications of asphalt concrete, which will lead to technical innovations for sustainable pavements.

| 17. Key Words | 18. Distribution Statement |
|---|---|
| Electrical Conductivity Control, Graphite, Asphalt Concrete, Percolation Threshold | No restrictions. This document is available to the public through NTIS:<br>National Technical Information Service<br>Alexandria, Virginia 22312<br>http://www.ntis.gov |

| 19. Security Classif. (of this report) | 20. Security Classif. (of this page) | 21. No. of Pages | 22. Price |
|---|---|---|---|
| Unclassified | Unclassified | 106 | |

**Form DOT F 1700.7 (8-72)** **Reproduction of completed page authorized**

# CONTROLLING CONDUCTIVITY OF ASPHALT CONCRETE WITH GRAPHITE

By

Philip Park
Younho Rew
And
Aishwarya Baranikumar

Report 600451-00025-1
Project Title: Controlling Electrical Conductivity of Asphalt Concrete for Multifunctional Applications

Sponsored by the

Southwest Region University Transportation Center
Texas A&M Transportation Institute
College Station, Texas 77843-3135

August 2014

## DISCLAIMER

The contents of this report reflect the views of the authors, who are responsible for the facts and the accuracy of the information presented herein. This document is disseminated under the sponsorship of the Department of Transportation University Transportation Centers Program in the interest of information exchange. The U.S. Government assumes no liability for the contents or use thereof.

## ACKNOWLEDGMENTS

The authors recognize that support for this research was provided by a grant from the U.S. Department of Transportation University Transportation Centers Program to the Southwest Region University Transportation Center.

The authors extend their gratitude to Asbury Carbons and Knife River Corporation for providing the raw materials used for the research at no cost. In addition, the authors acknowledge Dr. Amit Bhasin from the University of Texas at Austin for serving as a project monitor for this study.

# TABLE OF CONTENTS

# LIST OF FIGURES

**Page**

# LIST OF TABLES

# EXECUTIVE SUMMARY

Conductive asphalt concrete has a huge potential for various nonstructural applications such as self-healing, self-sensing, energy harvesting, and many others. Precise control of the electrical conductivity is an essential element to enable such applications of conductive asphalt concrete.

In this study, graphite powder is proposed as a conductive additive that allows conductivity control in wide range by mitigating the percolation threshold. The electrical volume resistivity of the mastic specimens containing various types and contents of graphite is examined, and the physical properties of the raw materials including scanning electron microscope analysis are obtained. Using two graphite types showed the best performance in the mastic tests. The conductive asphalt concrete specimens were fabricated, and their electrical and mechanical performances were evaluated for the various mixtures including different graphite contents and aggregate gradations.

Major findings from the study are as follows:

- A sudden change in electrical resistivity from no conduction to conduction, i.e., the so-called percolation threshold, is observed in specimens containing steel fibers. Achieving this threshold implies that the steel fibers form conductive paths by contacting to each other. The conductive paths is similar to a set of switches, and hence precise conductivity control with fibers is difficult.
- The electrical conductivity of asphalt mastics varies significantly with the type of conductive fillers. Natural flake graphite powder is the most efficient in imparting conductivity to asphalt. Sufficiently low electrical resistivity can be obtained by replacing a part of the fillers with the flake-type graphite powder in asphalt mastics (up to $10^{-2}/\Omega\bullet$cm).
- The volume resistivity of asphalt mastic and asphalt concrete containing natural flake graphite powder varies widely with the amount of graphite powder mixed into the mastic. The graphite does not completely eliminate the percolation threshold but substantially mitigates it. This implies that the electrical resistivity of asphaltic composite can be manipulated over a wide range.

- The different binder types do not have significant influence on the electrical conductivity of asphalt mastics, but some binder modifiers may reduce electrical conductivity.
- When a fixed amount of graphite is added to the mixture, a smaller amount of fine aggregate and binder results in higher electrical conductivity.
- The conductive asphalt concrete containing the flake-type graphite has improved indirect tensile strength when compared to control asphalt concrete. Dynamic shear rheometer tests for asphalt mastic show that the flake-type graphite additives increase complex modulus. This implies that adding graphite is beneficial for improving rutting resistance.

This study shows that the flake-type graphite is efficient to control the electrical conductivity of asphalt concrete up to a very low resistivity range. Moreover, the flake graphite improves the indirect tensile strength and viscosity. The mechanical and electrical benefits of the graphite filler will enable various multifunctional applications and improved durability of asphalt concrete for longer-lasting asphalt pavements.

# 1. INTRODUCTION

## 1.1 BACKGROUND

Asphalt concrete is a composite material that is heavily used in the construction of highways, runways, and parking lots. Riding comfort, durability, reliability, and water resistance are some of the driving mechanical characteristics that make asphalt concrete the most preferred choice in the pavement industry. With the increasing emphasis on the long-term well-being of individuals and environmental conservation, sustainability is becoming a key goal in planning and constructing civil infrastructures. Multifunctional materials have the simultaneous ability to exhibit nonstructural functions apart from their regular structural functions (Gibson 2010). Mechanical properties such as strength and stiffness are the primary functions of structural materials. However, by manipulating electrical, magnetic, optical, and other nonstructural properties, the material can exhibit advantages beyond the sum of the individual capabilities. Materials of this kind have tremendous potential for a wide range of real-life applications that can improve the efficiency and safety of daily lives. Asphalt concrete, by nature, is a nonconductive composite material, but its electrical conductivity can be improved by using conductive additives. Various nonstructural applications can be developed by controlling the conductivity, and the multifunctional asphalt concrete has strong potential that can lead to a breakthrough in sustainable pavement systems.

In 1968, Minsk (1968) initiated the concept of electrically conductive asphalt concrete, and this topic has gained immense interest in the last decade, resulting in an increased number of publications. The potential benefits of utilizing the electrical properties of asphalt composites have largely motivated these efforts. For instance, the electrical heating applications of conductive pavements have been studied to remove snow and ice (Xiangyang and Yuxing 2010). Electric heating is also expected to promote self-healing by reducing the rest period. In addition, the piezoresistivity of conductive asphalt, which refers to the change in electrical resistivity with applied mechanical pressure, can be used for self-sensing of strain (Liu and Wu 2009). Self-sensing of damage for evaluating pavement distress is possible if the relationship between the electrical property and internal damage is provided. Moreover, some conductive additives may improve the durability of asphalt concrete, thereby increasing the service life of the pavement systems (Park 2012).

Figure 1 shows the possible nonstructural functions and the benefits of conductive asphalt concrete, and Figure 2 summarizes the components of high-performance conductive asphalt concrete.

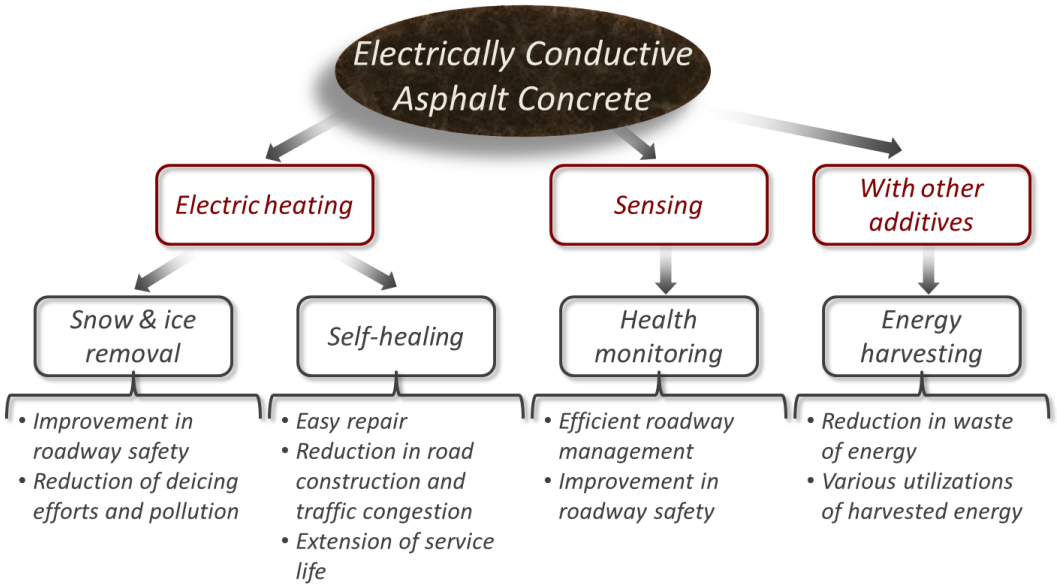


**Figure 1. Possible Applications and Benefits of Electrically Conductive Asphalt Concrete.**

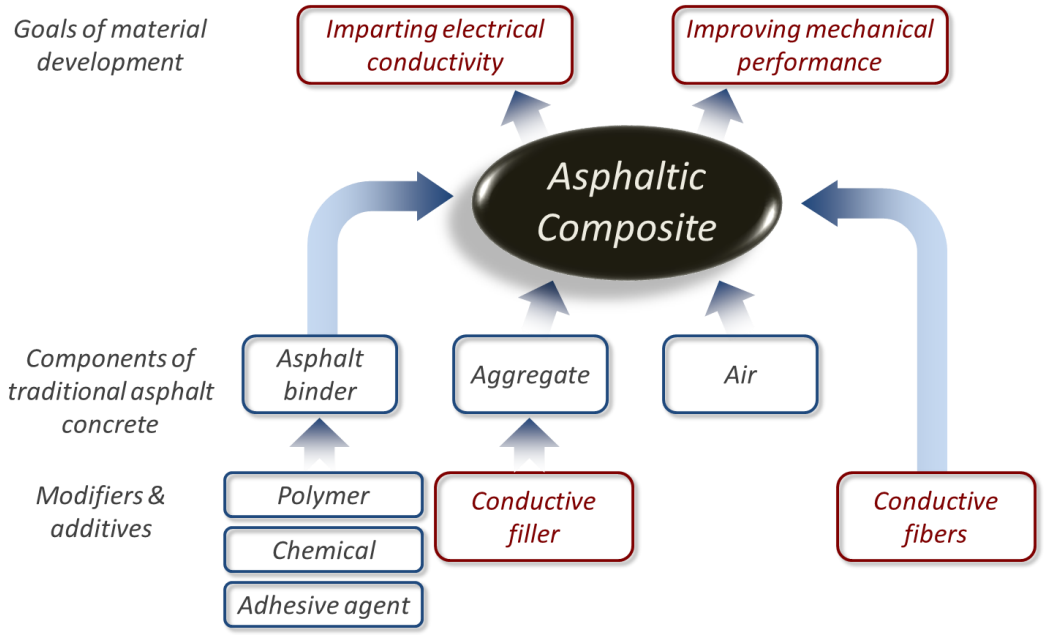


**Figure 2. Components of High-Performance Conductive Asphalt Concrete.**

## 1.2 PROBLEM STATEMENT

To use the full spectrum of applications of electrically conductive asphalt composites, precise control of the volume resistivity is needed. Previous investigators have tested various conductive fillers and fibers including micron-scale steel fibers (Huang et al. 2006, Serin et al. 2012), carbon fibers (Wu et al. 2005), steel wool (Garcia et al. 2009), carbon black (Wu et al. 2005), and graphite powder (Wu et al. 2005, Garcia et al. 2009) to impart electrical conductivity into asphalt concrete. Most of the previous investigators selected fiber-type additives as their primary conductive additives rather than powder-type additives because a relatively smaller number of fibers is needed to improve conductivity than graphite or carbon black (Huang et al. 2006). Fibers have longer lengths, which can facilitate the flow of electrons more easily than powder-type additives. On the other hand, asphalt concrete containing conductive fibers has a phenomenon called percolation threshold, which hinders the precise control of the electrical conductivity.

The percolation threshold is a sudden transition from the insulated to the conductive phase (Wu et al. 2005, Garcia et. al 2009). The dotted line in Figure 3 shows a typical relationship between the electrical resistivity and the content of the conductive additive reported from the previous investigators. The transition between the insulated phase and conductive phase can be characterized by a sudden drop in electrical resistivity at a specific content of conductive additive, the percolation threshold. According to Huang et al. (2006), the electrical conductivity of the asphalt composite comes from the formation of a continuous conductive path through the contacts between the conductive additives. By narrowing the adjustable volume resistivity range of conductive asphalt, the percolation threshold introduces limitations for developing various multifunctional applications. To enable precise manipulation of electrical resistivity over a wide range, a gradual resistance change with the increase of conductive additive is favorable; this is illustrated as a solid line in Figure 3. Another limitation in using discrete fiber-type additives is the dispersion and clumping of fibers during mixing (Abtahi et al. 2010). The clumping or balling of discrete fibers becomes severe as the fiber-length-to-thickness ratio (the aspect ratio) increases.

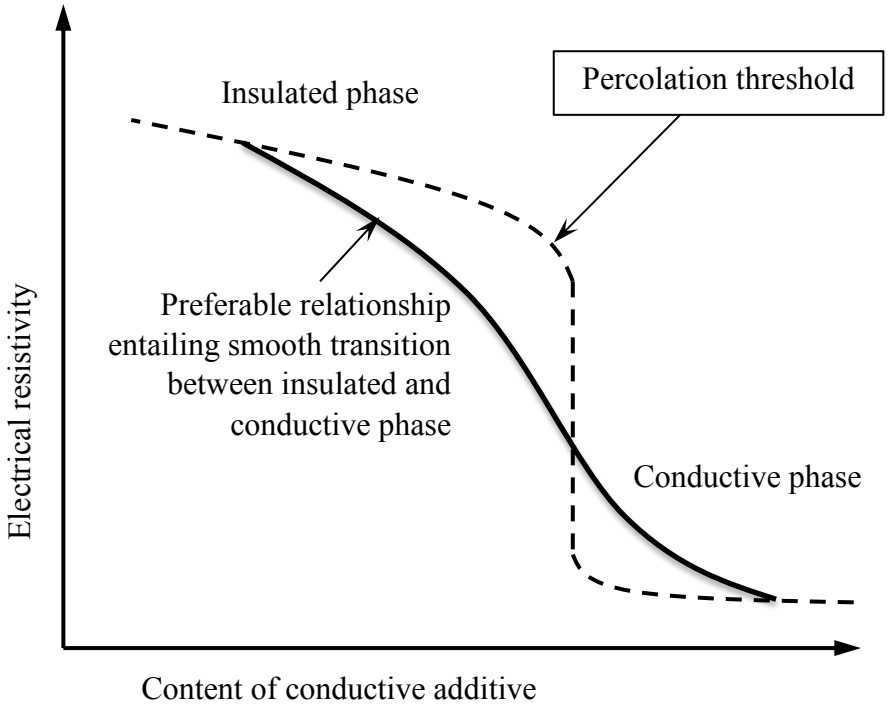


**Figure 3. Electrical Resistivity Transition Curve.**

Graphite is one of the powder-type conductive additives that some investigators used as a supplementary material (Huang et al. 2006, Garcia et al. 2009, Liu and Wu 2011b). While the percolation threshold is prevalent with fiber-type conductive additives, the use of graphite powder ensures relatively easy mixing and uniform dispersion. More importantly, the percolation threshold might be mitigated by using graphite powder even though larger quantities of graphite rather than conductive fibers are needed to reduce the electrical resistivity (Huang et al. 2009, Mo et al. 2005). On the other hand, the efficiency of graphite in imparting conductivity is not consistent in previous publications. According to Park (2012), this is due to the use of different types of graphite, but no other investigators have focused on the effect of graphite type, including the shape, size, and origin of the graphite powders. Motivated by this observation, this study investigated the effect of various graphite types on imparting conductivity, and identified the most efficient graphite type that ensures a smooth resistivity transition.

## 1.3 RESEARCH OBJECTIVES

The objective of this study was to find a proper conductive additive that enables a smooth transition from the insulated to the conductive phase. The following subjects were investigated through the study:

- A comprehensive literature review on conductive construction materials.
- Identification of the graphite types and their physical/geometrical characterizations.
- The effect of graphite types and amounts on the conductivity of asphalt mastic (asphalt binder and fillers).
- The effect of binder types on the conductivity of asphalt mastic.
- The effect of graphite on the viscoelastic properties of asphalt mastic.
- Verification of imparting conductivity into asphalt concrete.
- The effect of the aggregate gradation on electrical conductivity and adjustment of the optimum binder content.
- The strength of the conductive asphalt concrete.

Figure 4 shows the tasks of the research, and Figure 5 shows the schedule of the activities.

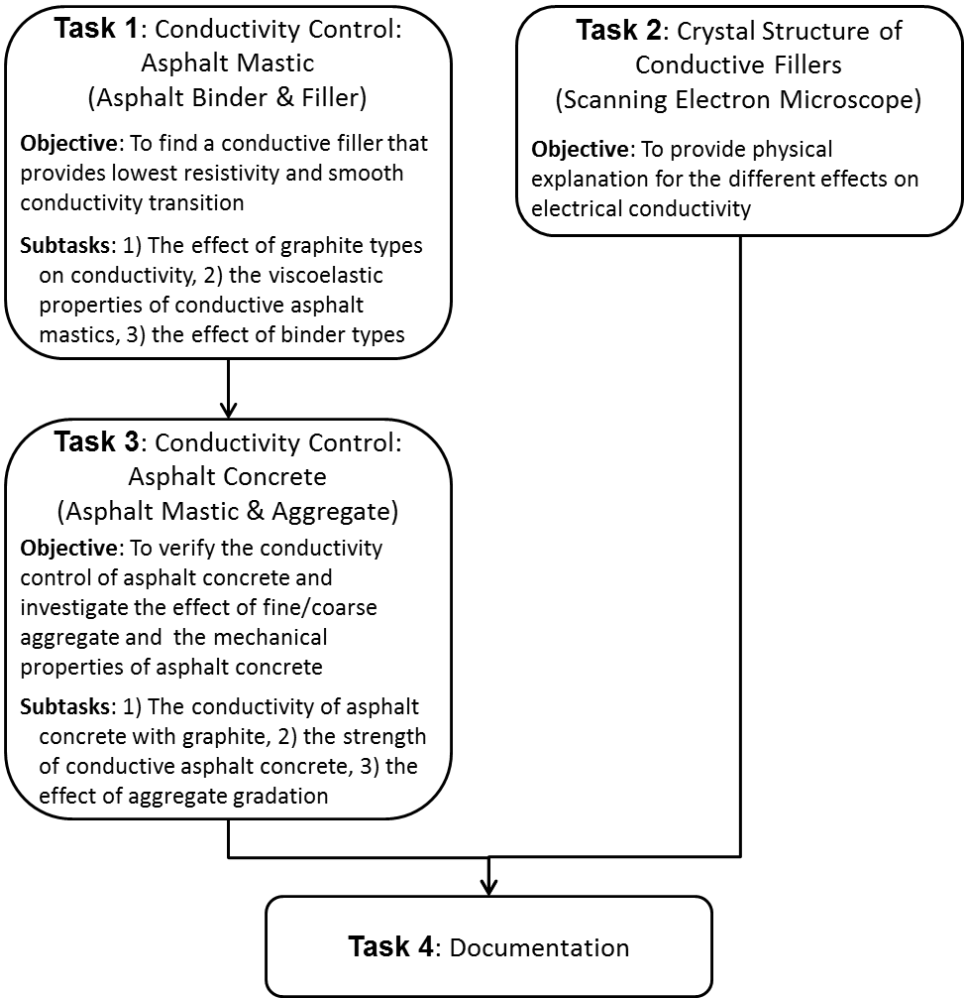


**Figure 4. Work Tasks.**

| | 13 | | | | | | | | | | | | 14 |
|---|---|---|---|---|---|---|---|---|---|---|---|---|---|
| | 1 | 2 | 3 | 4 | 5 | 6 | 7 | 8 | 9 | 10 | 11 | 12 | 1 |
| Task 1. Conductivity control of asphalt mastic | | | | | | | | | | | | | |
| Task 2. Crystal structure of conductive fillers | | | | | | | | | | | | | |
| Task 3. Conductivity control of asphalt concrete | | | | | | | | | | | | | |
| Task 4. Documentation | | | | | | | | | | | | | |

**Figure 5. Schedule of Activities.**

# 2. LITERATURE REVIEW

A review of the literature on imparting and controlling conductivity in asphalt concrete and the various possible multifunctional applications is summarized in this section.

## 2.1 APPROACHES TO IMPART CONDUCTIVITY INTO ASPHALT CONCRETE

The interest in imparting electrical properties into asphalt concrete dates back to the 1970s. Minsk (1971) patented electrically conductive asphaltic concrete using graphite as a conductive medium for the purpose of melting snow and ice on roadway surfaces by electrical heating. Stratfull (1974) and Fromm (1976) used coke breeze from the steel industry to produce conductive hot-mix asphalt (HMA) for cathodic protection of steel rebars in concrete bridges. Zaleski et al. (1998) patented a pavement system containing an electrically conductive layer for deicing purposes; the authors used graphite and coke as conductive additives. Parallel to asphalt concrete, extensive study on electrically conductive Portland cement concrete has been published. Barnard (1965) patented electrically conductive cementitious concrete. Since then, various efforts have been reported on the widened applications of conductive concrete (Chung 2003).

Findings from numerous research studies in the past have shown that the electrical conductivity of asphalt concrete can be improved with the addition of conductive fillers and/or fibers. Wu et al. (2003) showed that the inclusion of graphite beyond a critical content decreases the resistivity of asphalt-based composites. In this paper, the authors focused mainly on the self-sensing ability of conductive asphalt. In 2005, the electrical conductivity of asphalt concrete with other additives such as carbon black, graphite, and carbon fibers was investigated (Wu et al. 2005). It was found that pure carbon-fiber-modified asphalt concrete showed the best performance in conductivity, followed by graphite and carbon black, as illustrated in Figure 6. In the figure, the content of the conductive additive is presented as the volume percentage of the binder phase of the mixture. The electrical resistivity was found to decline rapidly when specific amounts of conductive additives were added, which is during the percolation threshold. Previous investigators (Wu et al. 2005, Huang et al. 2006) explained that a three-dimensional conductive network is established at the percolation threshold, and hence improvement in conductivity is not significant after this point. Wu et al. (2005) thus concluded that the desired electrical resistivity can be obtained by keeping the content of conductive additives slightly above the optimum

(percolation) level but making sure that the content does not go beyond to minimize the influence on the mechanical properties of asphalt concrete.

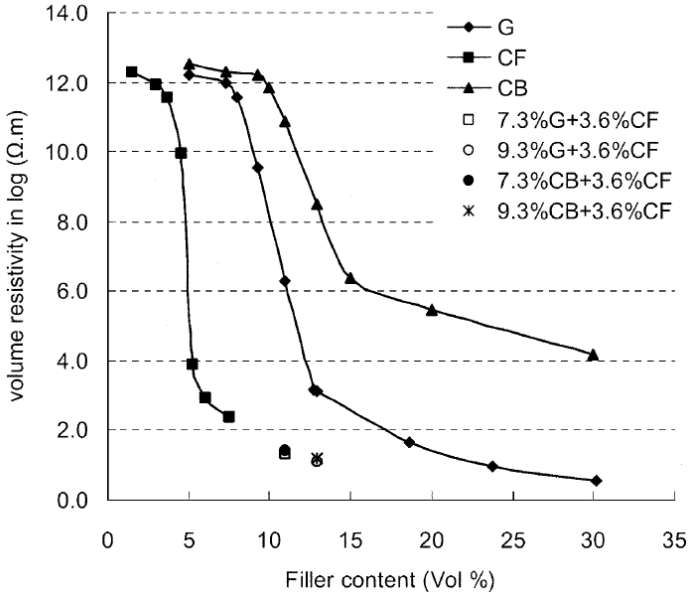


**Figure 6. Effect of Type of Conductive Additive on Electrical Resistivity of Asphalt Concrete (Wu et al. 2005).**

A research team at the University of Tennessee carried out similar studies. Huang et al. (2006) investigated the different options for producing electrically conductive asphalt. Micro scale steel fibers (8 μm in diameter and 6 mm in length), aluminum chips (passing a 0.10-mm sieve), and graphite (passing a 0.075-mm sieve) were examined for their ability in imparting conductivity. It was observed that aluminum chips are not effective in increasing the electrical conductivity of the mixture in spite of their excellent conductivity. The reason is that aluminum gets easily oxidized in the air and forms aluminum oxide, which has low conductivity. While aluminum is not the right choice for practical purposes, the mixtures with microscale steel fibers and graphite exhibited good electrical conductivity. Resistivity in the order of $10^3\,\Omega$.m was reached with the addition of 0.33 percent steel fibers by volume of asphalt binder. Approximately 2.3 percent graphite by volume of asphalt binder was needed to obtain a similar resistivity level. Variation in electrical conductivity during fatigue evolution was also studied through an indirect tensile test (IDT) and beam fatigue tests.

Huang et al. (2009) extended their investigation to the mechanical performance of conductive asphalt composites. They conducted the dynamic shear rheometer (DSR) test to study the effect of conductive additives (i.e., microscale steel fibers, carbon fibers, and graphite) on the viscoelastic properties of asphalt mastic (a mixture of asphalt binder and conductive additives). The results show that with increased conductive additives, the complex shear modulus, $G^*$, increases. This implies that the conductive additives can stiffen the asphalt binder. High contents of graphite were required to achieve sufficiently low resistivity; hence, the stiffness of the mastic was improved greatly. The mechanical performances of conductive HMA mixtures were investigated through an IDT and dynamic modulus tests. Though graphite reduces the IDT strength of the mixtures, it improves the dynamic modulus. On the other hand, the fracture energy of the mixtures with carbon or steel fibers was slightly improved due to the reinforcing effect of the fibers. Figure 7 depicts the IDT strength and dynamic modulus of asphalt concrete containing various additives.

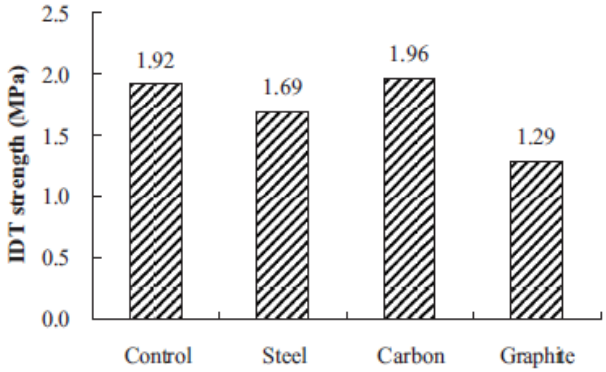


(a) IDT strength for various additives

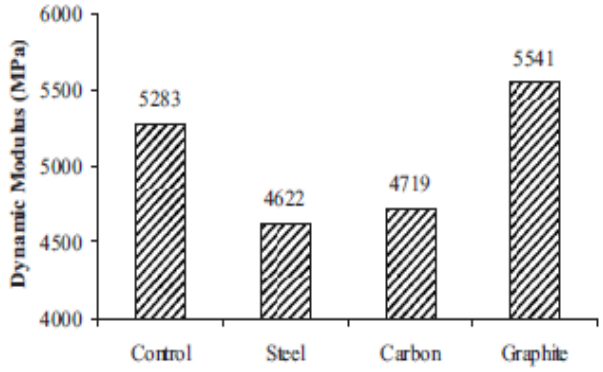


(b) Dynamic modulus at 10 Hz

**Figure 7. Mechanical Properties of HMA Mixture with Conductive Additives (Huang et al. 2009).**

Garcia et al. (2009) conducted a comprehensive study. They examined the effect of fiber content, the sand–bitumen ratio, and a combination of fillers and fibers (graphite and steel wool) on the resistivity of asphalt mortar. The authors divided the changes in the resistivity with volume percentages of conductive additive into four different phases:

- The insulated phase. The insulated phase is where the fibers are not connected with one another and the resistivity is approximately equal to that of plain asphalt concrete.
- The transition phase. The transition phase is where the percolation path of fibers forms and the resistivity rapidly drops, leading to the next phase.
- The conductive phase. The conductive phase is where the fibers are connected with each other, and the electrical resistivity of the composite becomes very low.
- The excess of fibers phase. The last phase is the excess of fibers phase, during which the reduction in length of conductive paths is no longer significant, and the electrical resistivity of the composite decreases slightly with the increased fiber content. In addition, the asphalt becomes difficult to mix when clusters of fibers start forming.

Figure 8 shows the schematic of the conductivity variation.

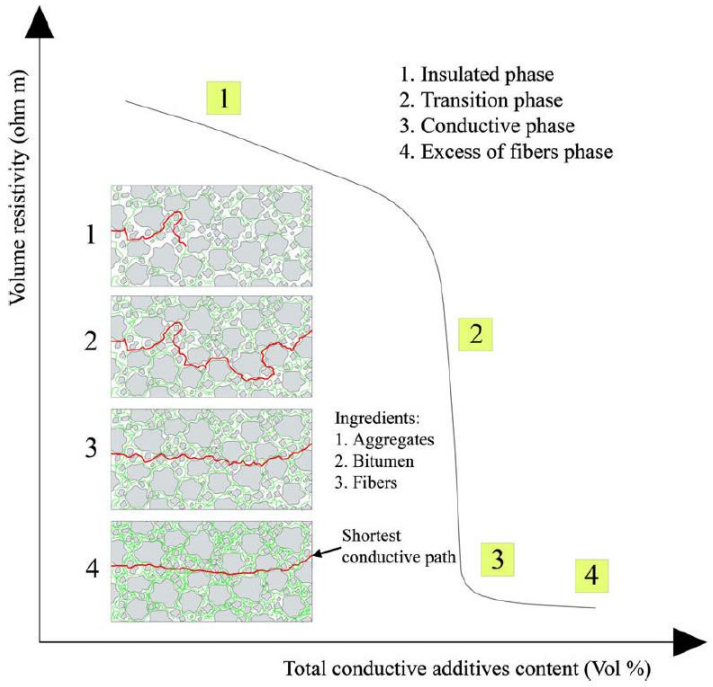


**Figure 8. Schematic Representation of Volume Resistivity versus Conductive Additive Content (Garcia et al. 2009).**

According to Garcia et al. (2009), the resistivity of the composite material varied not only with the content of conductive additives, but also with the sand-bitumen ratio. The authors observed that there exists an optimum conductive particles-bitumen ratio for each sand-bitumen ratio where the resistivity of the mixture reached a minimum level. Figure 9 shows the optimum sand-bitumen ratios for different amounts of conductive additives. Note that graphite significantly reduces the optimum sand-bitumen ratio when it is combined with steel wool.

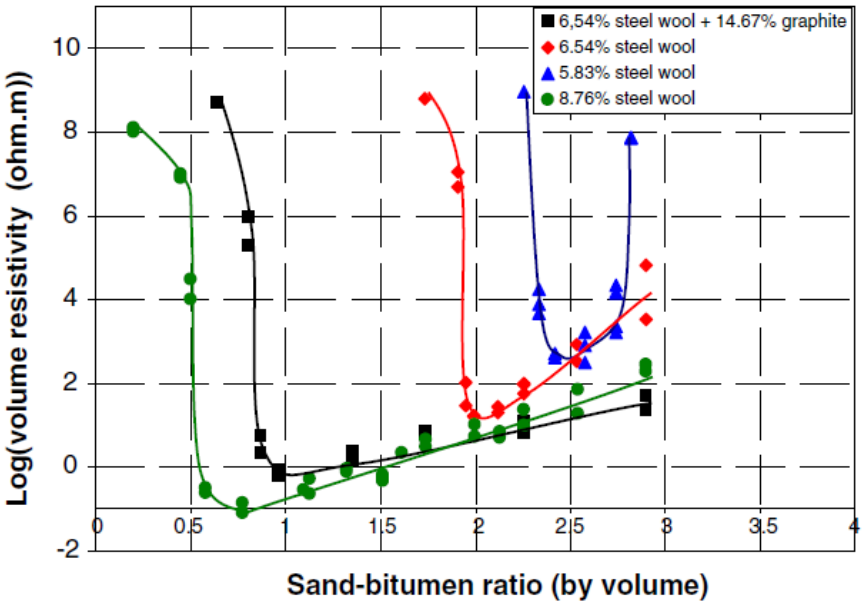


**Figure 9. Variation in Electrical Resistivity with Sand-Bitumen Ratio (Garcia et al. 2009).**

In addition, Liu et al. (2008a) and Liu and Wu (2009) investigated the piezoresistivity of conductive asphalt concrete. Piezoresistivity is an electrical property in which the electrical resistivity of a material changes due to applied stress or strain. It reflects the microstructural change in the material on application of load. This phenomenon was observed in conductive asphalt and implies that conductive asphalt could be used as a self-sensing material. The relationship between electrical property and mechanical condition broadens the possible multifunctional application of conductive asphalt.

Wu et al. (2010) investigated the mechanical characteristics of conductive asphalt concrete using graphite and carbon fiber. The authors studied the indirect tensile strength, indirect tensile resilient modulus, and indirect tensile fatigue life of the conductive asphalt concrete containing carbon fibers and graphite. The results indicated that conductive asphalt

concrete has higher tensile strength than regular asphalt concrete under dry conditions, but has lower wet tensile strength and tensile strength ratio (TSR). This means conductive asphalt concrete has relatively lower resistance to water, but fortunately the ratio is higher than the minimum required value. The indirect tensile resilient modulus increases with the addition of conductive components. The effect of carbon fibers on indirect resilient modulus is more prominent than that of graphite. The results of the indirect tensile fatigue test show that the fatigue life of conductive asphalt concrete at higher stress levels is greatly enhanced when compared to that of regular asphalt concrete. Figure 10 summarizes the findings of Wu et al. (2010).

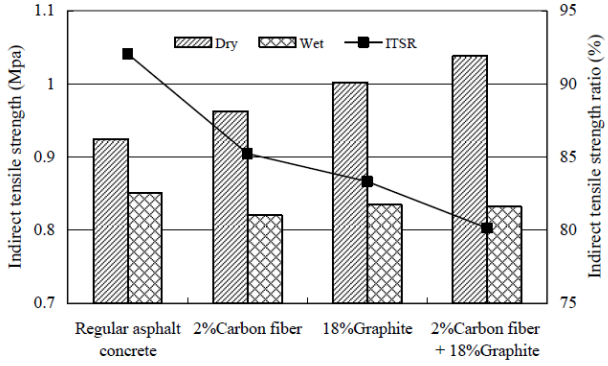


(a) Indirect tensile strength results for regular and conductive asphalt

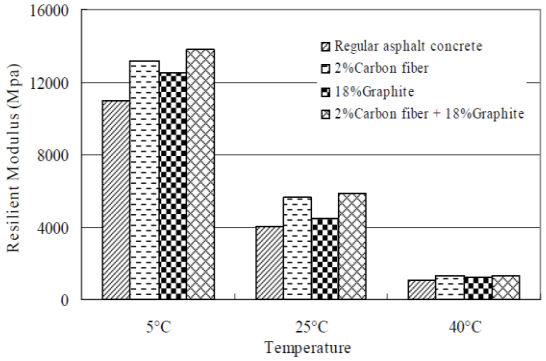


(b) Indirect tensile resilient modulus results at different temperatures

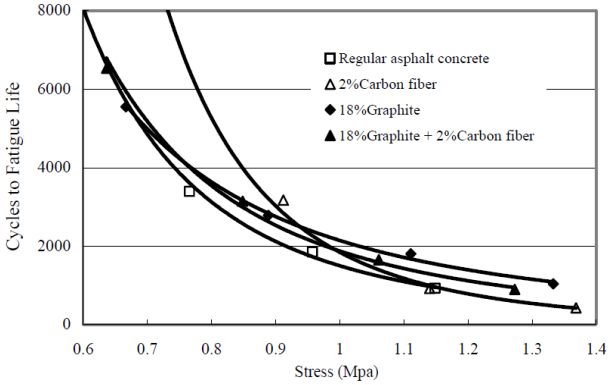


(c) Indirect tensile fatigue life graph for regular and conductive asphalt composites

**Figure 10. Mechanical Test Results of Conductive Asphalt Concrete (Wu et al. 2010).**

Liu et al. (2010b) conducted a similar study on the IDT strength of porous asphalt concrete with steel fibers. The authors observed that the IDT strength of the mixture increases

with the increase of steel fibers until a certain consistency. Beyond that, adding more fibers reduces the thickness of mastic film around the aggregates, leading to poor adhesion that reduces the IDT strength of porous asphalt concrete. Figure 11 shows the results of the IDT on conductive porous asphalt concrete.

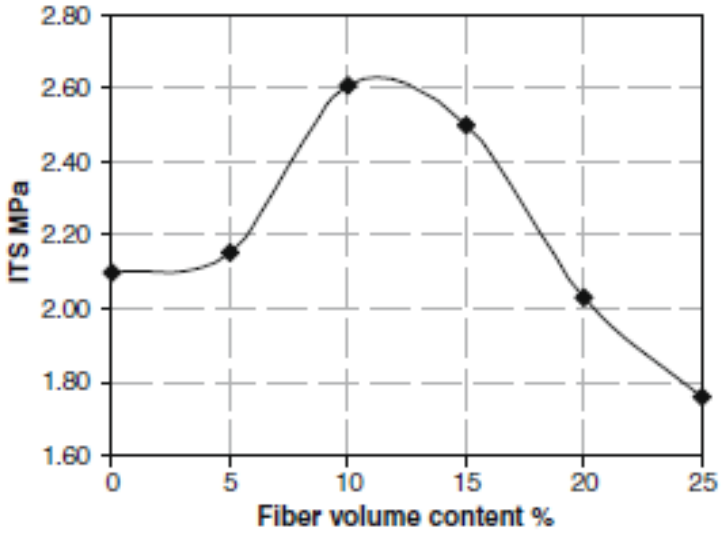


**Figure 11. Indirect Tensile Strength on Conductive Porous Asphalt Concrete (Liu et al. 2010b).**

Liu and Wu (2011a) investigated the variation of Marshall stability, resilient modulus, and dynamic stability of graphite- and carbon-fiber-modified asphalt concrete. According to Liu and Wu, the addition of graphite did not considerably enhance the mechanical strength of asphalt concrete. They concluded that graphite can be a good conductive filler, but its lubricating property caused by weak bonds between plain hexagonal crystal structures of graphite might impair the mechanical properties of asphalt concrete.

Park (2012) studied the effect of graphite powders on imparting electrical conductivity in asphalt mastic and showed that the electrical resistivity significantly varied with the type (shape and size) of graphite.

Zhang et al. (2011) proposed another type of conductive additive. Polyaniline (PANI) is a conductive polymer, and the authors tried to impart electrical conductivity into stone matrix asphalt using a self-made PANI/polypropylene (PP) compound. The conductivity increased by six orders of magnitude, and the percolation threshold was 1 percent.

As reviewed above, electrically conductive asphalt concrete has become popular during the last 10 years. Table 1 summarizes the previous research on conductive asphalt. As compared in Table 1, the amount of conductive additives required for specific resistivity varies significantly with the investigator. For example, the volume percentage of graphite at $10^3$ Ω·cm ranges from 11 percent to 30 percent. Therefore, the causes of this variability and the factors affecting the conductivity of asphalt mixtures should be clarified for precise conductivity control.

**Table 1. Summary of Previous Research on Conductive Asphalt Composites.**

| Author | Conductive Filler Used | Percentage of Additive to Attain Resistivity of $10^3$ Ω.cm (Percent Vol. by Binder) | Purpose |
|---|---|---|---|
| Minsk (1968) | Graphite (G) | G—17% and 21% | Snow and ice removal |
| Stratfull (1974) | Coke breeze | — | Cathodic protection of steel rebars in concrete bridges |
| Fromm (1976) | Coke breeze | — | Cathodic protection of concrete bridge decks |
| Zaleski et al. (1998) | Graphite and coke | — | Deicing |
| Wu et al. (2003) | Graphite | G—26% | Self-sensing applications |
| Wu et al. (2005) | Carbon black (CB), graphite, and carbon fibers (CF) | CB—13%, CF—6%, or G—30% | Imparting conductivity CF > G > CB |
| Huang et al. (2006) | Microscale steel fibers (SF), aluminum chips, and graphite | SF—0.75% or G—11% | Study conductivity, IDT, and beam fatigue test |
| Huang et al. (2009) | Microscale steel fiber, carbon fiber, and graphite | SF—0.99%, CF—5%, or G—18% | IDT strength, IDT fracture energy, dynamic modulus, flow number, and asphalt pavement analyzer (APA) rut depth |
| Garcia et al. (2009) | Graphite and steel wool (SW) | SW—6% or G—beyond 30% | Sand-bitumen ratio and effect of fiber content |
| Liu and Wu (2009) | Graphite and carbon fiber | G—12% | Piezoresistivity |
| Wu et al. (2010) | Graphite and carbon fiber | G—22% or CF—beyond 8% | IDT and indirect tensile fatigue life |
| Liu and Wu (2011a) | Graphite and carbon fiber | G—15% | Marshall stability, resilient modulus, and dynamic stability |
| Park (2012) | Graphite | G—21% | Electrical conductivity of different types of graphite |

## 2.2 MULTIFUNCTIONAL APPLICATIONS OF CONDUCTIVE ASPHALT CONCRETE

Multifunctional materials are considered smart and innovative materials due to their widespread technological impact and ability to respond to external stimuli in an environment-friendly manner. The technology necessary to build the next-generation devices includes:

- Autonomous robots.
- Smart homes.
- Intelligent sensors.
- Structural health monitoring.
- Smart transportation system.

The concept of developing multifunctional materials stems from the need to accomplish multiple applications and performances in a single system. The sought-after characteristics of these materials include energy-efficient nonstructural functions, such as self-sensing, self-healing, and electromagnetic properties, in addition to the traditional structural functions of resisting external forces. Hence, the research and development involved in multifunctional materials face a great technological challenge with various applications. Interdisciplinary investigations have been carried out for the molecular structure and nonstructural properties of various materials to explore multifunctional possibilities and to extend their use across different disciplines.

In the case of conductive asphalt concrete, the potential multifunctional applications include electrical heating, sensing, and energy harvesting. These features are discussed for a more thorough understanding of the benefits.

### Snow and Ice Removal Using Electric Heating

One of the major issues in society is improving transportation safety under freezing and/or snowy weather. Removing snow and ice, especially on highway and bridge surfaces, is a crucial step to enhance transportation safety. Deicing agents such as salt or sand can be used to remove ice from pavements (Blackburn et al. 2004). Salt is the most popular deicing agent because it is inexpensive and efficient. Deicing chemicals have obvious negative impacts, including concrete corrosion and environmental pollution. The International Energy Agency (IEA) and World Health Organization (WHO) pay much attention to these problems (Lofgren 2001, Sanzo and Hecnar 2006). Snow and ice on conductive asphalt pavement can be removed

by electric heating, which is the process of converting electric energy to heat (Chen et al. 2012). This method ensures reliable deicing and reduced pollution.

**Promoting Self-Healing**

Asphalt concrete is a self-healing material (Bommavaram et al. 2009). Once the load causing microcracks is removed, the molecules on either side of each crack start diffusing to the other end, and the microcracks are healed with time. The time required for this healing process is called the rest period. The challenge arises when the traffic flow is too heavy to allow a sufficient rest period for self-healing. One of the solutions is to increase the temperature of asphalt concrete because the healing can be accelerated with increased temperature (Bonnaure et al. 1982, Daniel and Kim 2001). Liu et al. (2010a, 2010b, 2010c), Garcia (2012), and Garcia et al. (2011a, 2011b) showed the possibility of promoting self-healing by inducting electrical energy into conductive asphalt concrete. Garcia et al. (2011a, 2011b) and Liu et al. (2010a, 2010b, 2010c) suggested a non-contact electric heating technique using electromagnetic fields. The induced current dissipates heat in the specimen via the eddy current effect.

**Strain and Damage Self-Sensing**

A self-sensing material can monitor its own strain and damage without an external sensor. Compared to the structural health-monitoring system based on the attached sensor network (extrinsic), self-sensing structural materials are intrinsically smart. Structures made with the intrinsically smart materials have possible advantages over extrinsically smart structures due to:

- Low cost.
- Good durability.
- Large sensing volume.
- Absence of mechanical property degradation due to the embedding of sensors (Chung and Wang 2003).

The contact resistance between the conductive filler governs the resistivity of the asphalt or cementitious composites. Upon application of an external compressive load, the filler particles get closer, resulting in decreased resistivity (Wen and Chung 2007d). Such a change in resistivity with application of mechanical stresses is referred to as piezoresistivity (Wu et al. 2006). This is the mechanism by which conductive asphalt pavements sense their own structural health.

Liu et al. (2008a, 2009, 2011a, 2011b) proposed a series-wound model to explain the piezoresistivity of conductive asphalt concrete by experimental studies. The number of electron carriers (conductive path) in the interior of the conductive asphalt concrete influences the electrical property, and the number of carriers is varied with different loading conditions. The relationship between the number of carriers and electrical resistivity is inversely proportional. In other words, resistance is reduced while under increased compressive stress during loading and increases during unloading until the stress reaches a certain value. Under compression, the contact resistance between graphite particles is reduced, and the insulating gaps between graphite particles are decreased, developing new conductive paths.

Another reason mentioned is the ability of microcracks to destroy the conductive network due to the large gap width of microcracks that prevent electron hopping.

The third effect is the dislocation of the conductive path, which results from the large vertical deformation that originates from the shear stress between aggregates. In addition, Liu et al. (2008b) studied the engineering properties and electrical properties of asphalt concrete with different graphite and carbon fiber content. The filler was 5 percent by weight, and the asphalt was 4.5 percent. Graphite of 150 μm and carbon fiber of 10-μm diameter and 5-mm length were used. The results from the IDT indicate that the addition of conductive fillers like graphite and carbon fiber influences or affects the mechanical properties of asphalt mixtures. The resilient modulus increased when a combination of graphite and carbon fibers was used, while smaller increases were observed with the use of only carbon fiber or graphite.

## 2.3 MULTIFUNCTIONAL APPLICATIONS OF CONDUCTIVE CEMENT CONCRETE

Concrete is the most widely used construction material nowadays and has a huge impact on the construction industry. Concrete by itself has strong structural properties but is a poor electrical conductor. Incorporation of electrically conductive materials in the cement matrix enhances the smart function of concrete for various multifunctional applications. The typical conductive additives are steel/carbon fibers and graphite powders. More recently, attempts to use carbon nanotubes have been made. The promising multifunctional applications include:

- Self-sensing.
- Self-heating.
- Self-healing.

- Electromagnetic shielding.
- Energy harvesting (more recently).

The factors affecting the conductivity of cement-based composites are:

- Volume fraction of fibers.
- Length of fibers.
- Temperature.
- Chloride content.
- Compressive, tensile, or flexure load.
- Sand-cement ratio.
- Relative humidity.
- Curing age.

The average length of carbon fibers found in the literature is between 5 mm and 10 mm; the average diameter is 10–15 μm. The typical volume fraction of fibers ranges from 0.2 to 1.5 percent. Carbon fibers are considered the most effective for strain sensing, while steel fibers are the most effective for thermal sensing and deicing purposes (Cao et al. 2001). Silica fume is a useful additive for enhancing fiber dispersion (Chen and Chung 1995). Carbon fibers are strong, durable, and not dense, but the one drawback is their high cost (Chung 1997, 1999, 2000, 2002, 2003, 2012).

**Conductivity of Cement-Based Composites**

Various investigators have verified that the conductivity of concrete increases with the increase of fiber volume fraction. Banthia (1992) showed that 5 percent fiber volume fraction produced hardly any increase in resistivity over time. In fact, samples with 3 percent fibers or less showed significant increases in resistivity over time. Chiarello and Zinno (2004) showed that longer fibers produced higher conductivity effects in concrete; e.g., 6-mm fibers yielded higher conductivity than 3-mm or shorter fibers. Several samples showed that conductivity is independent of specimen age. Chen et al. (2004) also showed the effect of fiber length on electric conductivity and declared a volume fraction around 0.3–0.4 percent to be the percolation threshold.

Chacko and Banthia (2007) examined the effect of various parameters on the resistivity of concrete. The electrical resistivity of carbon-fiber-reinforced cement composites increases

dramatically over time due to the microstructure change in the hydration of concrete. There was a considerable decrease in the conductivity of concrete when exposed to chloride ions, which present a dilemma because of their highly corrosive nature. On direct compressive loading, the resistivity decreased during the elastic stage, when fibers were coming in contact. The resistivity flattened out until the first crack was encountered; then it increased suddenly, further supporting the notion of self-sensing capability in concrete. The electrical resistivity decreased with temperature and vice versa. The water-cementitious material (w/cm) ratio did not affect the conductivity at high-volume fractions where the carbon fibers seem to provide most of the conductivity, so moisture/humidity levels do not play a major role in controlling the resistivity of cement materials. However, a w/cm ratio of 0.3 seemed to provide the least resistivity in low fiber content composites. Wen and Chung (2008) showed that saturated moisture levels had higher conductivity than less wet samples due to the effect of ionic conduction of cations of water.

Wen and Chung (2001a) studied the effect of carbon fibers on dielectric constant. Carbon fibers were found to be most effective in increasing dielectric constant (Wen and Chung 2001b). Wen and Chung (2004) summarized and showed the trends that different fillers and additives exhibited on the resistivity and thermoelectric power of concrete. Resistivity decreases with increasing fiber volume fraction. Carbon fiber is more effective in decreasing resistivity than carbon filament or graphite powder (Chung 2012). Carbon filaments were found more effective in conductivity than coke powder but less inferior in electromagnetic interference (EMI) shielding. A material stronger in thermoelectricity or electromagnetic shielding is not necessarily stronger in conductivity. Hong et al. (2003) studied the effect of graphite slurry infiltrated with steel fibers on the resistivity of fiber concrete. With a w/cm of 0.5 and 1:1 sand cement ratio, resistivity decreased with increasing graphite content and, more importantly, showed less resistance magnitudes with longer steel fibers. In the post-threshold zone, the resistivity decrease slowed. With the addition of fiber, the graphite particles connected the loose steel fibers, forming a graphite bridge and lowering the resistivity.

Vaidya (2011) attempted to impart electric conductivity in fly-ash-based composite. Replacing Portland cement with fly ash proved more effective than using only Portland cement in lowering resistivity with higher carbon fiber volume fractions. A fiber percentage of 0.1 percent is the required value to establish electric percolation. This was attributed to the

increased alkali content in supplementary cementitious materials, which contributed to higher ionic conduction.

### Self-Actuating Materials

The self-actuating capability allows material to respond to what has been sensed. The structural material provides strain or stress in response to an input such as an electric field or a magnetic field. The phenomenon known as reverse piezoelectric effect or electrostriction is responsible for this behavior (Chung 2002). Short carbon fiber reinforced cement has been observed to exhibit such behavior.

### Self-Sensing Cement Matrix Composites

Self-sensing refers to the ability of a material to sense its own condition such as strain, stress, damage, and temperature. Some applications of self-sensing include:

- Structural vibration control.
- Traffic monitoring.
- Weighing.
- Building facility management.
- Structural health monitoring.

Sensing is achieved by electrical resistance measurements. Thermocouples have been achieved when temperature adjustments are done on the structural materials. The development of cement-based materials containing short carbon fibers is opening new possibilities in the research field of multifunctional structural materials. The effects of numerous modes of loading on the piezoresistive phenomenon that have been investigated include:

- Flexure.
- Tension.
- Compression.
- Impact.
- Strain amplitude.
- Moisture.

The electrical resistance of self-sensing concrete varies with stress or strain. To measure the surface electrical resistance, the researchers used the four-probe method in which the outer

two contacts are meant for passing current and the inner two contacts are for voltage measurement (Chen and Liu 2007). The two-probe method gives less effective results. The gage factor, the fractional change in resistance per unit strain, ranges up to 700 for compression or tension. The resistance increases reversibly with tension and decreases with compression, due to fiber pull-out upon microcrack opening. Chung (1997) reported that concrete can contain as low as 0.2 percent carbon fiber content in order to exhibit piezoresistive capabilities. During the repeated loading test with various strain amplitudes in uniaxial compression, the peak resistivity varies linearly with peak strain. This implies that strain can be estimated by measuring electrical resistance. The gage factor for cementitious composites approaches 300, compared to a value of 2 that is typical of metal strain gages (Chung 2012). However, the gage factor does decrease with increasing strain amplitude.

Azhari and Banthia (2012) attempted to study the effects of carbon nanotubes on piezoresistivity. The combined use of carbon nanotubes and carbon fiber gives better sensing than the use of carbon nanotubes as the sole conductive admixture. However, the high cost of carbon nanotubes compared to carbon fiber is a significant disadvantage in view of the cost-conscious concrete industry. Carbon black is even less expensive than short carbon fiber, but it gives low values for the gage factor, so it is a useless material for controlling conductivity. Replacing 50 percent cement with carbon black maintains conductivity and electromagnetic shielding, but reduces strain sensing (Wen and Chung 2007a). Although research has emphasized the use of cement in the form of Portland cement, sulfoaluminate cement has been shown to be an effective cement matrix for providing piezoresistivity in the presence of short carbon fibers as filler (Wen and Chung 2007b).

**Damage Sensing**

Damage sensing has also been investigated when damage causes some breakage of the brittle carbon fibers, resulting in an irreversible increase in resistivity. The resistivity in both stress direction and transverse direction increases upon tension because of the fiber pull-out that accompanies crack opening and decreases upon compression, as a result of fiber push-in (Wen and Chung 2007c). Piezoresistivity allows the use of alternating current (AC) or direct current (DC) electrical resistance to monitor the strain of cement-based materials. The damage can be monitored by measuring the DC electrical resistivity via a four-probe method. Damage was

found to increase the electrical resistivity. In the case of major damage, this resistivity increase is irreversible because the strain never returned to zero, and it was found that fiber fracture controls the damage. Various resistance measurements used throughout the field include (Chen and Liu 2007):

- Volume resistance for measuring the damage of a volume.
- Surface resistance for measuring the damage of a surface.
- Contact resistance for measuring the damage of an interface.

**Temperature Sensing**

In regard to temperature sensing, cement-based materials have been developed into thermistors and thermocouples. Each thermocouple takes the form of a cement-based p-n junction. The thermoelectric effect of cement-based materials has been observed whereby a temperature gradient generates electricity. Wen and Chung (2000) showed the thermistor effect where electrical resistivity decreases with increasing temperature. The effect is attributed to the jump of electrons from one lamina to another across the interlaminar surface. Steel fiber was found to be very effective for heat resistance.

Wen and Chung (2000) reported that carbon fibers and graphite are less effective in heat sensing due to a higher voltage requirement and electrical resistivity. The use of steel fibers instead of carbon fibers results in highly positive thermoelectric power values because steel fibers provide electron conduction, whereas carbon fibers involve hole conduction. Steel fibers were found to produce a better thermoelectric material than carbon fiber. The thermoelectric effect is the basis of thermocouples for temperature measurement. The resistivity decreases upon heating, and the effect is quite reversible upon cooling. The fact that the resistivity is slightly increased after a heating and cooling cycle is probably due to thermal degradation of the material. Wen and Chung (2004) found that a cement-matrix composite containing 0.7 percent steel fibers (8-μm diameter) by volume and a mat of discontinuous uncoated carbon fibers for use as an interlayer are effective for self-heating. However, the effectiveness is low compared to flexible graphite, which is not a structural material.

**Electromagnetic Shielding**

Mainly due to their high reflectivity, carbon materials are also effective for shielding. The EMI shielding effectiveness of flexible graphite (made by compressing exfoliated graphite in the absence of a binder) reaches 130 dB (at 1 GHz), which is higher than or comparable to all EMI shielding materials, including carbon and non-carbon materials. The high effectiveness of flexible graphite is due to the high electrical conductivity and high surface area, which is valuable due to the skin effect. Flexible graphite has the additional advantages of:

- Resiliency (needed for EMI gaskets, which are particularly challenging due to the requirement of resiliency).
- Low density.
- Low thermal expansion.
- Thermal conductivity (which helps microelectronic heat dissipation).
- Chemical resistance.

**Percolation Theory**

The percolation theory describes the behavior of concrete reinforced with conductive carbon fibers. The conductivity changes significantly at a critical fiber content that is found to be independent of the matrix. This refers to the volume fraction above which the fibers touch one another to form a continuous electrical path (Sui and Liu 2006). Longer fibers were found to decrease the threshold where the threshold is between 0.5 and 1.0 percent fiber volume fractions. Wen and Chung (2007a) observed double percolation in cement-based composites where one percolation threshold was attributed to the fiber percolation and the other to cement percolation. Baeza et al. (2010) also observed triple percolation.

# 3. CHARACTERIZATIONS OF RAW MATERIALS

This section introduces the physical properties of the materials used in the research. The properties of graphite, including density, particle size, and surface area, play a major role in deciding the electrical resistivity, mixing, and compaction difficulties of the conductive asphalt concrete. Scanning electron microscope (SEM) images of the graphite provide an explanation of the observed conductivity variation within the graphite types. In addition, the researchers investigated the physical properties of other materials used in this study, such as:

- Aggregate.
- Binders.
- Fillers.
- Wood stick.
- Silver paste.
- Copper tape.

## 3.1 TYPES OF GRAPHITE

Eight different types of graphite and a carbon black produced by Asbury Carbons, Inc., were selected to study the effect of these materials on imparting conductivity into asphalt concrete. Graphite has a two-dimensional hexagonal crystal structure; hence, the ideal shape of a graphite particle is a hexagonal plate. However, the shape and size of the particles vary according to the source and manufacturing process. The graphite types are classified into:

- Three flake types (F146, F3204, and F516).
- Two amorphous types (505 and 508).
- One artificial type (A99).
- Two types with ultra-high surface area (SA4827 and TC307).

Although the graphite types 505 and 508 are called amorphous types because of their particle shape, they are actually crystalline materials. On the other hand, carbon black is a genuine amorphous material, which does not have a long-range order in its atomic structure. Table 2 presents the properties of the graphite types and carbon black.

**Table 2. Properties of Graphite Used for Research (Asbury Carbons, Inc.).**

| Asbury ID | Percent Carbon | Typical Size (µm) | True Density | Surface Area ($m^2/g$) | Typical Resistivity (Ω·cm) | TL Price ($/lb) | Note |
|---|---|---|---|---|---|---|---|
| F146 | 96.86 | 20 (< 44) | 2.25 | 6.35 | 0.03–0.05 | $1.27 | Flake type |
| F3204 | 97.05 | 15 (< 44) | 2.25 | 7.41 | 0.03–0.05 | $1.18 | Flake type |
| F516 | 95.45 | — (< 212) | 2.26 | 5.0 | 0.03–0.05 | $1.66 | Flake type |
| 505 | 84.50 | 35 (< 75) | 2.30 | 22 | 0.13 | $0.55 | Amorphous type |
| 508 | 81.77 | 20 (97% < 44) | 2.30 | 21 | 0.13 | $0.59 | Amorphous type |
| A99 | 99.68 | 20 | 2.23 | 8.47 | 0.047 | $1.01 | Artificial type |
| SA4827 | 99.66 | < 1 um | 2.20 | 248.92 | 0.184 | $4.15 | Artificial graphite nanoplatelet |
| TC307 | 99.92 | < 1 um | 2.20 | 352 | 0.289 | $4.58 | Artificial graphite nanoplatelet |
| CB5303 | 99.90 | 0.03 | 1.8 | 254 | 0.341 | $7.87 | Carbon black |

## 3.2 SCANNING ELECTRON MICROSCOPE ANALYSIS

Figure 12 shows scanning electron microscope images of the graphite powders that were taken to investigate the shape of the graphite particles. The images labeled (a) through (i) show the SEM images of the nine conductive powders, with the magnification scale set at 2000 times for all images. As shown in (a), (b), and (c), the flake graphite particles have thin plate shapes. The rest of the figures show that the amorphous and artificial graphite types have irregular shapes. Graphite has super conductivity along the flat surface, while conductivity through the plate is significantly lower; hence, the difference in the particle shapes may lead to a difference in conductivity. Particle size and shape can affect mixture properties. For instance, the particle size of TC307 is small, resulting in a very high surface area (352 $m^2/g$). This implies that TC307 will require more binder to coat its surface than other types of graphite.

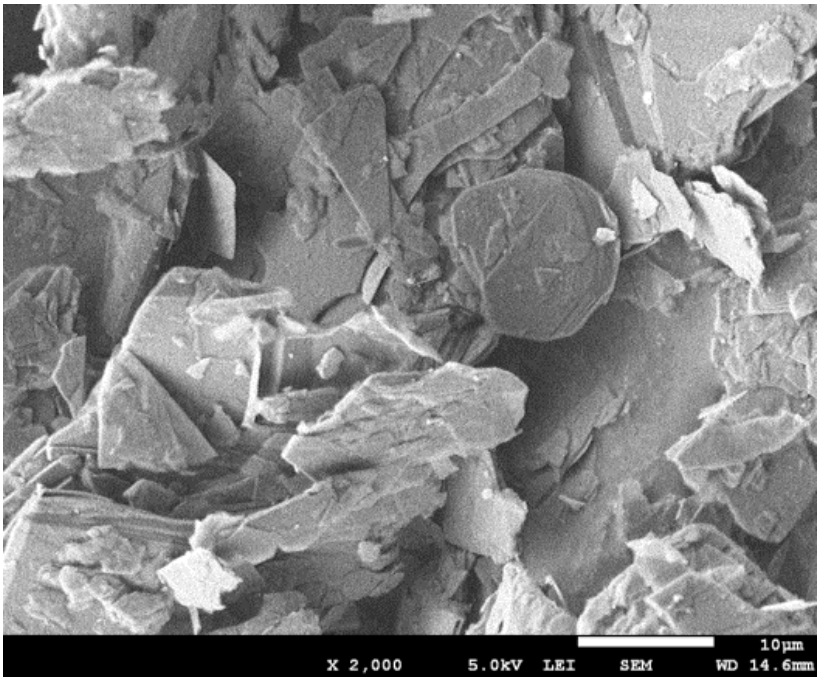


(a) Flake graphite F146

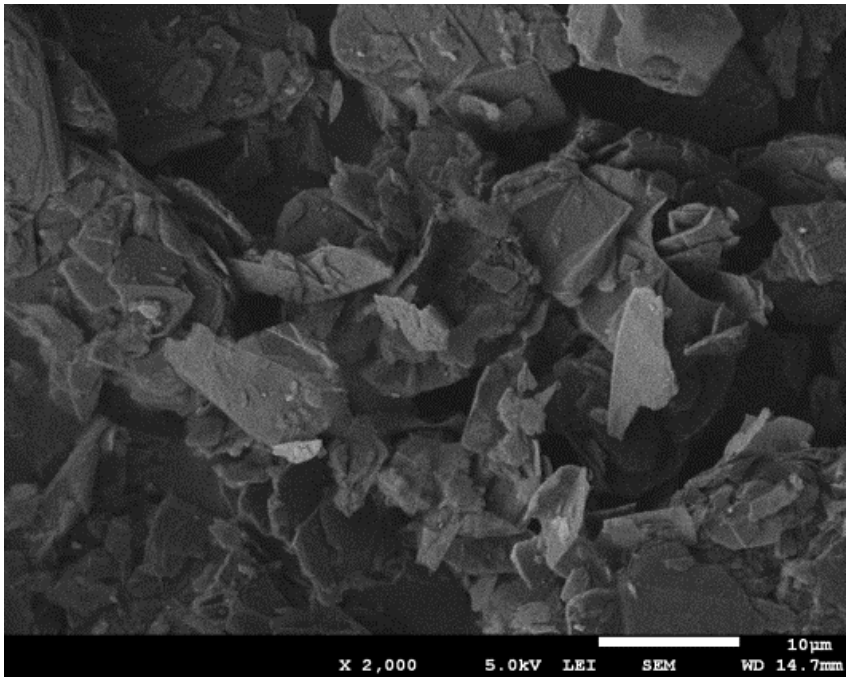


(b) Flake graphite F3204

**Figure 12. SEM Images of Graphite Powders.**

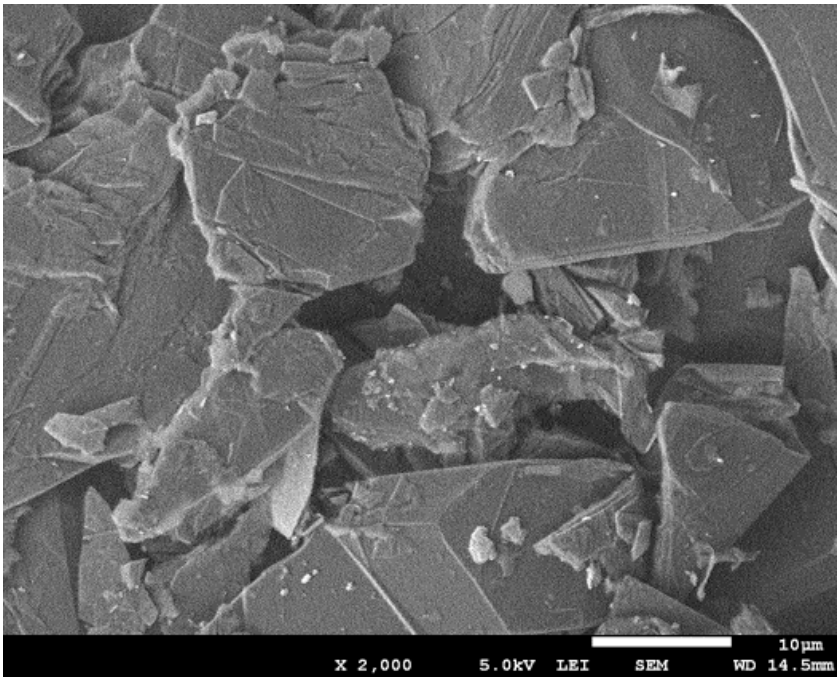


(c) Flake graphite F516

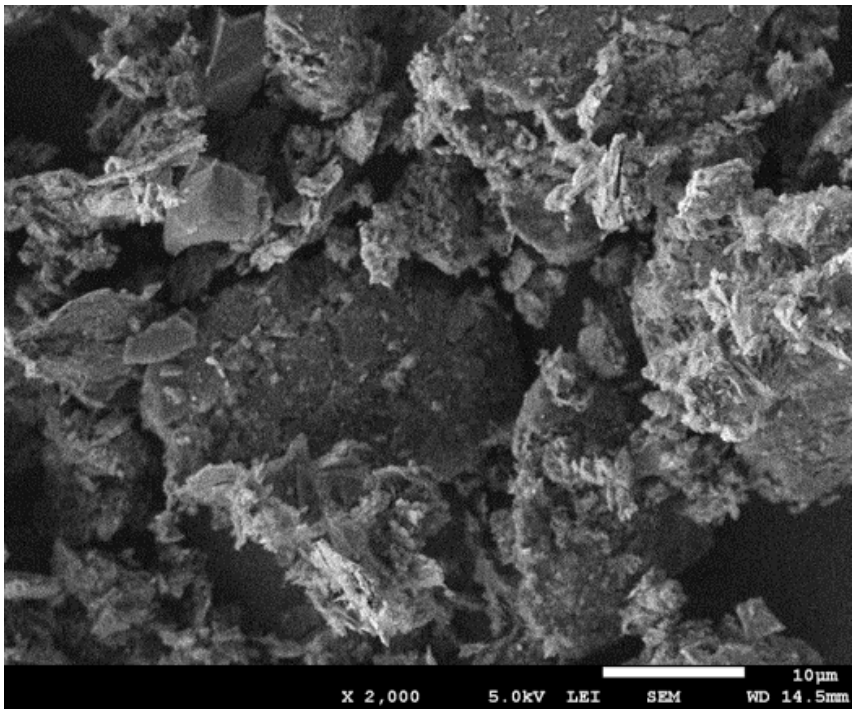


(d) Amorphous graphite 505

**Figure 12. SEM Images of Graphite Powders (Continued).**

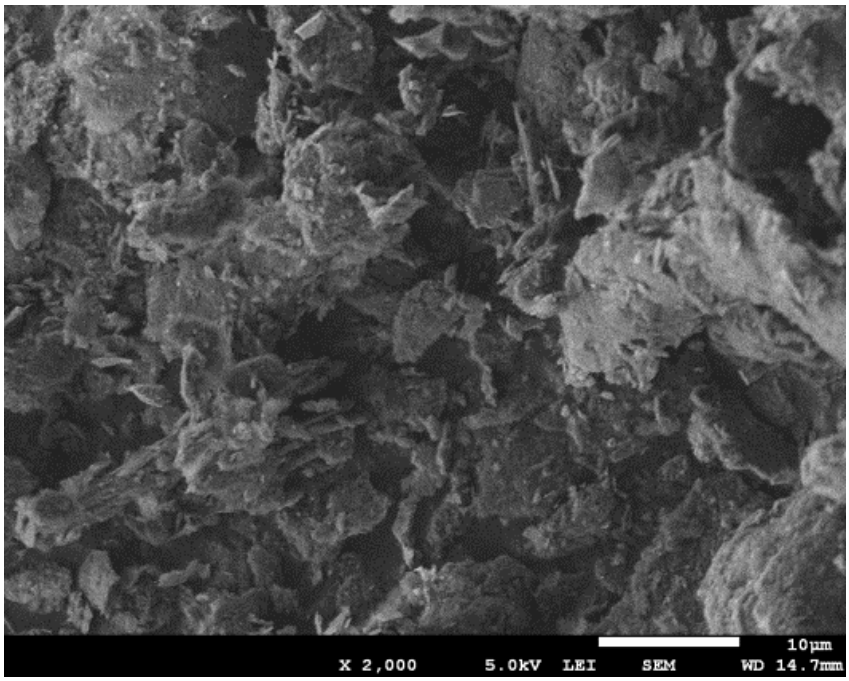


(e) Amorphous graphite 508

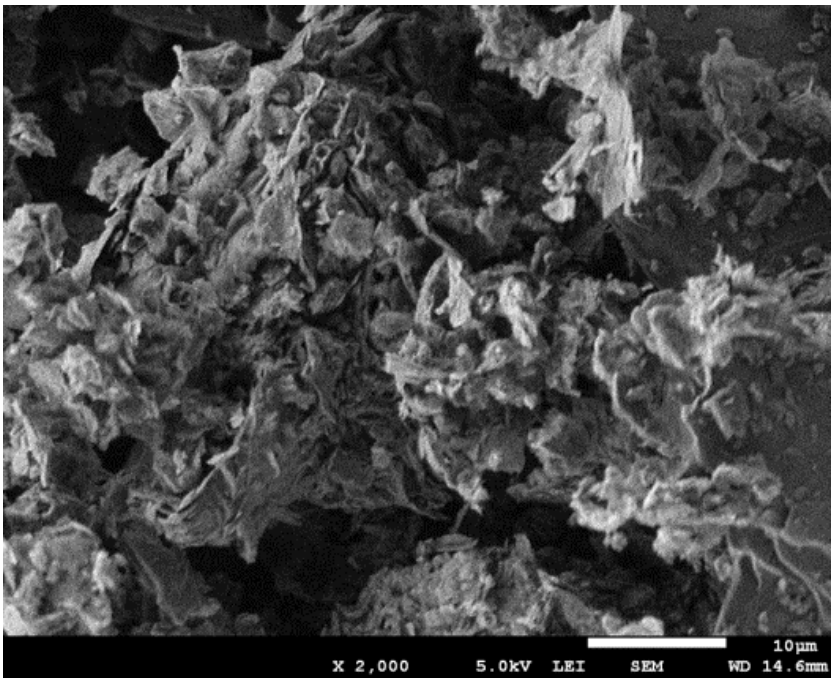


(f) Artificial graphite A99

**Figure 12. SEM Images of Graphite Powders (Continued).**

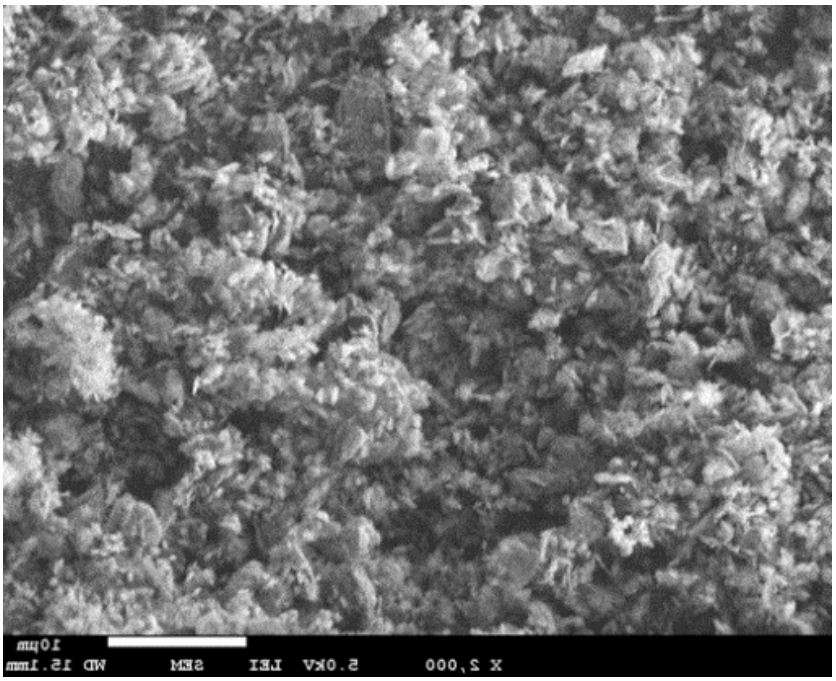

(g) Ultra-high-surface-area graphite SA4827

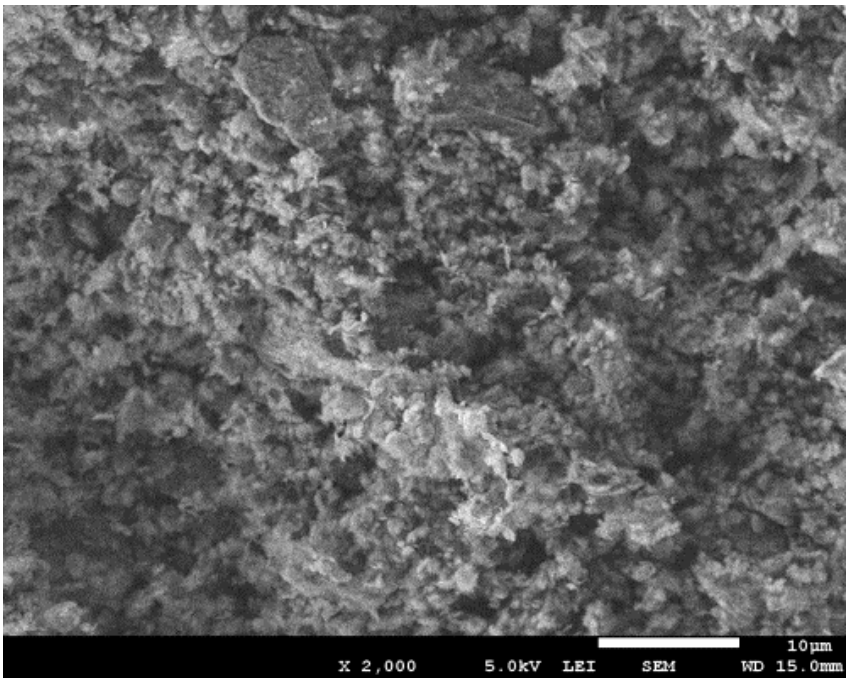


(h) High-surface-area graphite TC307

**Figure 12. SEM Images of Graphite Powders (Continued).**

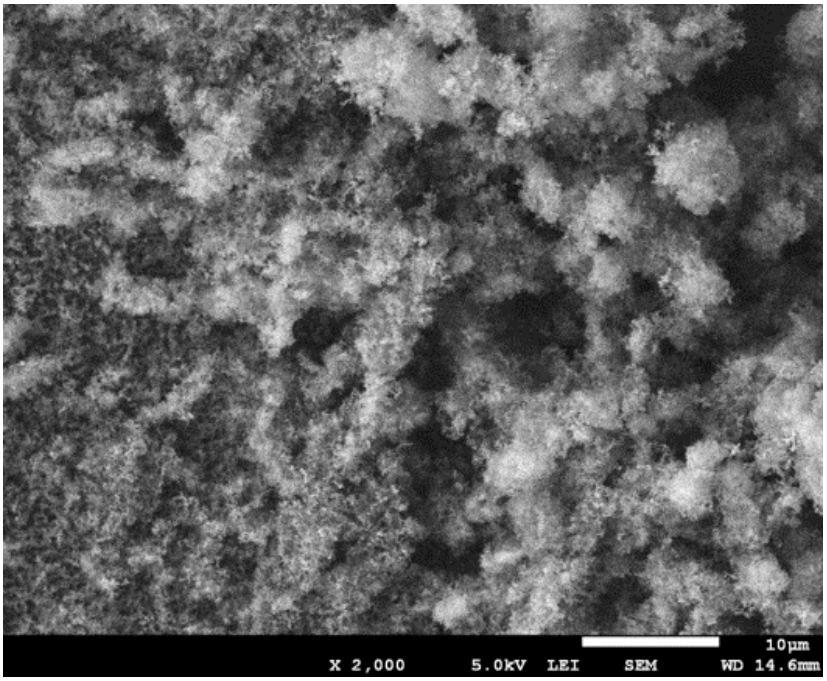


(i) Carbon black CB5303

**Figure 12. SEM Images of Graphite Powders (Continued).**

### 3.3 PHYSICAL PROPERTIES OF OTHER MATERIALS

The research team used several materials for the experiment and investigated their properties. For fixing asphalt mastic specimens in a thin film form, the researchers used wood sticks as a non-conductive base. The electrical volume resistivity of pinewood ranges from $10^{14}$ to $10^{16}$ ($\Omega \cdot m$) and varies with the moisture content. The wood base was heated in the oven for 24 hours to remove moisture. Asphalt concrete is a mixture of coarse aggregate, fine aggregate, filler, and binder. In this study, the conductive additives are considered to replace traditional fillers to minimize the effect on the skeleton structure of asphalt concrete. As the traditional filler for manufacturing the control specimens, Type II Portland cement was used. Silver paste and copper tape were used as the electrodes for measuring the electrical resistivity.

Three different performance-grade binders (PG 64-22, PG 58-22, and PG 70-22) were selected to investigate the effects of binder grade on electrical resistivity. PG 64-22 and PG 58-22 are produced from different crude oils, while PG 70-22 is a modified binder of PG 64-22. The modifiers used for PG 70-22 are 2 percent Styrene-Butadiene-Styrene (SBS) and 0.5 percent sulfur. Table 3 lists the physical properties of the materials used in the research.

**Table 3. Materials Used for Research.**

| Material | Typical Size | Density | Thermal Conductivity (W/mK) | Electrical Resistivity (Ω·m) | Note |
|---|---|---|---|---|---|
| Coarse aggregate | 4.75 mm–25 mm | Specific gravity 2.57 g/cc | 1.25–1.75 | $10^9$ | |
| Fine aggregate | 0.075 mm–4.75 mm | Specific gravity 2.63 g/cc | 1.25–1.75 | $10^9$ | |
| Fillers | < 0.075 mm | Specific gravity 3.15 g/cc | 0.29 | $10^9$ | Type II Portland cement measured temp.: 25°C |
| Binder | Liquid | 1.032 g/cm$^3$ | | | Jebro, Inc. PG 76-22/PG 70-22 PG 64-22/PG 58-22 |
| Wood stick | 1″×2″×8′ | 400–420 kg/m$^3$ | 0.12 W/mK | $10^{14}$–$10^{16}$ | Radiata Pine Claymark, Inc. |
| Silver paste | Particle size: 0.4–1.0μm | Specific gravity 2.25g/cc$^3$ | - | Sheet resistance 0.02–0.05 ohms/sq/mil (25 μm) | Ted Pella, Inc. |
| Copper tape | W: 6.3 mm L: 16.46 m T: 2.4 mils (66 μm) | 8.94kg/cm$^3$ | - | Sheet resistance (ohms/sq): 0.001 | Ted Pella, Inc. |

# 4. ELECTRICAL CONDUCTIVITY OF ASPHALT MASTIC

## 4.1 INTRODUCTION

The literature review highlighted the possible applications of electrically conductive asphalt and some of the attempts of previous investigators. Steel wool, steel fibers, carbon fibers, and some anonymous types of graphite have been used as the conductive additive to impart conductivity. Among these additives, graphite showed the possibility for precise conductivity control—a gradual drop in resistivity with increasing graphite content. The present study focuses on the effect of various types of graphite on controlling the conductivity of asphalt composites. In this section, the test procedure, specimen preparation, and test results for asphalt mastic are presented. In addition, mixing difficulties observed in certain graphite types are discussed.

## 4.2 MATERIALS AND EXPERIMENTS—ELECTRICAL AND VISCOELASTIC

The asphalt mastic specimens were prepared using PG 70-22 asphalt binder (ASTM International 2007b) and various combinations of conductive and non-conductive fillers. The density of the binder is 1.032 g/cm$^3$.

The asphalt mastics are composed of 50 percent asphalt binder and 50 percent filler by weight. This proportion was kept constant throughout the experiment. The research team used Type II Portland cement as the non-conductive traditional filler. Graphite or carbon black replaced part of the cement filler in the mastic specimens and ranged from 10 percent to 50 percent by weight of the mastic. For example, when the graphite content is 20 percent, cement content is 30 percent to maintain the 50 percent filler content in the mastic.

Figure 13(a) shows that the mastic specimens were prepared in thin film shape. Dry pinewood was used as a base for spreading the asphalt mastic. The wooden base blocks were coated with heat-resistant epoxy to prevent the absorption of asphalt binder. The wood, binder, and filler were conditioned at 150°C for 2 hours in the oven before mixing. Once the materials were heated, the binder and filler (a combination of cement and graphite with various proportions) were mixed manually by hand for 3–5 minutes to ensure uniform and complete dispersion of the filler in the mastic. The mastic was then spread on the epoxy-coated wooden blocks. The researchers measured the average thickness of the mastic by reading the weight of

the wooden block before and after spreading the mastic. Once they found the weight of the mastic on the wooden block, they divided this weight by the density of mastic and the spread area to obtain its average thickness. The density of the mastic was estimated using the individual densities of the binder, cement, and graphite, and their respective weight proportions in the mastic. For each type and content of graphite, three mastic specimens were prepared to improve the reliability of the results.

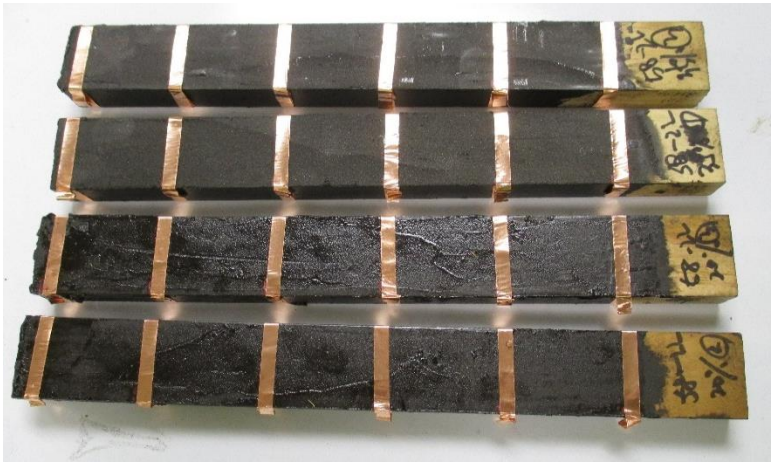

(a) Mastic specimens

(b) Resistivity measurement setup: Solartron 1296 and 1260A

**Figure 13. Experimental Setup for Measuring Electrical Property.**

The mastic specimens were conditioned at room temperature for 8 hours before testing. Figure 13(a) shows that copper tape was installed at every 50 mm and was used as electrodes.

Silver paste was painted between the mastic and copper tape to ensure full contact between these items. The research team used the two-point sensing method to measure impedance of the mastic specimens. Because of the copper tape at various locations on the specimen, the researchers were able to select different combinations of electrodes (i.e., the distance between electrodes can be 50 mm, 100 mm, or 200 mm) and to observe the impedance change with distance.

Figure 13(b) shows the Solartron 1260A and 1296 that the research team used to measure the resistance of the specimens. The Solartron 1260A can measure resistance only up to 100 MΩ. To extend the measurable range up to 100 TΩ, the Solartron 1296 was combined with the 1260A. The electrical impedances of the specimens were measured at 0.1 V with an AC frequency sweep ranging from 0.01 Hz to 1000 Hz. Once the resistances were obtained, the volume resistivity was calculated using Equation (1):

$$\rho = R\,\frac{A}{L} \qquad \textbf{Eq. (1)}$$

where ρ is the volume resistivity measured in ohm·centimeter (Ω-cm); *R* is the resistance in ohm (Ω) obtained from the experiment; *A* is the cross-sectional area of the mastic in square centimeters; and *L* is the distance between the electrodes in centimeters. The electric field is assumed to be constant, and the end effect is assumed to be negligible.

Figure 14 shows the DSR that was used to obtain the rheological parameters of the mastics at intermediate and high temperatures. The tests are conducted in accordance with American Association of State Highway and Transportation Officials T315, and the investigators obtain complex shear modulus (|G*|) and phase angle of binder (δ). |G*| represents the stiffness of a binder that includes the contribution of elastic property and viscous property of an asphalt. δ represents the contribution of viscosity in the viscoelastic behavior of asphalt binder. In the DSR test, the asphalt specimen was placed between two plates (see Figure 14[a]). The bottom plate was fixed, while the top one was oscillating with a frequency of 10 radians per second. The diameter of the mastic sample was 25 mm.

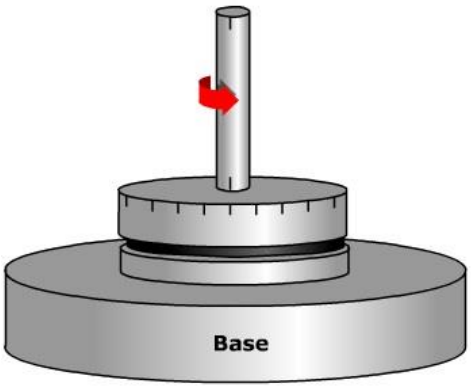


(a) DSR plates


(b) DSR test equipment

**Figure 14. Experimental Setup for Measuring Viscoelastic Property.**

## 4.3 RESULT AND DISCUSSION

### Effect of Steel Fiber on Electrical Conductivity

Prior to the tests for the graphite, the effect of steel fibers on the electrical conductivity was demonstrated. Figure 15 shows the conductivity measurements for the specimens containing 30-mm steel fibers. The electrical resistance was measured using AC current for the frequency range from 0.1 to 106 Hz. The flat line at the bottom is the resistance of the specimen containing 1.5 percent steel fibers. As shown in the figure, when the conductivity of the material is in the measurable range, the measured resistivity is constant over the frequency range. The other three lines in Figure 15 show a typical signal pattern for non-conductive materials. For those,

resistance fluctuates up to 100 Hz and exceeds 100 MΩ, which is the measurable limit of the Solartron 1260A. In addition, the resistances drop as the frequency rises above 100 Hz. Such a signal pattern indicates that the resistance of the material is above the measurable range.

Figure 15 implies that only the specimen containing 1.5 percent steel fiber passes over the percolation threshold. The steel fibers in the specimen form continuous conductive paths by contacting each other, making the material conductive. The result supports the physical explanation of the percolation threshold illustrated in Figure 3, and implies that conductivity cannot be manipulated only with conductive fibers.

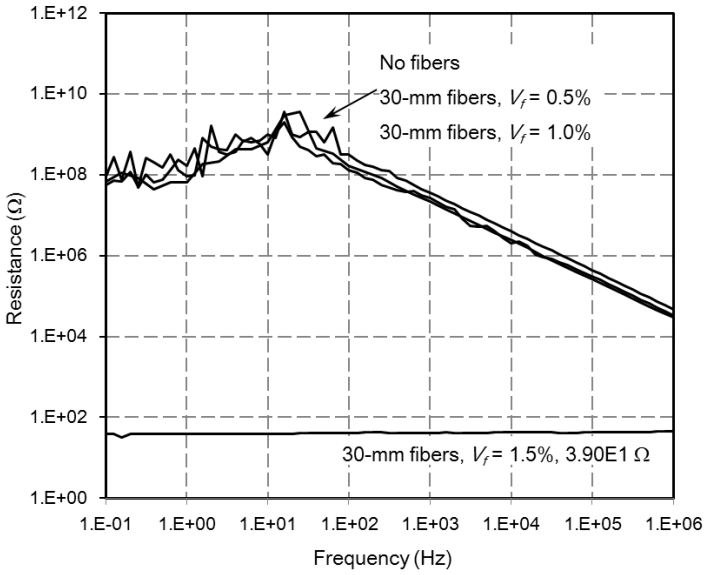


**Figure 15. Electrical Resistance of Asphalt Concrete Containing 30-mm-Long Steel Fibers.**

### Effect of Graphite Types on Electrical Conductivity

Figure 16 compares the variations of electrical resistivities with the contents of conductive additives for the eight different graphite types and carbon black. The research team obtained approximately 24 readings for each mastic specimen. The figure shows that the mastic resistance varies with the type of graphite. The specimens with the flake-type graphite (F146, F3204, and F515) display the lowest conductivity, whereas the mastics with amorphous graphite (505 and 508) still remain non-conductive at 40 percent content. These results can be compared with the particle shape of graphite observed from the SEM analysis. The thin plate shape of the flake-type graphite particles is similar to the ideal crystal structure of graphite and allows super-

conductivity along the flat surface. On the other hand, the irregular shapes of the amorphous graphite particles seem to work as a barrier against the flow of electrons, leading to poor conductivity. These graphs demonstrate the importance of selecting the proper type of graphite for imparting conductivity.

As shown in Figure 16(a) through (c), the resistance gradually decreases with the increase of the graphite content. A relatively rapid drop in resistivity exists between 13 and 16 percent (F146 and F3204) or 10 and 13 percent (F516) by mastic volume; after that point, the resistivity drops gradually from $10^5$ Ω·cm and reaches resistivity at about $10^2$ Ω·cm. This implies that the electrical resistivity can be controlled within the range of $10^2$–$10^5$ Ω·cm, and sufficiently low conductivity ($10^{-2}$/Ω·cm) can be obtained only by using graphite.

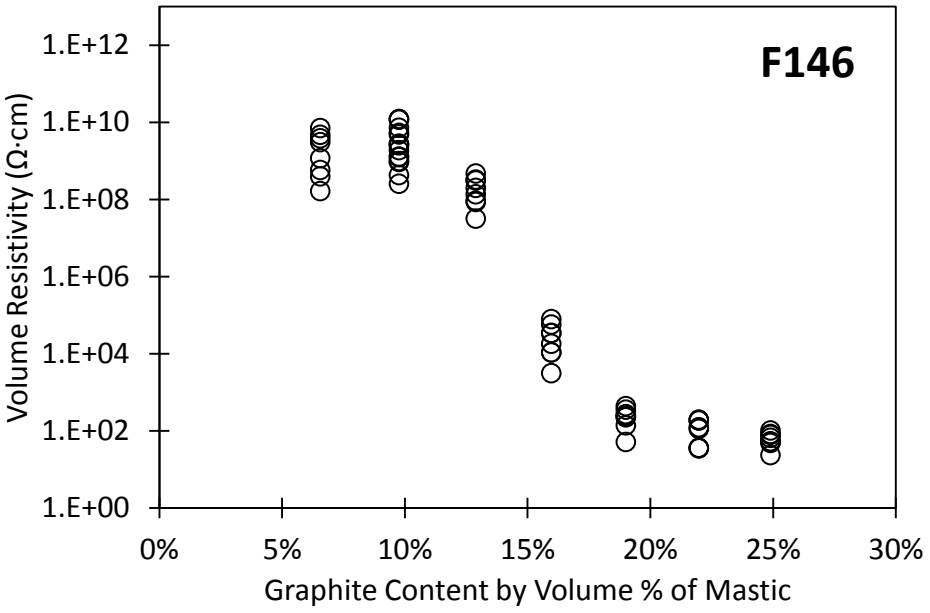


(a) Flake graphite F146

**Figure 16. Electrical Resistivity of Asphalt Mastics Containing Various Graphite Types.**

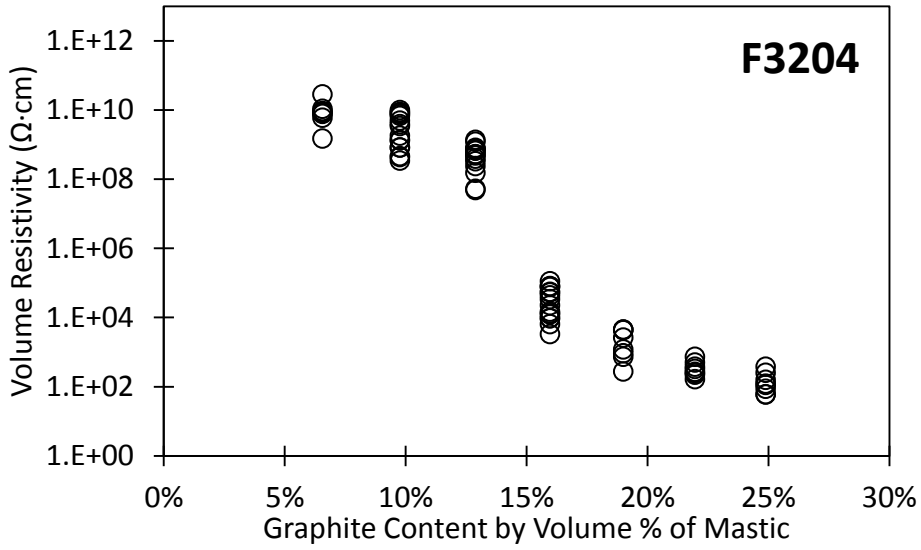


(b) Flake graphite F3204

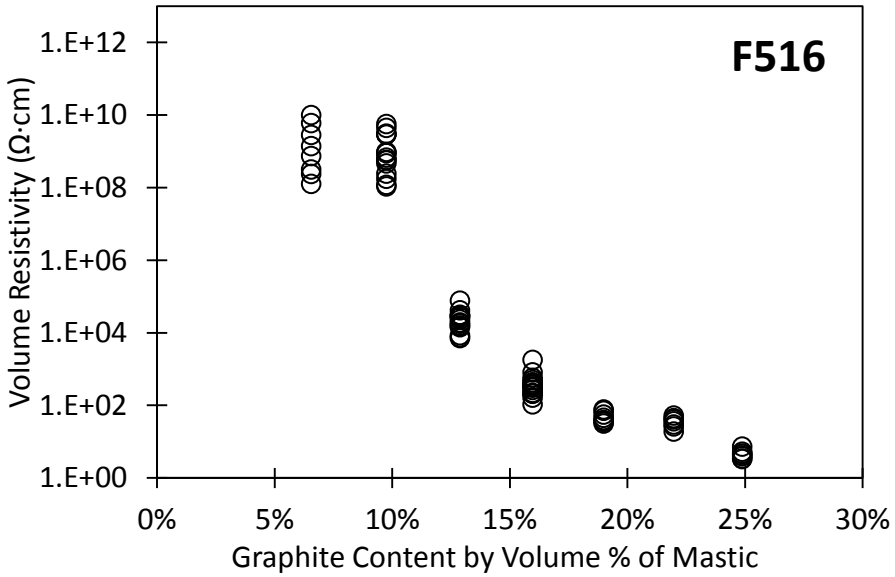


(c) Flake graphite F516

**Figure 16. Electrical Resistivity of Asphalt Mastics Containing Various Graphite Types (Continued).**

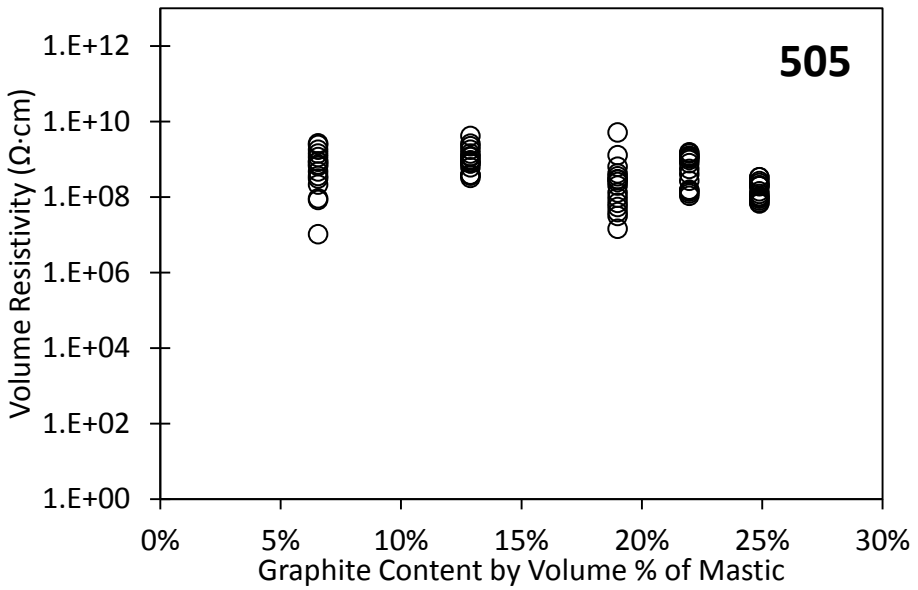


(d) Amorphous graphite 505

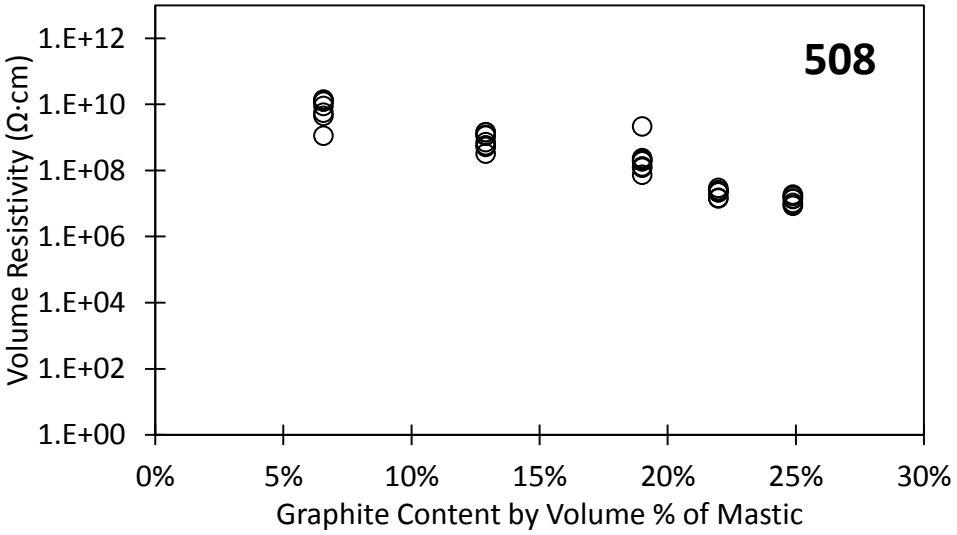


(e) Amorphous graphite 508

**Figure 16. Electrical Resistivity of Asphalt Mastics Containing Various Graphite Types (Continued).**

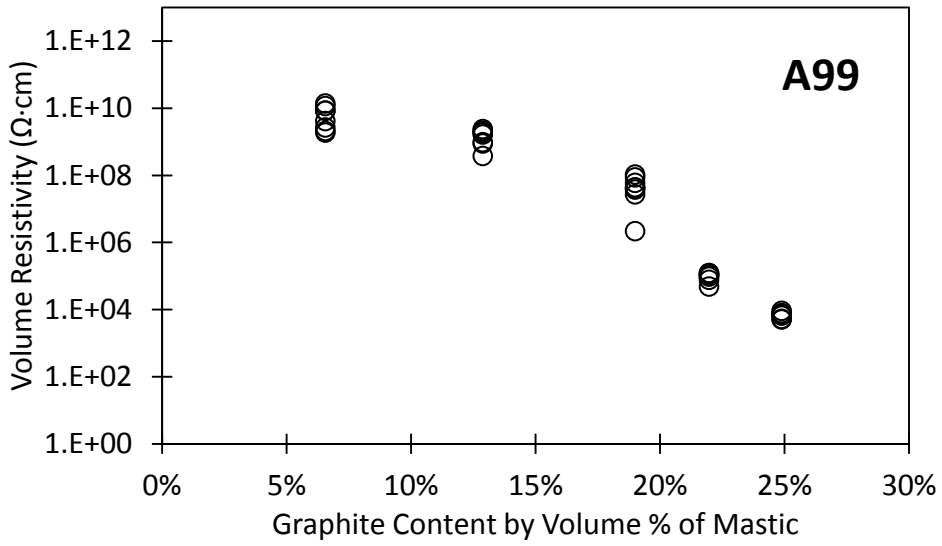


(f) Artificial graphite A99

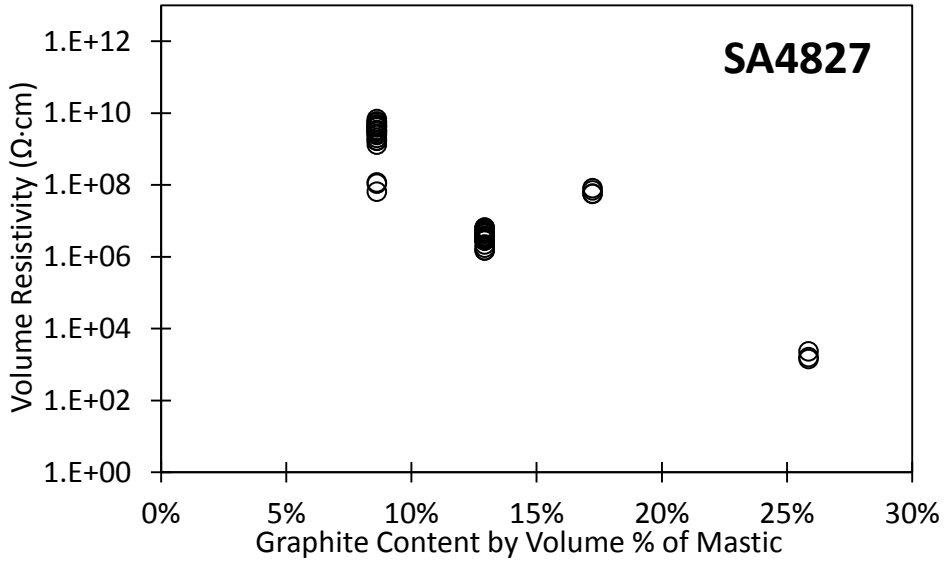


(g) Ultra-high-surface-area graphite SA4827

**Figure 16. Electrical Resistivity of Asphalt Mastics Containing Various Graphite Types (Continued).**

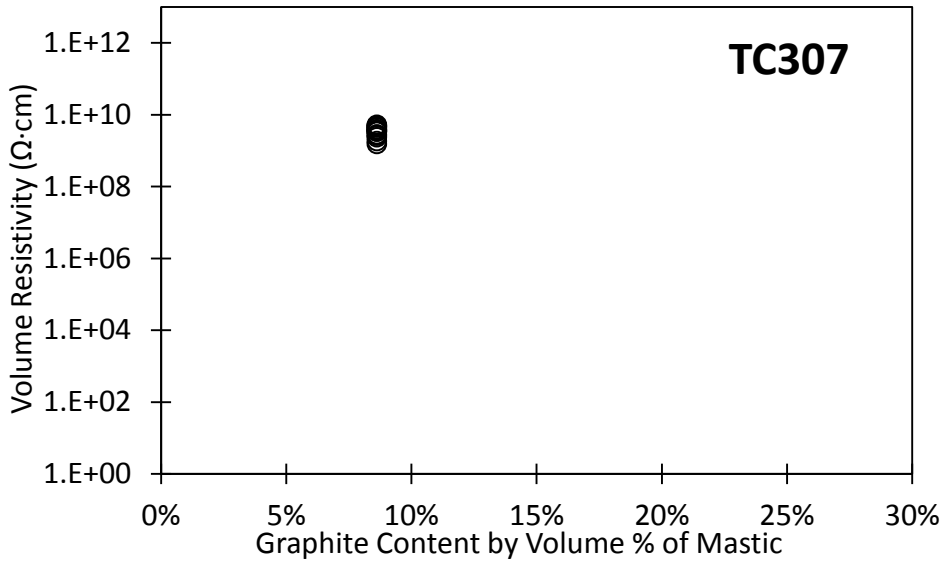


(h) High-surface-area graphite TC307

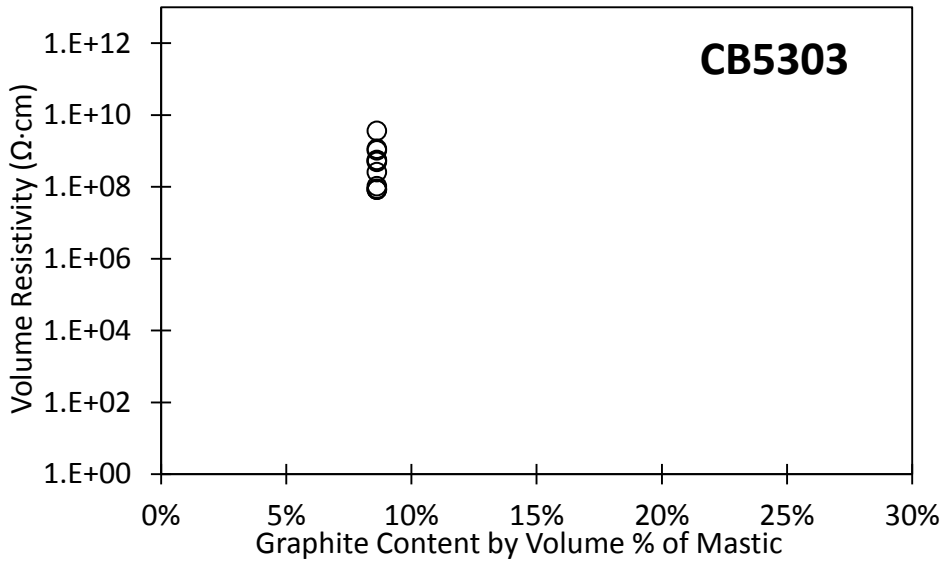


(i) Carbon black CB5303

**Figure 16. Electrical Resistivity of Asphalt Mastics Containing Various Graphite Types (Continued).**

Figure 17 summarizes the measured electrical resistivity. Each dot in the figure represents the average value of 24 volume resistivity readings. The first noticeable observation is the similar trends in resistivity of all the flake-type graphite. As noted earlier, the gradual resistivity that dropped to sufficiently low levels implies the possibility of precise conductivity

control with the flake-type graphite. The amorphous and artificial types of graphite proved ineffective in improving conductivity. The specimens have high volume resistivity even at high content.

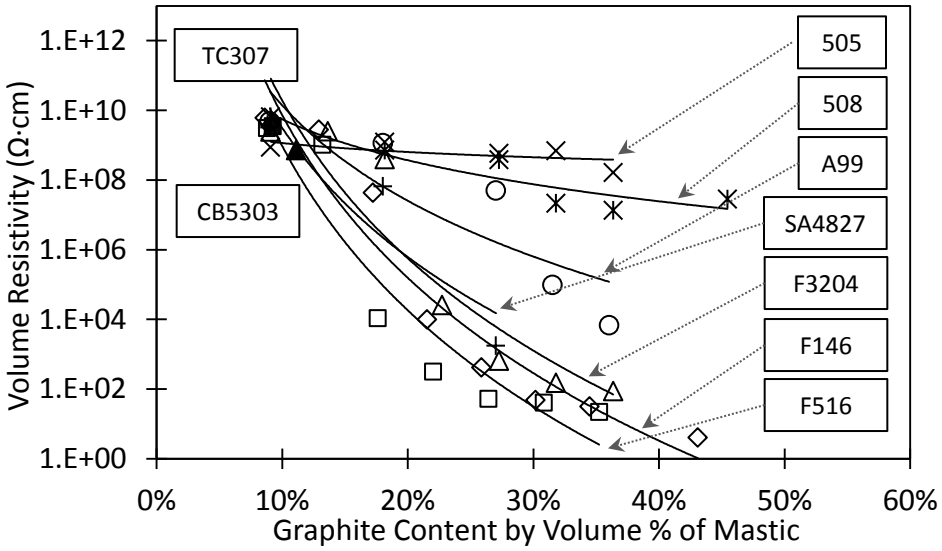


**Figure 17. Comparison of Volume Resistivity of Various Graphite Types.**

Mixing difficulty was observed with the high-surface-area graphite. The mastics became thick and sticky beyond a certain concentration. Specimens with SA4827 graphite were prepared with up to 18 percent by volume graphite content because of the mixing difficulty. TC307 and CB5303 were even harder to mix, and specimens with only 7 percent by volume graphite content were prepared. This limits the use of this type of graphite. The mastics containing flake-type graphite (F146, F3204, and F516) also became sticky as the concentration in the mastic increased. However, in the mixing of asphalt concrete including aggregate, no significant difficulty was observed with high concentrations of graphite. The artificial type, A99, produced a watery mix that was easier to spread on the wood than the other graphite types. In contrast, the amorphous types 505 and 508 were difficult to mix beyond a graphite content of 18 percent by volume of the mastic.

**DSR Test Results**

The DSR test measured the complex shear modulus (|G*|) and phase angle (δ) of the mastics. The mastics containing the traditional filler (cement) and F516 graphite with various proportions were tested at three different temperatures (64°C, 70°C, and 76°C).

Figure 18 shows that the complex modulus (|G*|) increases as the graphite content increases. On the other hand, the phase angle (δ) of the mastic is not affected as significantly as |G*|. Figure 19 shows that δ drops slightly (22–25 percent by volume) at high graphite content. Correspondingly, |G*| · Sinδ (Figure 20) and |G*|/Sinδ (Figure 21) show a trend similar to that in Figure 18. This implies that graphite can improve rutting resistance but may reduce fatigue resistance.

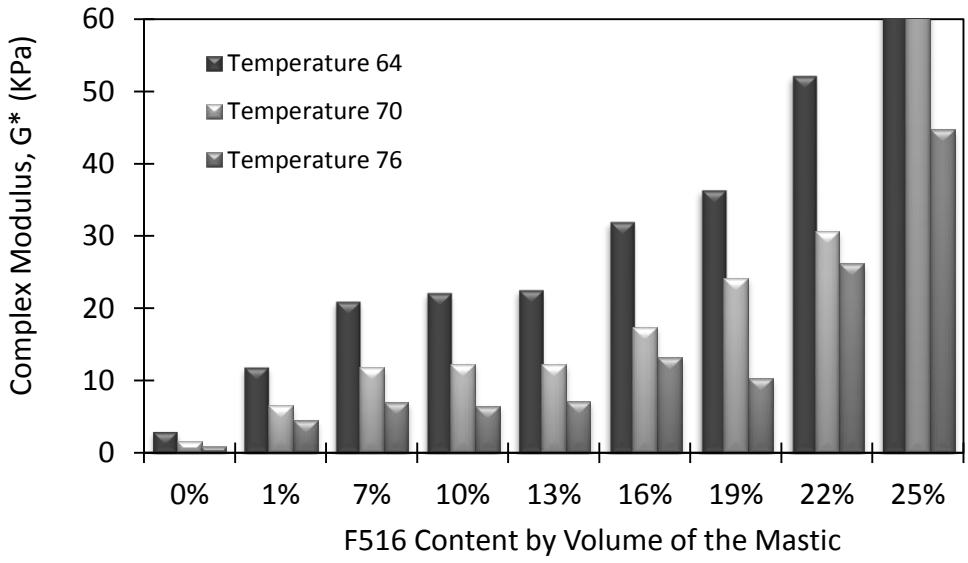


**Figure 18. Variation of Complex Modulus with Graphite Contents.**

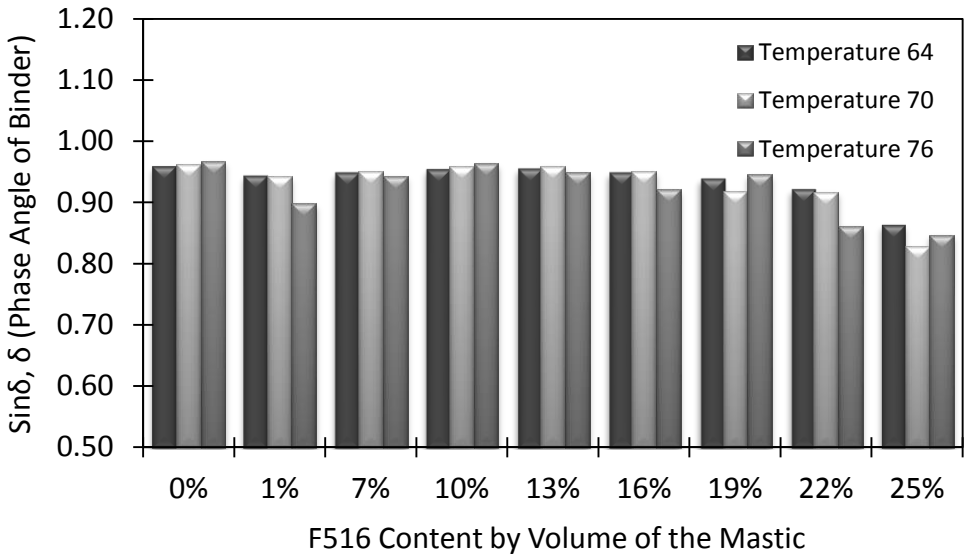


**Figure 19. Variation of Phase Angle with Graphite Contents.**

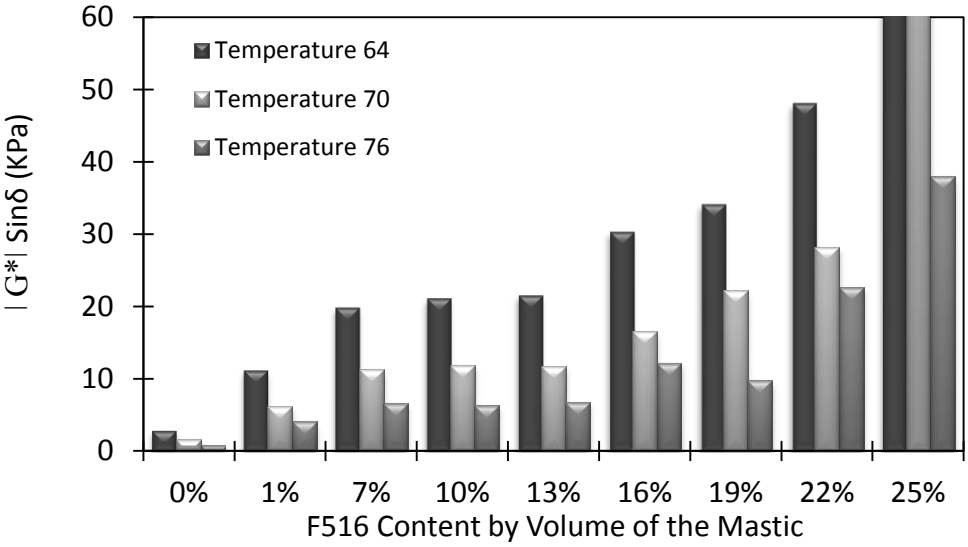


**Figure 20. Variation of |G*| · sinδ (KPa) with Graphite Contents.**

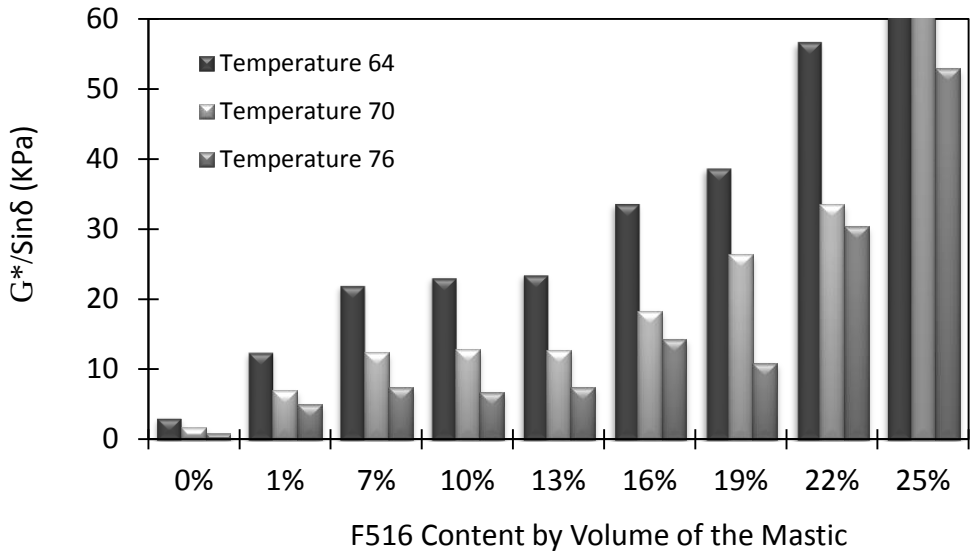


**Figure 21. Variation of G*/sinδ (KPa) with Graphite Contents.**

**Effect of Different Binder Types**

To find the effect of different binder grades for the electrical properties, the research team prepared asphalt mastic specimens with PG 70-22, PG 64-22, and PG 58-22 binders. These specimens also contain various proportions of F516 graphite and non-conductive fillers.

Figure 22 illustrates the resistivity data obtained from three types of binder grade. The three cases do not show clear differences. To examine the effect of binder types more closely, the researchers selected the data for the conductive range (16–22 percent graphite by volume of mastic) and plotted their fitting curves (see Figure 23). The fitting curves of PG 64-22 and PG 58-22 are almost identical to each other, while the electrical resistivity of PG 70-22 is approximately one order higher than the others. Considering that PG 64-22 and PG 58-22 are produced from different crude oils, the sources of the binder do not influence the electrical resistivity. PG 70-22 is a modified binder of PG 64-22 with 2 percent SBS and 0.5 percent sulfur. This means that the binder modifiers can be an important factor in controlling electrical conductivity and may increase the volume resistivity.

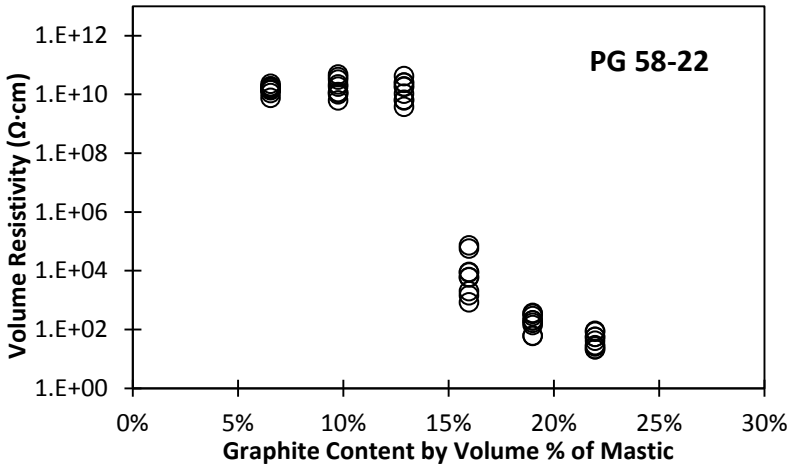


(a) PG 58-22

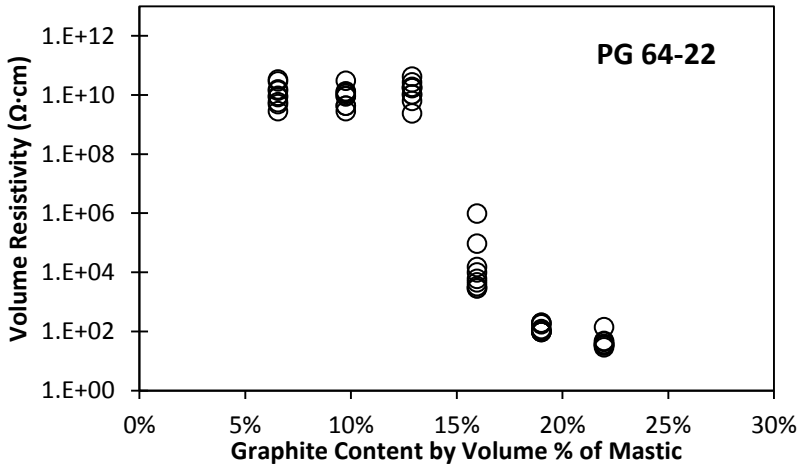


(b) PG 64-22

**Figure 22. Volume Resistivity of Various Binder Types.**

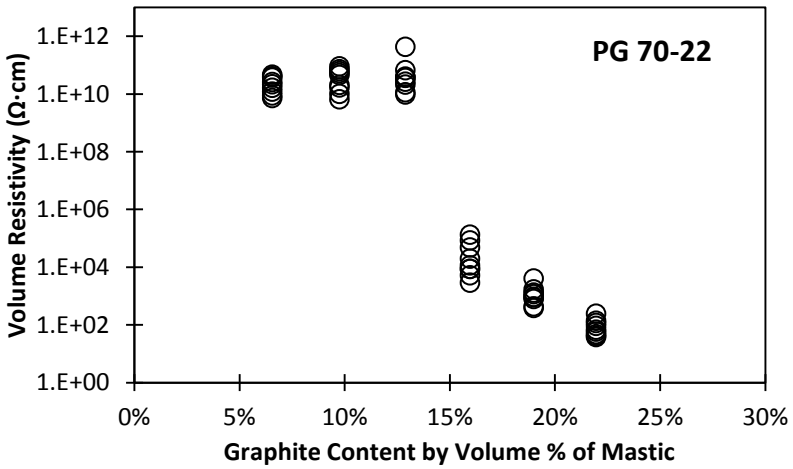


(c) PG 70-22

**Figure 22. Volume Resistivity of Various Binder Types (Continued).**

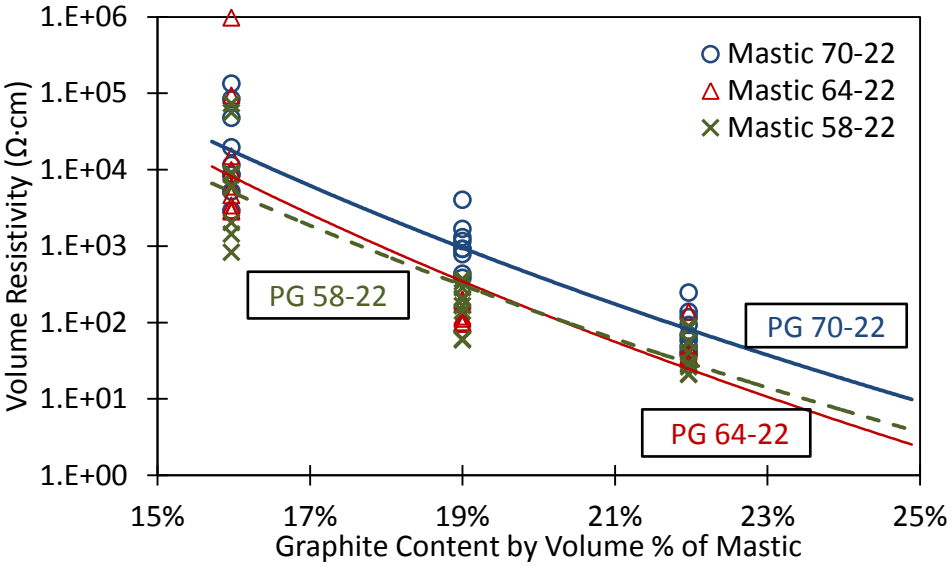


**Figure 23. Effect of Binder Types on Electrical Resistivity**

# 5. ASPHALT CONCRETE TEST

## 5.1 INTRODUCTION

Asphalt concrete is composed of asphalt binder, aggregate, and air voids. Traditional asphalt concrete is a good insulator by nature with resistivity ranging from $10^9$ to $10^{11}$ Ω.cm. From the experiments with asphalt mastics containing various graphite types, the two best performing graphite types (F146 and F516) were selected as conductive additives for asphalt concrete. This section presents the mix design, specimen preparation, test method, and test results of the conductive asphalt concrete.

## 5.2 MATERIALS AND EXPERIMENTS—ELECTRICAL AND MECHANICAL

### Materials and Mix Design

Asphalt concrete specimens were prepared using PG 70-22 asphalt binder (density 1.032 g/cc). The specimens were prepared in accordance with the Superpave mixture design method. Appendix A presents the sieve analysis results of fine and coarse aggregates used in this study. The specific gravities of coarse aggregates, fine aggregates, and filler are measured as 2.57 g/cc, 2.63 g/cc, and 3.15 g/cc, respectively. The research team selected the proportion of coarse and fine aggregates to satisfy mixture requirements specified in ASTM D3515. Table 4 shows the standard aggregate gradations for D-3, D-5, and D-6. In this study, D-6_1 gradation (Table 5) was used to investigate the effect of different gradation types. For D-6_1 gradation, the team used the Superpave method and determined the optimum binder content to be 5.3 percent by weight of the total mixture. Also, the optimum binder contents for D-3, D-5, and D-6_2 gradations were determined to be 4.0 percent, 4.8 percent, and 4.86 percent, respectively, by weight of the total mixture. Appendix Bshows the test data for these optimum binder contents.

**Table 4. Composition of Bituminous Paving Mixtures.**

| | D-3 | D-5 | D-6 |
|---|---|---|---|
| **1½ in.** | 100 | | |
| **1 in.** | 90–100 | | |
| **¾ in.** | | 100 | |
| **½ in.** | 56–80 | 90–100 | 100 |
| **⅜ in.** | | | 90–100 |
| **No. 4** | 29–59 | 44–74 | 55–85 |
| **No. 8** | 19–45 | 28–58 | 32–67 |
| **No. 16** | | | |
| **No. 30** | | | |
| **No. 50** | 5–17 | 5–21 | 7–23 |
| **No. 100** | | | |
| **No. 200** | 1–7 | 2–10 | 2–10 |

**Table 5. Aggregate Gradation.**

| Sieve size (mm) | 37.5 | 25 | 19 | 12.5 | 9.5 | 4.75 | 2.36 | 1.18 | 0.6 | 0.3 | 0.15 | 0.075 |
|---|---|---|---|---|---|---|---|---|---|---|---|---|
| D-3 % passing | 100 | 95 | 87 | 72 | 63 | 45 | 25 | 15 | 11 | 8 | 5 | 5 |
| D-5 % passing | 100 | 100 | 100 | 95 | 88 | 65 | 40 | 20 | 12 | 8 | 5 | 5 |
| D-6_1 % passing | 100 | 100 | 100 | 99.9 | 95.3 | 68.1 | 50.8 | 35.3 | 21.0 | 11.5 | 7.2 | 6.1 |
| D-6_2 % passing | 100 | 100 | 100 | 100 | 95 | 75 | 55 | 35 | 20 | 12 | 5 | 5 |

## Specimen Preparation

The research team conducted specimen preparation and volumetric analysis in accordance with Superpave mixture design and ASTM standards. The aggregates and fillers were heated at 150°C for at least 4 hours to eliminate moisture, and the binder was heated for 2 hours at the same temperature prior to mixing. The researchers first mixed the fillers with aggregates and then added the binder. They used a mechanical mixer to mix the materials until the aggregates and fillers were coated well with the binder. The mixture was then conditioned in the oven at the compaction temperature (135°C).

The researchers used the Superpave gyratory compactor to compact the specimens. Cylindrical specimens measuring 150 mm in diameter and 95 mm in height were compacted with gyration until these reached 4 percent air voids. Figure 24 shows the compacted specimens. For

each test case, the team prepared four cylindrical specimens: three for measuring indirect tensile strength and one for measuring the electrical conductivity. The specimen for electrical conductivity was drilled to make three core samples out of it. This cutting eliminated the error in conductivity measurement by removing the conductive mastic at the side of the specimens.


**Figure 24.Compacted Asphalt Concrete Specimens.**

### Electrical Resistivity Measurement Setup

Copper tape was installed as electrodes at the top and bottom of the core-cut specimens. The rough top and bottom surfaces of the specimen were cut. A highly conductive silver paste was applied on the specimen surface to maintain full contact between the specimen and copper tape. The researchers used the Solartron 1260A and 1296 (Figure 13) to measure the resistance of the specimens. The measured resistance was then converted to volume resistivity corresponding to the dimensions of the specimen. Figure 25 shows the specimens and measurement setup.

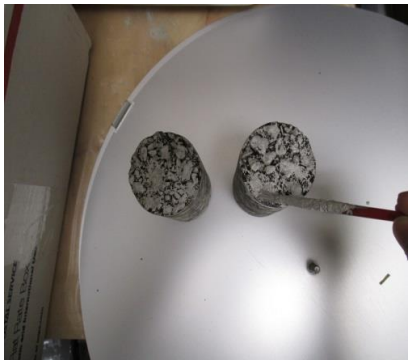

(a) Painting silver paste on top and bottom

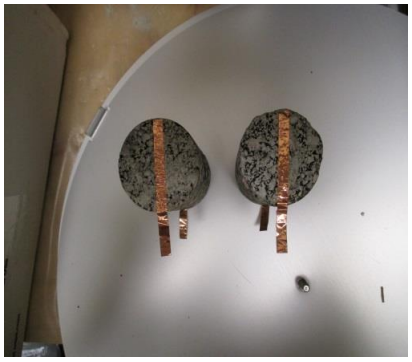

(b) Installing copper tape

surfaces of specimens as electrodes

**Figure 25. Asphalt Concrete Specimens.**

**Indirect Tensile Strength Test**

For each case, the research team conditioned three compacted specimens at room temperature (25°C) before testing. An electromechanical materials testing instrument, Instron 5583, was used for performing the IDT. During the IDT, a monotonic compressive load was applied on the specimen at a constant displacement rate of 50.8 mm/min. (2 in./min.) until fracture. The load and displacement were recorded. The IDT strength was computed as follows:

$$S_T = \frac{2 \times P}{\pi \times t \times D} \quad \textbf{Eq. (2)}$$

where $S_T$ is the IDT strength in MPa, *P* is the maximum load in N, *t* is the specimen height immediately before test in millimeters, and *D* is the specimen diameter in millimeters. The researchers performed the test in accordance with ASTM D6931-07. Figure 26 shows the IDT setup and the fractured specimen.

**Figure 26. Indirect Tension Test Setup.**

## 5.3 RESULTS AND DISCUSSION

### Volumetrics

Four specimens for each case were prepared, and their volumetric properties were evaluated. Table 6 provides the average values of these volumetric properties.

**Table 6. Volumetric Properties of the Mixture.**

| Specimen | Optimum Binder Content (OBC) (%) | Bulk Specific Gravity ($G_{sb}$) (g/cc) | Maximum Specific Gravity ($G_{mm}$) | Bulk Specific Gravity of Compacted Hot Mix Asphalt ($G_{mb}$) | Air Voids (%) | Voids in Mineral Aggregate (VMA) | Voids Filled with Asphalt (VFA) |
|---|---|---|---|---|---|---|---|
| Control Mix | 5.3 | 2.642 | 2.428 | 2.329 | 4.09 | 16.52 | 75.27 |
| F146-20% | 5.3 | 2.625 | 2.394 | 2.298 | 4.01 | 17.09 | 76.57 |
| F146-25% | 5.3 | 2.621 | 2.411 | 2.311 | 4.14 | 16.50 | 74.92 |
| F146-30% | 5.3 | 2.617 | 2.427 | 2.315 | 4.60 | 16.22 | 71.65 |
| F516-10% | 5.3 | 2.633 | 2.415 | 2.316 | 4.10 | 16.44 | 75.06 |
| F516-15% | 5.3 | 2.628 | 2.424 | 2.322 | 4.21 | 16.06 | 73.80 |
| F516-20% | 5.3 | 2.624 | 2.389 | 2.285 | 4.38 | 17.55 | 75.01 |
| F516-25% | 5.3 | 2.620 | 2.402 | 2.302 | 4.19 | 16.79 | 75.07 |
| F516-30% | 5.3 | 2.615 | 2.386 | 2.288 | 4.10 | 17.14 | 76.09 |
| F516-35% | 5.3 | 2.611 | 2.406 | 2.311 | 3.95 | 15.92 | 75.19 |
| F516-40% | 5.3 | 2.606 | 2.423 | 2.331 | 3.80 | 15.02 | 74.73 |
| D-3 Gradation | 4.0 | 2.618 | 2.444 | 2.358 | 4.34 | 15.16 | 71.39 |
| D-5 Gradation | 4.8 | 2.634 | 2.425 | 2.325 | 4.12 | 16.14 | 76.18 |
| D-6 Gradation | 4.9 | 2.638 | 2.465 | 2.354 | 4.50 | 15.23 | 70.43 |
| D-6 25% Gradation | 3.9 | 2.638 | 2.431 | 2.335 | 3.95 | 15.91 | 75.18 |

To determine the effect of various graphite contents, this mixture design was kept constant for the control specimens and the specimens containing graphite. In addition, 5 percent of filler content in the mixture was kept constant, but the proportion of the graphite and traditional filler varies. The contents of graphite were 7 percent, 10 percent, 13 percent, 16 percent, 19 percent, 22 percent, and 25 percent by volume of asphalt mastics, which are 1.1 percent, 1.6 percent, 2.1 percent, 2.6 percent, 3.1 percent, 3.6 percent, and 4.1 percent, respectively, by weight of the total mix. On the other hand, for experiments related to the effect

of aggregate gradation, the researchers chose F516 graphite for the mixture and kept the graphite content at 25 percent of mastic weight.

Most of the specimens have air voids in the 4±0.5 percent (ASTM International 2005) range. The specific gravity of aggregates (coarse aggregate, fine aggregate, and filler), $G_{sb}$, slightly decreases with an increase in graphite content because the density of graphite is lower than that of cement. $G_{mm}$ and $G_{mb}$ are the theoretical and bulk-specific gravity of the mixture, respectively. The VMA and VFA are calculated from the following equations:

$$\text{VMA} = 100 - \frac{\text{Gmb} \times \text{Ps}}{\text{Gsb}} \quad \textbf{Eq. (3)}$$

$$\text{VFA} = 100 \times \frac{\text{VMA} - \text{AV}}{\text{VMA}} \quad \textbf{Eq. (4)}$$

where Ps is the percentage of aggregates in the total mixture, and AV is the percent air voids. Table 7 compares the number of gyrations needed to obtain 4 percent target air voids for the specimens with various graphite contents. The control mixture has 56 gyrations, and the number of gyrations increases with increased graphite content. As shown in the mastic DSR test, adding graphite causes an increase in the G* value and results in additional compaction efforts. This means that the mixtures with graphite require extra care in compaction.

The mixtures with F516 (bigger particles) require fewer gyrations to achieve the target air voids than the mixtures with F146 when the same amount of graphite is added.

**Table 7. Average Number of Gyrations for Different Mixes.**

| Specimen | Number of Gyrations | Specimen | Number of Gyrations |
|---|---|---|---|
| Control Mix | 56 | F516-30% | 127 |
| F146-20% | 48 | F516-35% | 159 |
| F146-25% | 110 | F516-40% | 192 |
| F146-30% | 232 | D-3 Gradation | 75 |
| F516-10% | 41 | D-5 Gradation | 75 |
| F516-15% | 52 | D-6 Gradation | 75 |
| F516-20% | 77 | D-6_25% Gradation | 75 |
| F516-25% | 98 | | |

**Electrical Resistivity Test**

Figure 27 shows the variation of volume resistivity of asphalt concrete specimens and asphalt mastic specimens containing F146 graphite. Figure 28 represents volume resistivity according to the F516 graphite content of the specimens. The lines in Figure 27 and Figure 28 show the volume resistivity from the asphalt mastic specimens. In Figure 28, the volume resistivity of the control mixture (no graphite) is $1.03 \times 10^{13}$ Ω.cm. The specimens with the two types of conductive graphite (F146 and F516) show a similar trend to the mastic test results—resistivity decreases with increased graphite content. Although there are exceptions, the volume resistivity data of asphalt concrete specimens in the conductive range (13–25 percent by volume of mastics) are higher than those of the mastic specimens because of the additional non-conductive volume of aggregate. Appendix C presents all of the electrical resistivity values.

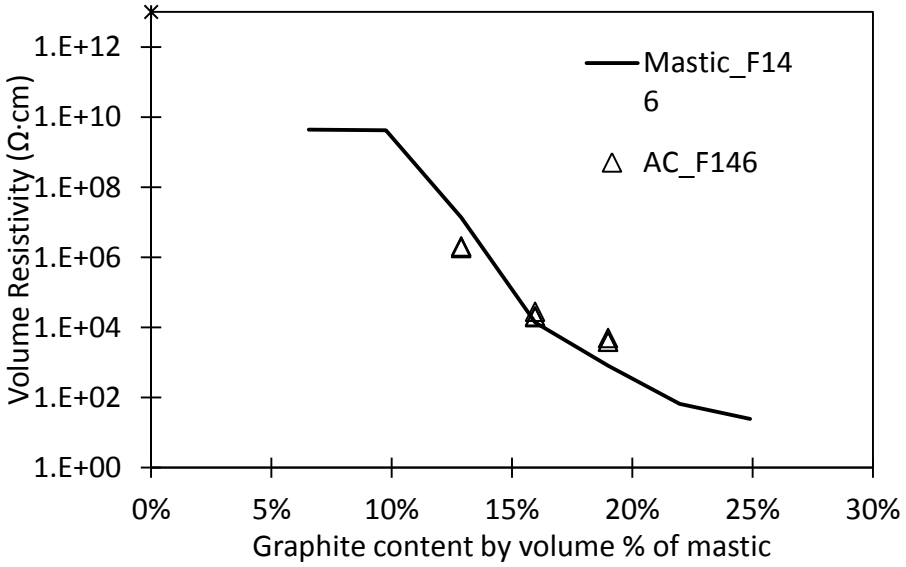


**Figure 27. Volume Resistivity versus F146 Graphite Content for Conductive Asphalt Concrete.**

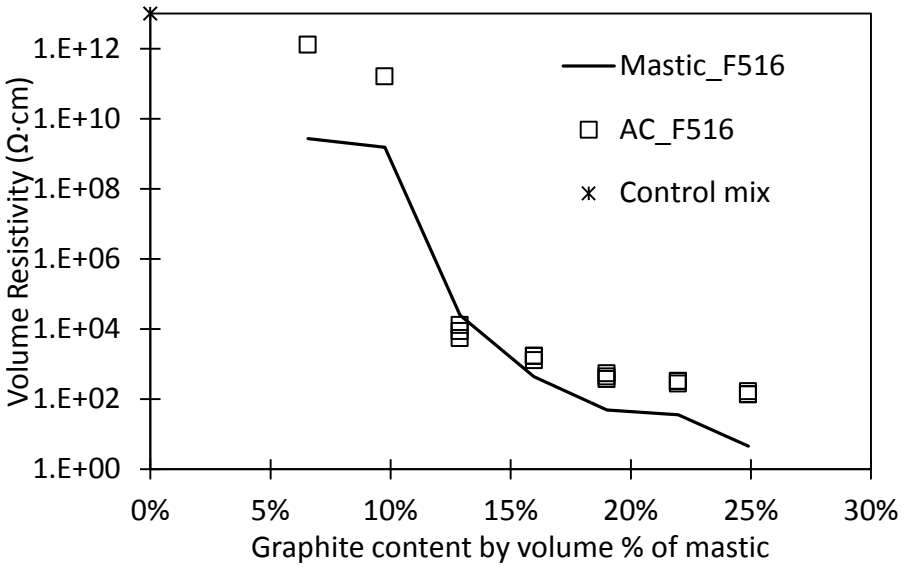


**Figure 28. Volume Resistivity versus F516 Graphite Content for Conductive Asphalt Concrete.**

**Indirect Tensile Strength**

The research team measured the IDT strengths to investigate the effect of adding graphite on the mechanical properties of the conductive asphalt concrete. Figure 29 shows the IDT strength obtained from three specimens for each case. The average IDT strength of the control mixture is 1.12 MPa. The strengths of the specimens containing 13 percent, 16 percent, and 19 percent graphite (in volume in the mastics, equivalent to 2.1 percent, 2.6 percent, and 3.1 percent volume in the mixtures, respectively) are higher than those of other specimens, including the control mixture. The maximum improvement in IDT strength is 41 percent in the specimens containing 16 percent graphite by volume of the asphalt mastic. Addition of more graphite in the mix results in the decrease of IDT strength. This result is similar to the IDT strength results of porous asphalt concrete containing steel fibers (Liu et al. 2010b). Figure 30 shows that the effects of F516 and F146 on the IDT strength are almost identical.

Thus, the addition of 16 percent (by volume of asphalt mastic) F516 to asphalt concrete has sufficiently low electrical resistivity ($1.6 \times 10^3$ Ω.cm) and also improves the mechanical strength of the mix. Considering the efficiency in imparting conductivity and mechanical performance, it can be concluded that flake-type F516 graphite is the best graphite for multifunctional applications. Appendix D presents the load-versus-time curves of all IDT specimens obtained from this experiment.

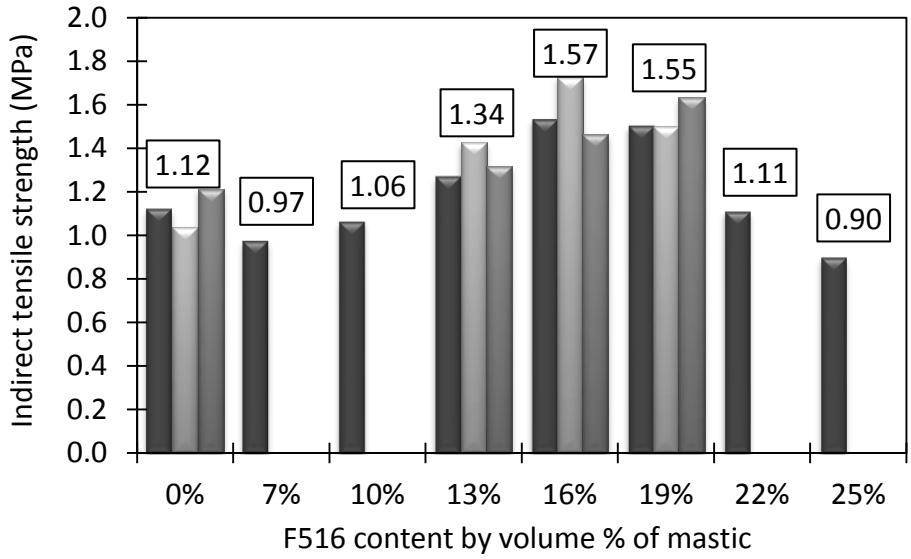


**Figure 29. Effect of Graphite Contents on IDT Strength.**

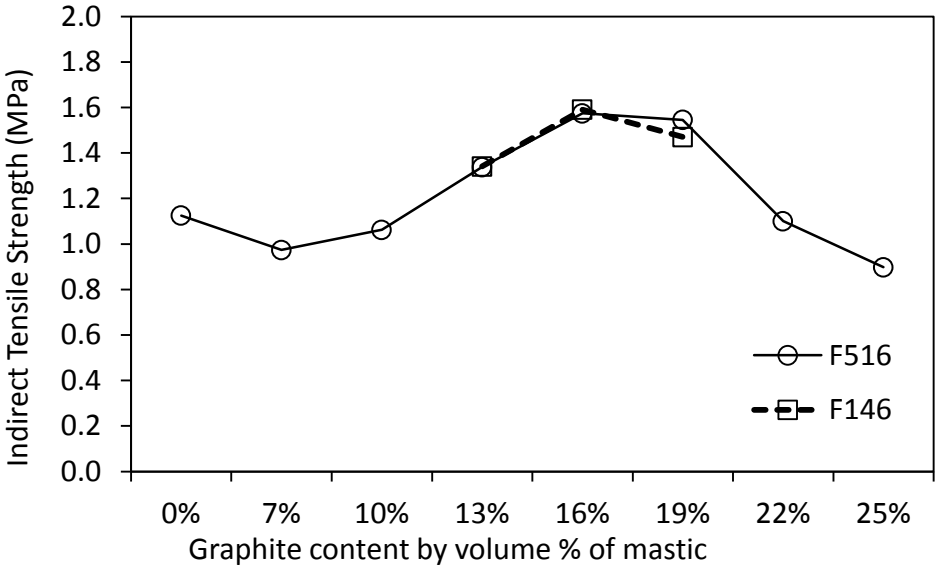


**Figure 30. Comparing IDT Strength of F146 and F516.**

**Electrical Resistivity Test Related to Effect of Gradation**

Figure 31 compares the volume resistivity of asphalt concrete specimens with different aggregate gradations. The volume resistivity of the control mixture (no graphite) of each gradation is almost the same value, $3.01 \times 10^{12}$ Ω.cm, $2.99 \times 10^{12}$ Ω.cm, and $3.17 \times 10^{12}$ Ω.cm. In this test set, the content ratio of the graphite and binder is fixed, but the binder contents vary

according to the optimum binder content test results. The different binder contents cause the slight differences in the volume percent of graphite in the mixture shown in Figure 31. The electrical resistivity increases in the order of D-6, D-5, and D-3 mixtures. Since the D-3 mixture has the biggest maximum aggregate size, it contains the least amount of fine aggregate and binder. Therefore, the results indicate that the electrical resistivity is dependent on the ratio of graphite content to asphalt mortar (fine aggregate and binder). In other words, when the same amount of graphite is added, the specimen containing more coarse aggregates has higher electrical conductivity. Appendix C presents all the electrical resistivity data.

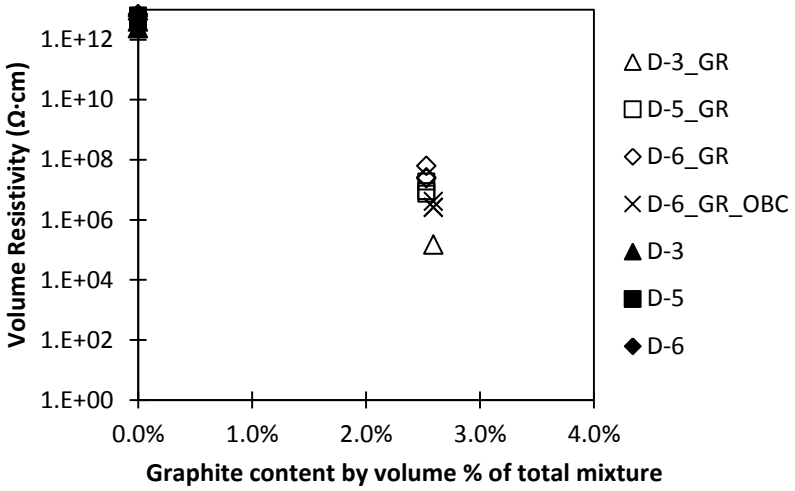


**Figure 31. Comparing Volume Resistivity in Accordance with Gradation Types.**

### Indirect Tensile Strength Related to Effect of Gradation

Indirect tensile strengths (ITSs) are measured to investigate the mechanical effect of graphite in different aggregate gradations. Figure 32 shows the ITSs obtained from three specimens for each case. The ITS of the control mixture for each gradation type are 1.35MPa (D-3), 1.24MPa (D-5), and 1.5MPa (D-6); and the ITSs with graphite (approximately 2.5 percent by mixture volume) are 1.55MPa (D-3_GR), 1.55MPa (D-5_GR), and 1.83MPa (D-6_GR), respectively. The improvement in ITS for each case is about 20 percent, with D-6 having the greatest rate at 32 percent and containing the highest amount of fine aggregate.

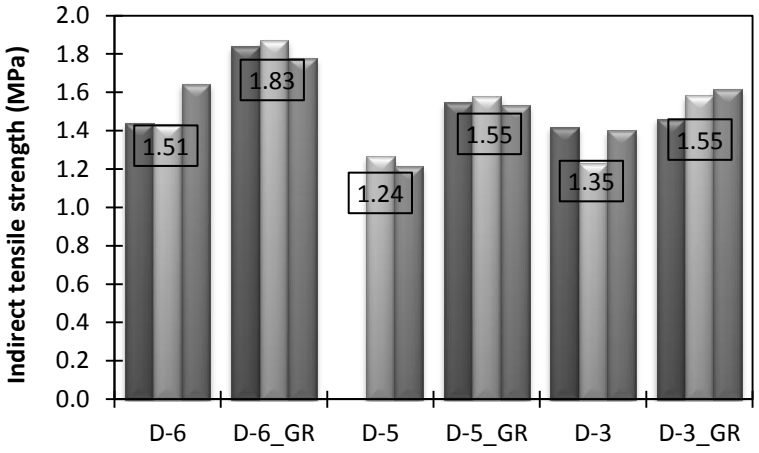


**Figure 32. Effect of Graphite Contents on IDT Strength of Conductive Asphalt Concrete.**

# 6. CONCLUSIONS AND SUMMARY

The effects of graphite additives on the electrical conductivity and mechanical properties of asphalt concrete were investigated in this study. The electrical volume resistivity of the mastic specimens containing various types and contents of graphite was examined, and the physical/geometrical properties of the graphite particles were evaluated through the SEM analysis. From the mastic test results, two graphite types were selected and added to the asphalt concrete. The conductivity of these asphalt concrete samples was compared with that of asphalt mastics. The effects of binder type and aggregate gradation were investigated as well.

Major findings from the study are listed as follows:

- A sudden change in electrical resistivity from no conduction to conduction, i.e., the so-called percolation threshold, is observed in specimens containing steel fibers. Achieving this threshold implies that the steel fibers form conductive paths, which behave like a switch. Therefore, it is difficult to manipulate the electrical resistivity of asphalt concrete only with fibers.
- The electrical conductivity of asphalt mastics varies significantly with the type of conductive fillers. Natural flake graphite powder is the most efficient in imparting conductivity into asphalt. Sufficiently low electrical resistivity can be obtained by replacing a part of the fillers with the flake-type graphite powder in asphalt mastics.
- The volume resistivity of asphalt mastic and asphalt concrete containing natural flake graphite powder varies widely with the amount of graphite powder mixed in the mastic. The graphite does not completely eliminate the percolation threshold but substantially mitigates it. This implies that the electrical resistivity of asphaltic composite can be manipulated over a wide range of resistivity.
- The different binder types do not have significant influence on the electrical conductivity of asphalt mastics, but binder modifiers may reduce electrical conductivity.
- When a fixed amount of graphite is added to the mixture, using less fine aggregate and binder results in higher electrical conductivity.
- The conductive asphalt concrete containing the flake-type graphite has improved ITS when compared to the control asphalt concrete. DSR tests for asphalt mastic show

that the flake-type graphite additives increase complex modulus. This implies that adding graphite is beneficial for improving rutting resistance.

Flake graphite exhibits good electrical conductivity along with mechanical performance. As discussed in the previous chapters, the stepwise decrease in electrical resistivity of this conductive asphalt concrete can be used for various multifunctional applications.

# REFERENCES


Abtahi, S. M., M. Sheikhzadeh, and S. M. Hejazi (2010). "Fiber-Reinforced Asphalt-Concrete—A Review." *Construction and Building Materials*, 24 (6), pp. 871–877.

American Society for Testing and Materials (2000) (reapproved 2004). "Standard Specification for Coarse Aggregate for Bituminous Paving Mixtures." *ASTM D692-00,* West Conshohocken, PA.

Asbury Carbons (2013). *Materials*. http://asbury.com/materials/graphite/.

ASTM International (2001). "Standard Specification for Hot-Mixed, Hot-Laid Bituminous Paving Mixtures." *ASTM D3515-01,* West Conshohocken, PA.

ASTM International (2003). "Standard Test Method for Theoretical Maximum Specific Gravity and Density of Bituminous Paving Mixtures." *ASTM D2041-03,* West Conshohocken, PA.

ASTM International (2005). "Standard Test Method for Percent Air Voids in Compacted Dense and Open Bituminous Paving Mixtures." *ASTM D3203-05,* West Conshohocken, PA.

ASTM International (2006). "Standard Test Method for Sieve Analysis of Fine and Coarse Aggregates." *ASTM C136-06,* West Conshohocken, PA.

ASTM International (2007a). "Standard Specification for Fine Aggregate for Bituminous Paving Mixtures." *ASTM D1073-07,* West Conshohocken, PA.

ASTM International (2007b). "Standard Specification for Performance Graded Asphalt Binder." *ASTM D6373-07,* West Conshohocken, PA.

ASTM International (2007c). "Standard Test Method for Bulk Specific Gravity and Density of Compacted Bituminous Mixtures Using Coated Samples." *ASTM D1188-07,* West Conshohocken, PA.

ASTM International (2007d). "Standard Test Method for Indirect Tensile (IDT) Strength of Bituminous Mixtures." *ASTM D6931-07*, West Conshohocken, PA.

Azhari, F., and N. Banthia (2012). "Cement-Based Sensors with Carbon Fibers and Carbon Nanotubes for Piezoresistive Sensing." *Cement and Concrete Composites*, 34 (7), pp. 866–873.

Baeza, J. F., D. D. Chung, E. Zornoza, L. G. Andion, and P. Carces (2010). "Triple Percolation in Concrete Reinforced with Carbon Fiber." *ACI Material Journal*, 107 (4), pp. 396–402.

Banthia, N. (1992). "Electrical Resistivity of Carbon and Steel Micro-fiber Reinforced Cements." *Cement and Concrete Research*, 22 (5), pp. 804–814.

Barnard, E. H. (1965). “Electrically Conductive Concrete.” U.S. Patent 3,166,518.

Blackburn, R. R., K. M. Bauer, D. E. Amsler, Sr., S. E. Boselly III, and A. D. McElroy (2004). *NCHRP Report 526: Snow and Ice Control: Guidelines for Materials and Methods*. Transportation Research Board, National Cooperative Highway Research Program, Washington, DC.

Bommavaram, R. R., A. Bhasin, and D. N. Little (2009). “Determining Intrinsic Healing Properties of Asphalt Binders.” *Transportation Research Record*, 2126 (1), pp. 47–54.

Bonnaure, F. P., A. H. Huibers, and A. Boonders (1982). “A Laboratory Investigation of the Influence of Rest Periods on the Fatigue Characteristics of Bituminous Mixes.” *Journal of the Association of Asphalt Paving Technologists*, 51, pp. 104–128.

Cao, J., S. Wen, and D. D. L. Chung (2001). “Defect Dynamics and Damage of Cement-Based Materials, Studied by Electrical Resistance Measurement.” *Journal of Materials Science*, 36 (18), pp. 4351–4360.

Chacko, R., and N. Banthia (2007). “Carbon Fiber Reinforced Cement Based Sensors.” *Canadian Journal of Civil Engineering*, 34 (3), pp. 284–290.

Chen, B., and J. Liu (2007). “Damage in Carbon Fiber-Reinforced Concrete, Monitored by Both Electrical Resistance Measurement and Acoustic Emission Analysis.” *Construction and Building Materials*, 22 (11), pp. 2196–2201.

Chen, B., K. Wu, and W. Yao (2004). “Conductivity of Carbon Fiber Reinforced Cement-Based Composites.” *Cement and Concrete Composites*, 26 (4), pp. 291–297.

Chen, F., M. Chen, S. Wu, and J. Zhang (2012). “Research on Pavement Performance of Steel Slag Conductive Asphalt Concrete for Deicing and Snow Melting.” *Key Engineering Materials*, 509, pp. 168–174.

Chen, P., and D. D. L. Chung (1995). “Improving the Electrical Conductivity of Composites Comprised of Short Conducting Fibers in a Non-conducting Matrix: The Addition of a Non-conducting Particulate Filler.” *Journal of Electronic Materials*, 24 (1), pp. 47–51.

Chiarello, M., and R. Zinno (2004). “Electrical Conductivity of Self-Monitoring CFRC.” *Cement and Concrete Composites*, 27 (4), pp. 463–469.

Chung, D. D. L. (1997). “Self-Monitoring Structural Materials.” *Materials Science and Engineering*, 22 (2), pp. 57–78.

Chung, D. D. L. (1999). "Cement Reinforced with Short Carbon Fibers: A Multifunctional Material." *Composites*, 31 (6), pp. 511–526.

Chung, D. D. L. (2000). "Cement-Matrix Composites for Smart Structures." *Smart Materials and Structures*, 9 (4), pp. 389–401.

Chung, D. D. L. (2002). "Piezoresistive Cement-Based Materials for Strain Sensing." *Journal of Intelligent Material Systems and Structures*, 13 (9), pp. 599–609.

Chung, D. D. L. (2003). *Multifunctional Cement-Based Materials*. Marcel Dekker, Inc., New York, NY.

Chung, D. D. L. (2012). "Carbon Materials for Structural Self-Sensing, Electromagnetic Shielding and Thermal Interfacing." *Carbon*, 50 (9), pp. 3342–3353.

Chung, D. D. L., and S. Wang (2003). "Self-Sensing of Damage and Strain in Carbon Fiber Polymer-Matrix Structural Composites by Electrical Resistance Measurement." *Polymer and Polymer Composites*, 11 (7), pp. 515–525.

Daniel, J. S., and Y. R. Kim (2001). "Laboratory Evaluation of Fatigue Healing of Asphalt Mixtures." *Journal of Materials in Civil Engineering*, 13 (6), pp. 434–440.

Fromm, H. J. (1976). "Electrically Conductive Asphalt Mixes for the Cathodic Protection of Concrete Bridge Decks." *Proceedings of Association of Asphalt Paving Technologists*, pp. 382–399.

Garcia, A. (2012). "Self-Healing of Open Cracks in Asphalt Mastic." *Fuel*, 93, pp. 264–272.

García, A., E. Schlangen, M. Van de Ven, and D. Van Vliet (2011a). "Crack Repair of Asphalt Concrete with Induction Energy." *Heron*, 56 (1/2), pp. 37–48.

García, A., E. Schlangen, M. Van de Ven, and D. Van Vliet (2011b). "Induction Heating of Mastic Containing Conductive Fibers and Fillers." *Materials and Structure*, 44, pp. 499–508.

García, A., E. Schlangen, M. Van de Ven, and Q. Liu (2009). "Electrical Conductivity of Asphalt Mortar Containing Conductive Fibers and Fillers." *Construction and Building Materials*, 23 (10), pp. 3175–3181.

Gibson, R. F. (2010). "A Review of Recent Research on Mechanics of Multifunctional Composite Materials and Structures." *Composite Structures*, 92, pp. 2793–2810.

Hong, L. (2003). "Experimental Study on Graphite Slurry Infiltrated Fiber Concrete Slab for Snow Melting." *Journal of Building Materials*, 12 (1), pp. 96–100.

Huang, B., J. Cao, X. Chen, X. Shu, and W. He (2006). "Laboratory Investigation into Electrically Conductive HMA Mixtures." *Journal of the Association of Asphalt Paving Technologists*, 75, pp. 1235–1253.

Huang, B., X. Chen, and X. Shu (2009). "Effects of Electrically Conductive Additives on Laboratory-Measured Properties of Asphalt Mixtures." *Journal of Materials in Civil Engineering*, 21, pp. 612–617.

Liu, Q., E. Schlangen, M. Ven, and M. Poot (2010a). "Optimization of Steel Fiber Used for Induction Heating in Porous Asphalt Concrete." *Proceedings of the Seventh International Conference on Traffic and Transportation Studies, ASCE, Kunming, China, August 3–5*, pp. 1320–1330.

Liu, Q., E. Schlangen, A. García, and M. Ven (2010b). "Induction Heating of Electrically Conductive Porous Asphalt Concrete." *Construction and Building Materials*, 24 (7), pp. 1207–1213.

Liu, Q., E. Schlangen, M. Ven, and A. Garcia (2010c). "Healing of Porous Asphalt Concrete via Induction Heating." *Road Materials and Pavement Design,* 11 (S1), pp. 527–542.

Liu, X., and S. Wu (2009). "Research on the Conductive Asphalt Concrete's Piezoresistivity Effect and Its Mechanism." *Construction and Building Materials*, 23 (8), pp. 2752–2756.

Liu, X., and S. Wu (2011a). "Study on the Graphite and Carbon Fiber Modified Asphalt Concrete." *Construction and Building Materials*, 25, pp. 1807–1811.

Liu, X., and S. Wu (2011b). "Study on the Piezoresistivity Character of Electrically Conductive Asphalt Concrete." *Advanced Materials Research*, Vol. 233–235, pp. 1756–1761.

Liu, X., S. Wu, L. Ning, and G. Bo (2008a). "Self-Monitoring Application of Asphalt Concrete Containing Graphite and Carbon Fibers." *Materials Science Edition,* 23 (2), pp. 268–271.

Liu, X., S. Wu, Y. Qunshan, Q. Jian, and L. Bo (2008b). "Properties Evaluation of Asphalt-Based Composites with Graphite and Mine Powders." *Construction and Building Materials,* 22, pp. 121–126.

Lofgren, S. (2001). "The Chemical Effects of Deicing Salt on Soil and Stream Water of Five Catchments in Southeast Sweden." *Water, Air, and Soil Pollution*, 130, pp. 863–868.

Minsk, L. D. (1968). "Electrically Conductive Asphalt for Control of Snow and Ice Accumulation." *Highway Research Record*, 227, pp. 57–63.

Minsk, L. D. (1971). "Electrically Conductive Asphaltic Concrete." U.S. Patent 3,573,427.

Mo, L., S. Wu, X. Liu, and Z. Chen (2005). "Percolation Model of Graphite-Modified Asphalt Concrete." *Journal of Wuhan University of Technology Materials Science Edition,* 20 (1), pp. 111–113.

Park, P. (2012). *Characteristics and Applications of High-Performance Fiber Reinforced Asphalt Concrete*. Ph.D. Dissertation, University of Michigan, Ann Arbor, MI.

Sanzo, D., and S. J. Hecnar (2006). "Effects of Road Deicing Salt (NaCl) on Larval Wood Frogs." *Environmental Pollution*, 140, pp. 247–256.

Serin, S., N. Morova, M. Saltan, and S. Terzi (2012). "Investigation of Usability of Steel Fibers in Asphalt Concrete Mixtures." *Construction and Building Materials*, 36, pp. 238–244.

Stratfull, R. F. (1974). "*Experimental Cathodic Protection of a Bridge Deck*." Highway Research Report CA_DOT-TL-5117-4-74-02, California Department of Transportation, Sacramento, CA.

Sui, L., and T. Liu (2006). "State of the Art of Multi-functional and Smart Concrete." *Key Engineering Materials*, pp. 302–303, 424–431.

Vaidya, S., and E. Allouche (2011). "Experimental Evaluation of Electrical Conductivity of Carbon Fiber Reinforced Fly Ash Based Geopolymer." *Smart Structure and Systems*, 7 (1), pp. 27–40.

Wen, S., and D. D. L. Chung (2000). "Cement as a Thermoelectric Material." *Journal of Materials Research*, 15 (12), pp. 2844–2848.

Wen, S., and D. D. L. Chung (2001a). "Effect of Admixtures on the Dielectric Constant of Cement Paste." *Cement and Concrete Research*, 31 (4), pp. 673–677.

Wen, S., and D. D. L. Chung (2001b). "Effect of Stress on the Electric Polarization in Cement." *Cement and Concrete Research*, 31 (2), pp. 291–295.

Wen, S., and D. D. L. Chung (2004). "Effect of Fiber Content on the Thermoelectric Behavior of Cement." *Journal of Materials Science*, 39 (13), pp. 4103–4106.

Wen, S., and D. D. L. Chung (2007a). "Double Percolation in the Electrical Conduction in Carbon Fiber Reinforced Cement-Based Materials." *Carbon*, 45 (2), pp. 263–267.

Wen, S., and D. D. L. Chung (2007b). "Electrical Resistance Based Damage Self-Sensing in Carbon Fiber-Reinforced Cement." *Carbon*, 45 (4), pp. 710–716.

Wen, S., and D. D. L. Chung (2007c). "Partial Replacement of Carbon Fiber by Carbon Black in Multifunctional Cement-Matrix Composites." *Carbon*, 45 (3), pp. 505–513.

Wen, S., and D. D. L. Chung (2007d). "Piezoresistivity-Based Strain Sensing in Carbon Fiber Reinforced Cement." *ACI Materials Journal*, 104 (2), pp. 171–179.

Wen, S., and D. D. L. Chung (2008). "Effect of Moisture on Piezoresistivity of Carbon Fiber-Reinforced Cement Paste." *ACI Materials Journal*, 105 (3), pp. 274–280.

Wu, S., L. Mo, and Z. Shui (2003). "Piezoresistivity of Graphite Modified Asphalt-Based Composites." *Key Engineering Materials*, 249, pp. 391–396.

Wu, S., L. Mo, Z. Shui, and Z. Chen (2005). "Investigation of the Conductivity of Asphalt Concrete Containing Conductive Fillers." *Carbon*, 43 (7), pp. 1358–1363.

Wu, S., X. Liu, Q. Ye, and N. Li (2006). "Self-Monitoring Electrically Conductive Asphalt-Based Composite Containing Carbon Fillers." *Transactions of Nonferrous Metals Society of China*, 16 (S2), pp. 512–516.

Wu, S., Y. Zhang, and M. Chen (2010). "Research on Mechanical Characteristics of Conductive Asphalt Concrete by Indirect Tensile Test." *Proceedings of SPIE*, pp. 752265-752265.

Xiangyang, W., and G. Yuxing (2010). "Research on the Preparation of Conductive Asphalt Concrete for Deicing and Snow Melting." *Proceedings of* the *3rd International Conference on Advanced Computer Theory and Engineering*, pp. 381–384.

Zaleski, P. L., D. J. Derwin, and W. H. Flood (1998). "Electrically Conductive Paving Mixture and Paving System." U.S. Patent 5**,**707,171.

Zhang, H., X. H. Wu, and X. L. Wang, (2011). "Conductivity mechanism of asphalt concrete with the PANI/PP compound conductive fiber." *In Materials Science Forum*, Vol. 689, pp. 69-73.

# APPENDICES

## A. Sieve Analysis of Aggregates

(1) Asphalt concrete with various contents of graphite

**Table A1. Sieve Analysis of Coarse Aggregate.**

| Sieve Size | Sieve Size (mm) | Mass Sieve (g) | Mass Sieve + Agg. (g) | Mass Retained (g) | Total % Retained | Total % Passing |
|---|---|---|---|---|---|---|
| 3/4" | 19 | 794 | 794 | 0 | 0 | 100 |
| 1/2" | 12.5 | 787 | 789.5 | 2.5 | 0.17 | 99.83 |
| 3/8" | 9.5 | 804.5 | 1,003.5 | 199 | 13.43 | 86.57 |
| #4 | 4.75 | 777 | 1,939.5 | 1,162.5 | 90.93 | 9.07 |
| #8 | 2.36 | 717 | 840.5 | 123.5 | 99.17 | 0.83 |
| #16 | 1.18 | 630.5 | 634 | 3.5 | 99.40 | 0.60 |
| Pan | 0 | 383 | 392 | 9 | 100.00 | 0.00 |

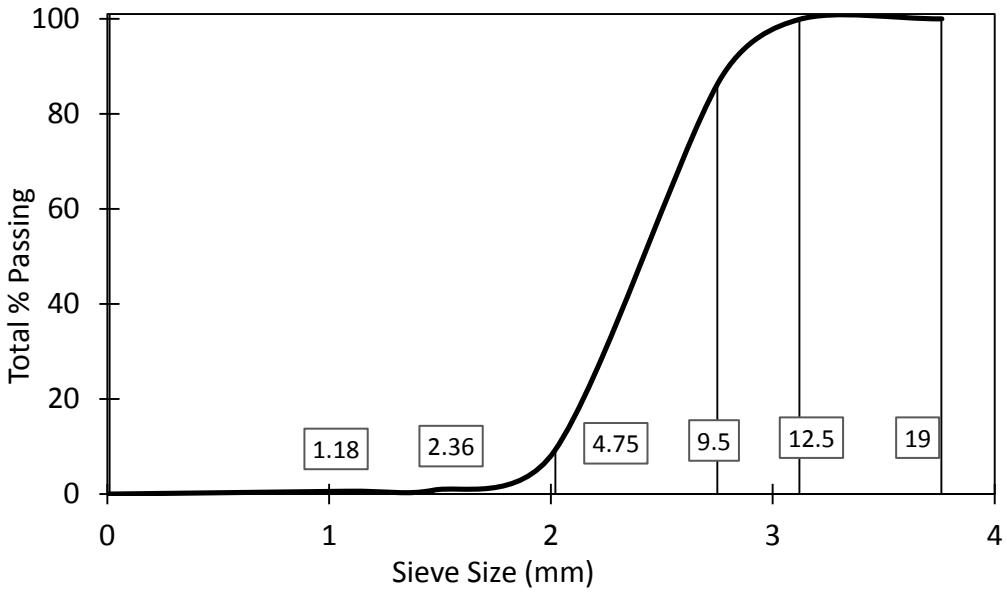


**Figure A1. Gradation of Coarse Aggregate.**

**Table A2. Sieve Analysis of Fine Aggregate.**

| Sieve Size | Sieve Size (mm) | Mass Sieve (g) | Mass Sieve + Agg. (g) | Mass Retained (g) | Total % Retained | Total % Passing |
|---|---|---|---|---|---|---|
| 3/8" | 9.5 | 804.5 | 804.5 | 0 | 0 | 100 |
| #4 | 4.75 | 777 | 778.5 | 1.5 | 0.10 | 99.90 |
| #8 | 2.36 | 717 | 1,079 | 362 | 24.23 | 75.77 |
| #16 | 1.18 | 630.5 | 1,016 | 385.5 | 49.93 | 50.07 |
| #30 | 0.6 | 575 | 925.5 | 350.5 | 73.30 | 26.70 |
| #50 | 0.3 | 545.5 | 782.5 | 237 | 89.10 | 10.90 |
| #100 | 0.15 | 529 | 636.5 | 107.5 | 96.27 | 3.73 |
| #200 | 0.075 | 294 | 323.5 | 29.5 | 98.23 | 1.77 |
| Pan | 0 | 383 | 409.5 | 26.5 | 100.00 | 0.00 |

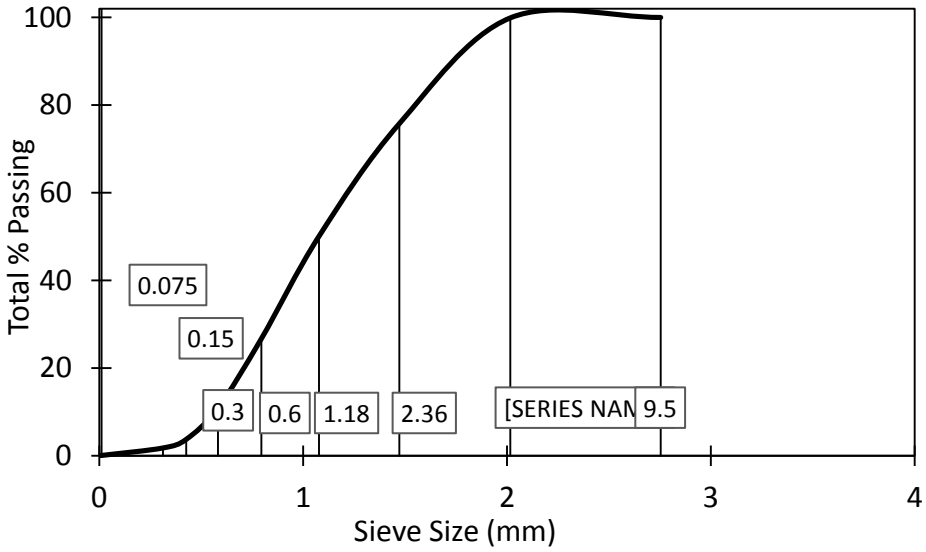


**Figure A2. Gradation of Fine Aggregate.**

**Table A3. Sieve Analysis of Aggregate.**

| Sieve Size (mm) | % Passing Coarse Aggregate (CA) | % Passing Fine Aggregate (FA) | % Passing Filler | Gradation (0.35/0.6/0.05) | Specification D-6 Mix |
|---|---|---|---|---|---|
| 19 | 100 | 100 | 100 | 100.0 | |
| 12.5 | 99.83 | 100 | 100 | 99.9 | 100 |
| 9.5 | 86.57 | 100 | 100 | 95.3 | 90–100 |
| 4.75 | 9.07 | 99.90 | 100 | 68.1 | 55–85 |
| 2.36 | 0.83 | 75.77 | 100 | 50.8 | 32–67 |
| 1.18 | 0.60 | 50.07 | 100 | 35.3 | |
| 0.6 | 0.00 | 26.70 | 100 | 21.0 | |
| 0.3 | 0.00 | 10.90 | 100 | 11.5 | 7–23 |
| 0.15 | 0.00 | 3.73 | 100 | 7.2 | |
| 0.075 | 0.00 | 1.77 | 100 | 6.1 | 2–10 |

Nominal maximum size: 9.5 mm

Maximum size: 12.5 mm

(2) Asphalt concrete of various aggregate gradation

- D-6 and D-6_OBC gradation

**Table A4. Aggregate Gradation of D-6 Mixture.**

| Sieve Size (mm) | % Passing Aggregate | % Remain Aggregate | Specification D-6 Mix |
|---|---|---|---|
| 19 | 100 | 0 | |
| 12.5 | 100 | 0 | 100 |
| 9.5 | 95 | 5 | 90–100 |
| 4.75 | 75 | 20 | 55–85 |
| 2.36 | 60 | 15 | 32–67 |
| 1.18 | 35 | 25 | |
| 0.6 | 20 | 15 | |
| 0.3 | 12 | 8 | 7–23 |
| 0.15 | 5 | 7 | |
| 0.075 | 5 | 0 | 2–10 |

Nominal maximum size: 4.75 mm

Maximum size: 9.5 mm

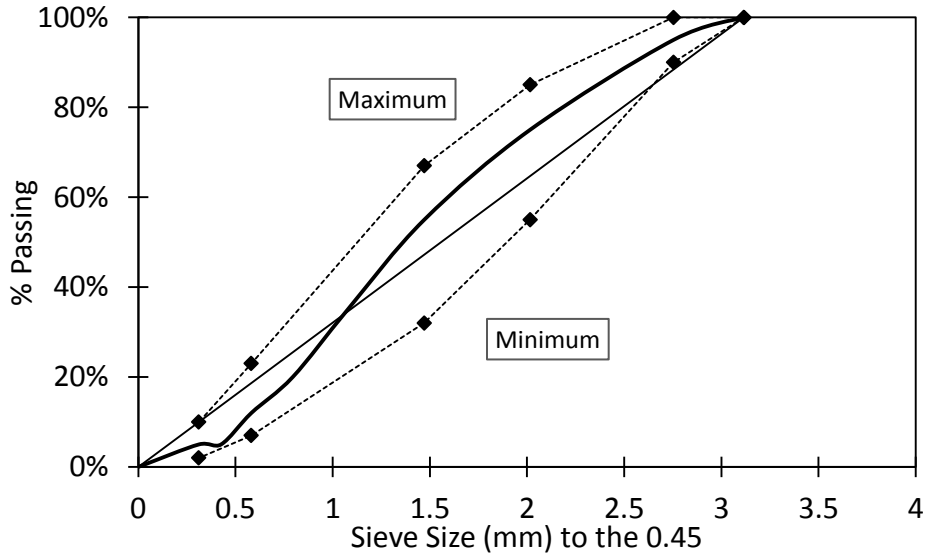


**Figure A3. Sieve Analysis of D-6 Mix.**

- D-5 gradation

**Table A5. Aggregate Gradation of D-5 Mixture.**

| Sieve Size (mm) | % Passing Aggregate | % Remain Aggregate | Specification D-5 Mix |
|---|---|---|---|
| 19 | 100 | 0 | 100 |
| 12.5 | 95 | 5 | 90–100 |
| 9.5 | 88 | 7 | |
| 4.75 | 65 | 23 | 44–74 |
| 2.36 | 40 | 25 | 28–58 |
| 1.18 | 20 | 20 | |
| 0.6 | 12 | 8 | |
| 0.3 | 8 | 4 | 5–21 |
| 0.15 | 5 | 3 | |
| 0.075 | 5 | 0 | 2–10 |

Nominal maximum size: 9.5 mm

Maximum size: 12.5 mm

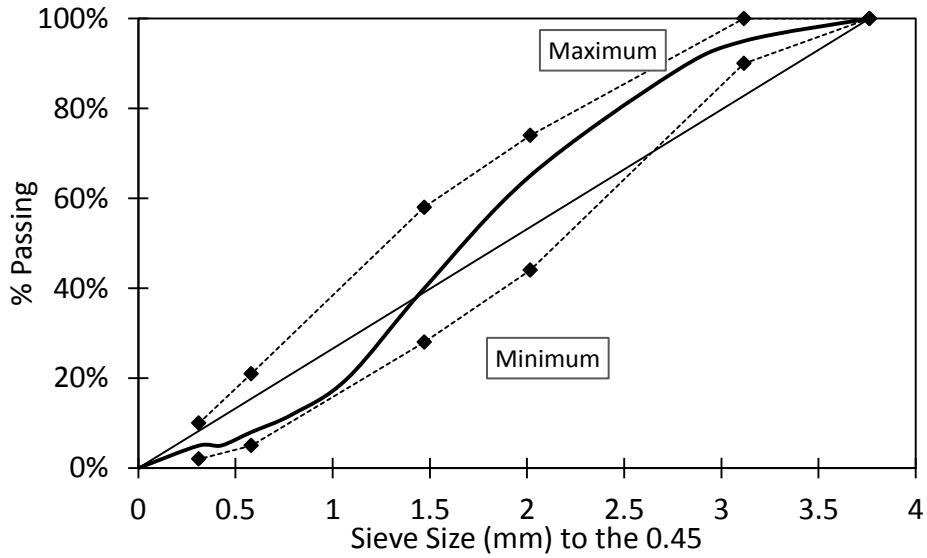


**Figure A4. Sieve Analysis of D-5 Mix.**

- D-3 gradation

**Table A6. Aggregate Gradation of D-3 Mixture.**

| Sieve Size (mm) | % Passing Aggregate | % Remain Aggregate | Specification D-3 Mix |
|---|---|---|---|
| 37.5 | 100 | 0 | 100 |
| 25 | 95 | 8 | 90–100 |
| 19 | 87 | 15 | |
| 12.5 | 72 | 15 | 56–80 |
| 9.5 | 63 | 9 | |
| 4.75 | 45 | 18 | 29–59 |
| 2.36 | 25 | 20 | 19–45 |
| 1.18 | 15 | 10 | |
| 0.6 | 11 | 4 | |
| 0.3 | 8 | 3 | 5–17 |
| 0.15 | 5 | 3 | |
| 0.075 | 5 | 0 | 1–7 |

Nominal maximum size: 19 mm

Maximum size: 25 mm

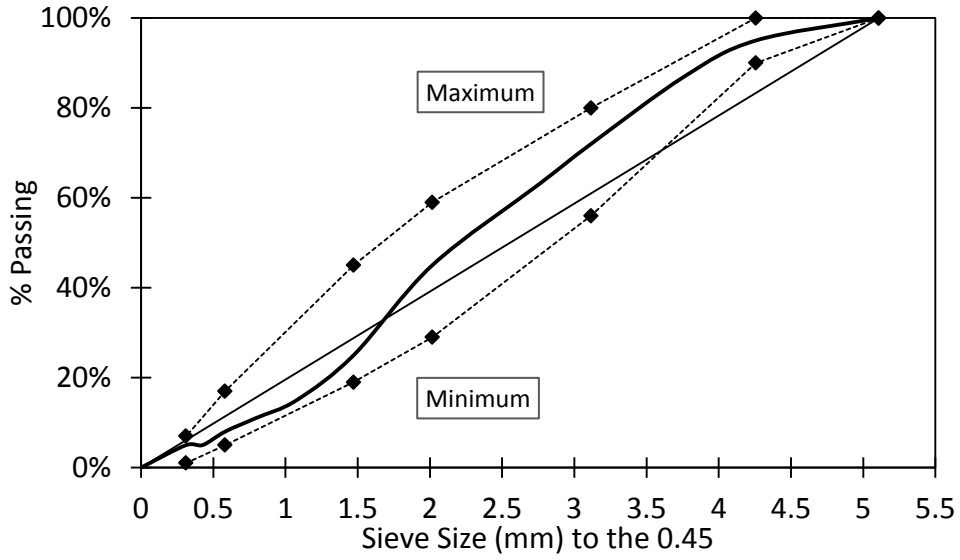


**Figure A5. Sieve Analysis of D-5 Mix.**

**B. Determination of Binder Content**

(1) Asphalt concrete with various contents of graphite

- 5.3% for 4% air void

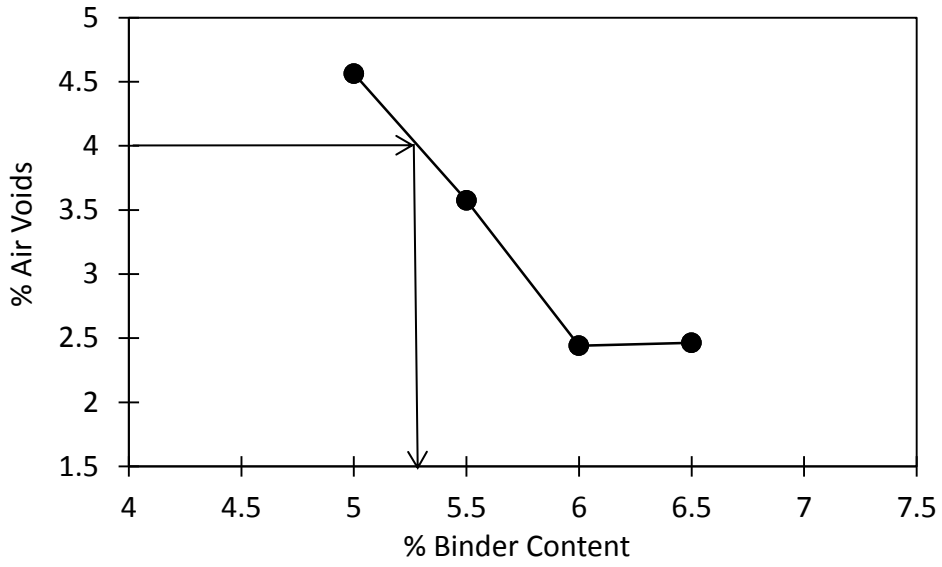


**Figure B1. Air Voids versus Percent Binder Content of D-6 Mixture.**

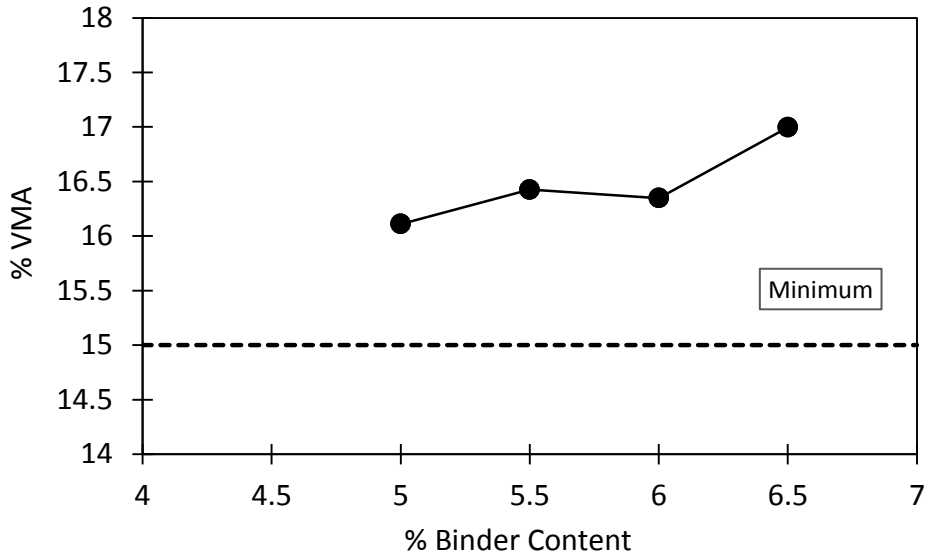


**Figure B2. VMA versus Percent Binder Content of D-6 Mixture.**

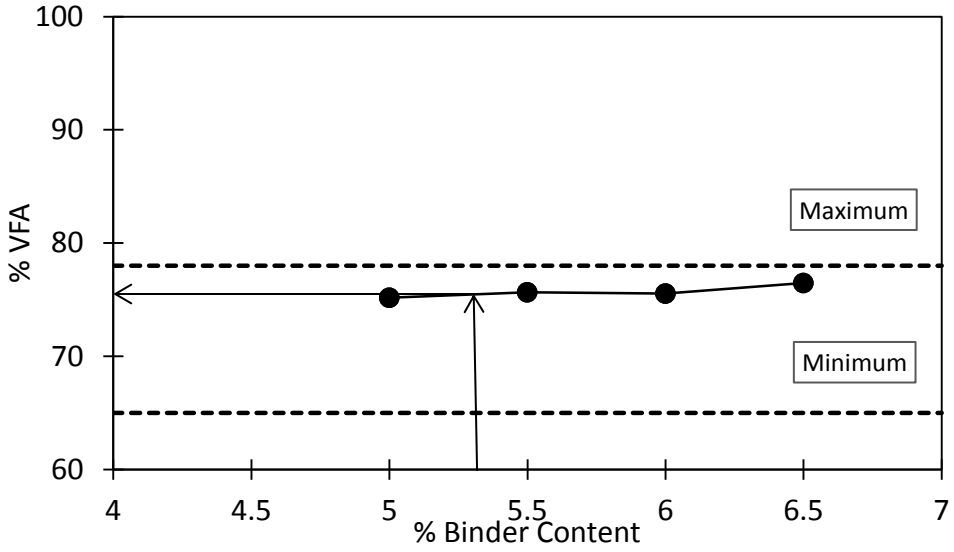


**Figure B3. VFA versus Percent Binder Content of D-6 Mixture.**

(2) Asphalt concrete with various aggregate gradation

- D-6 (4.86% for 4% air void)

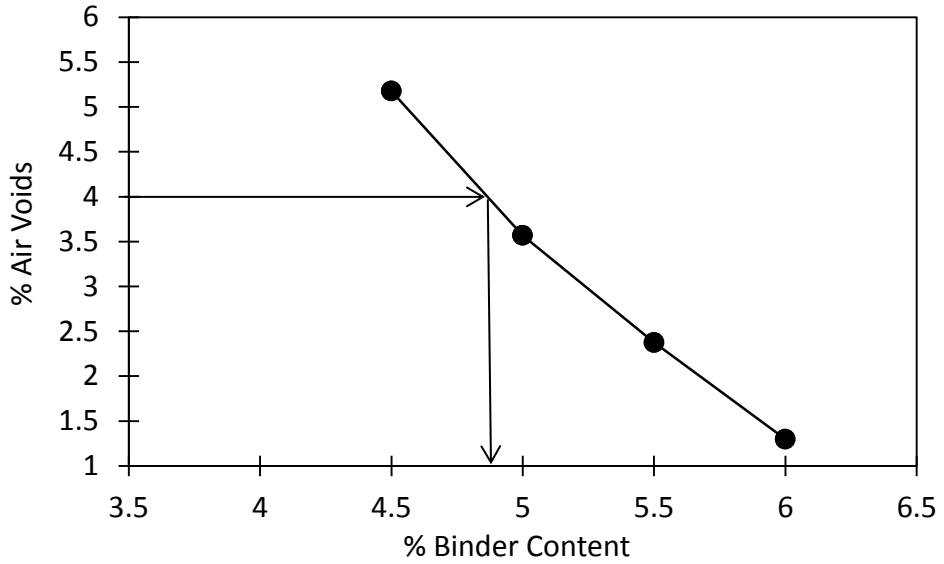


**Figure B4. Air Voids versus Percent Binder Content of D-6 Mixture.**

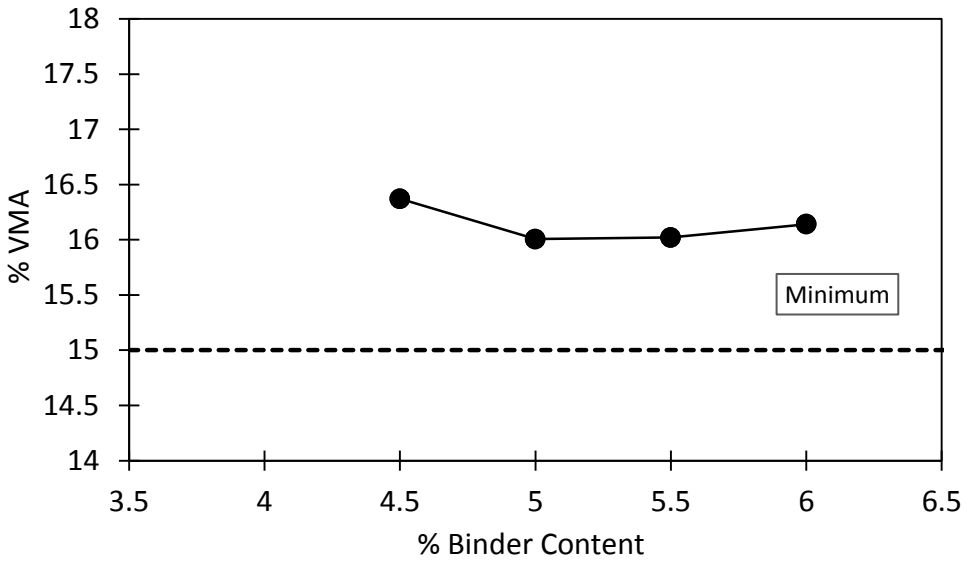


**Figure B5. VMA versus Percent Binder Content of D-6 Mixture.**

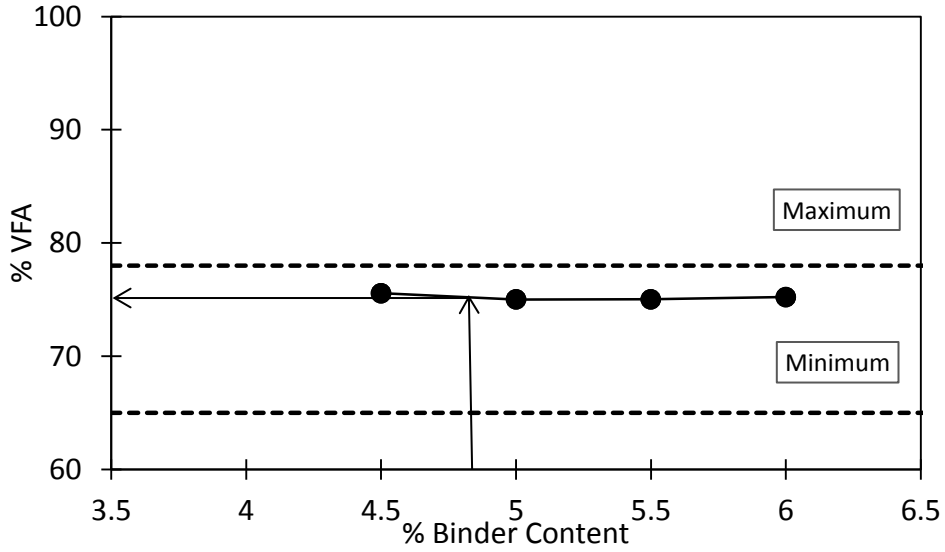


**Figure B6. VFA versus Percent Binder Content of D-6 Mixture.**

- D-5 (4.8% for 4% air void)

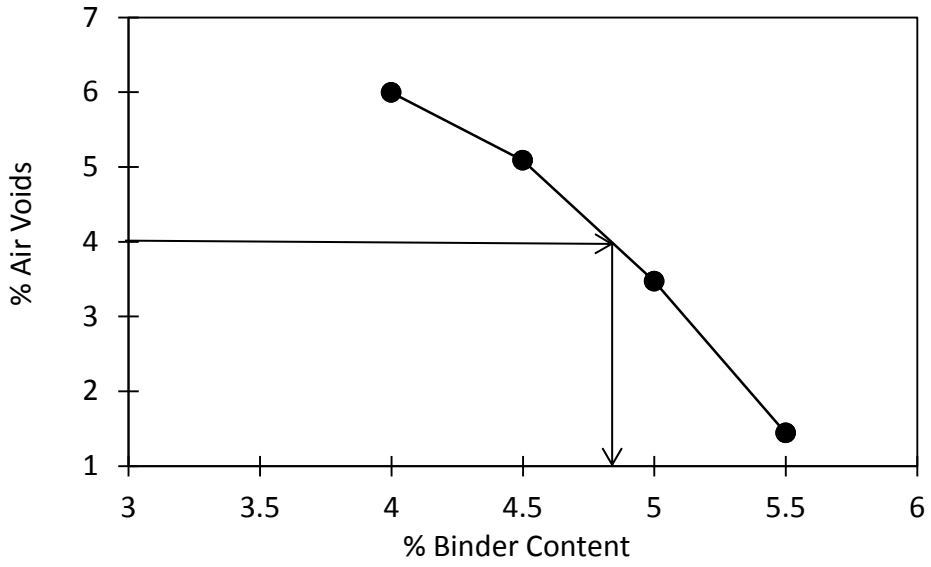


**Figure B7. Air Voids versus Percent Binder Content of D-5 Mixture.**

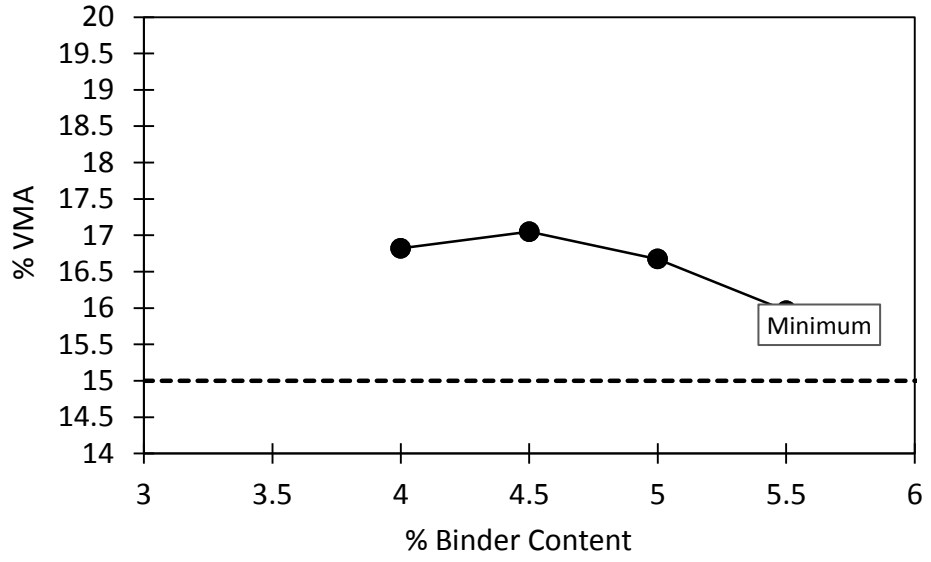


**Figure B8. VMA versus Percent Binder Content of D-5 Mixture.**

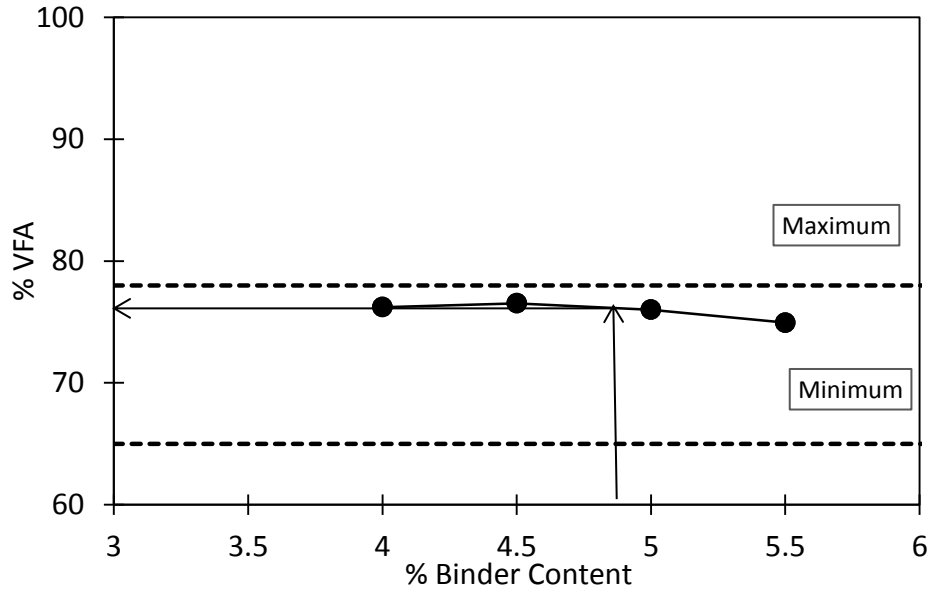


**Figure B9. VFA versus Percent Binder Content of D-5 Mixture.**

- D-3 (4.08% for 4% air void)

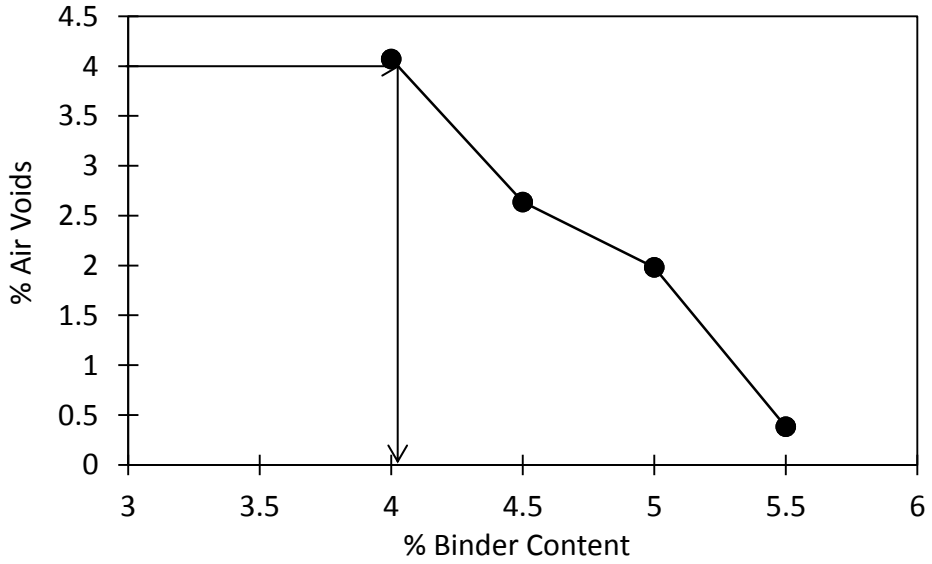


**Figure B10. Air Voids versus Percent Binder Content of D-3 Mixture.**

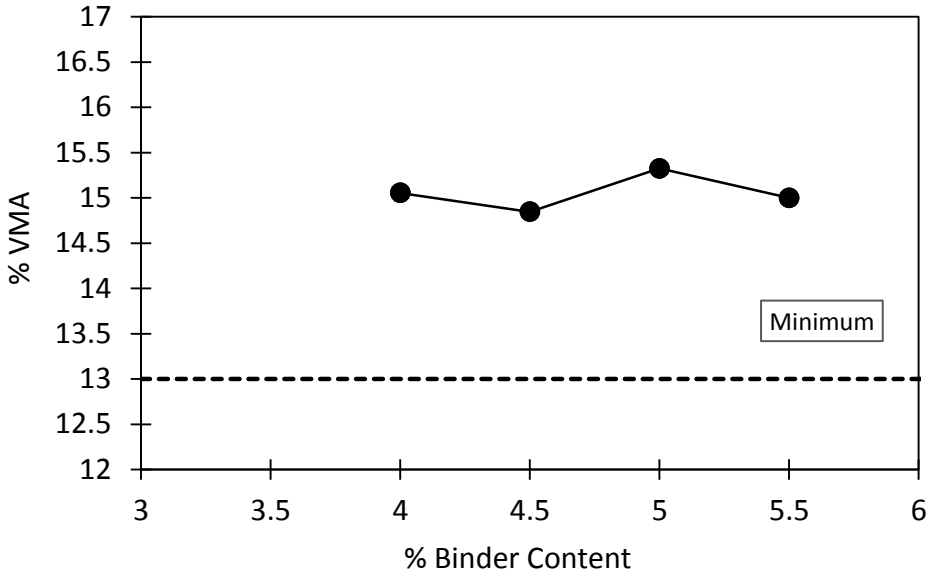


**Figure B11. VMA versus Percent Binder Content of D-3 Mixture.**

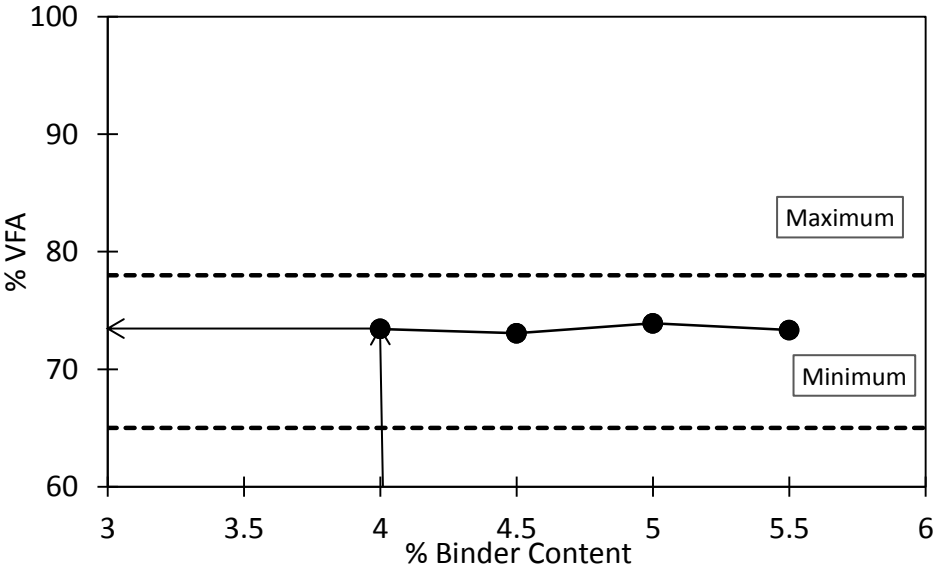


**Figure B12. VFA versus Percent Binder Content of D-3 Mixture.**

- D-6_OBC (3.92% for 4% air void)

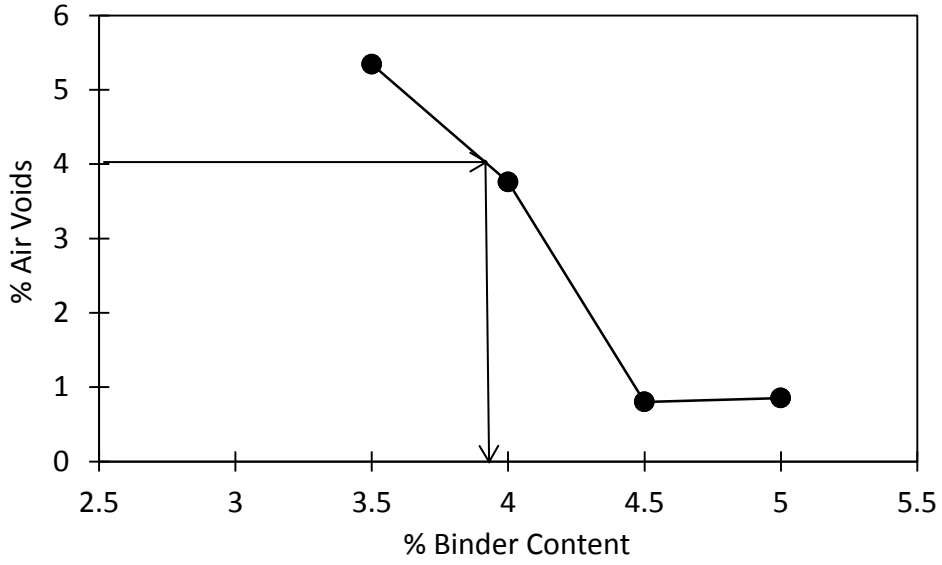


**Figure B13. Air Voids versus Percent Binder Content of D-6 Mixture with Graphite.**

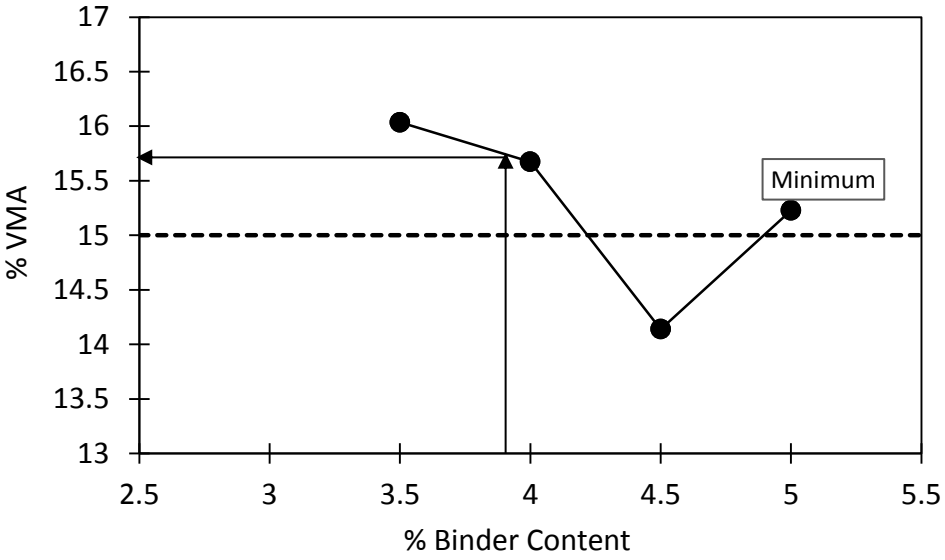


**Figure B14. VMA versus Percent Binder Content of D-6 Mixture with Graphite.**

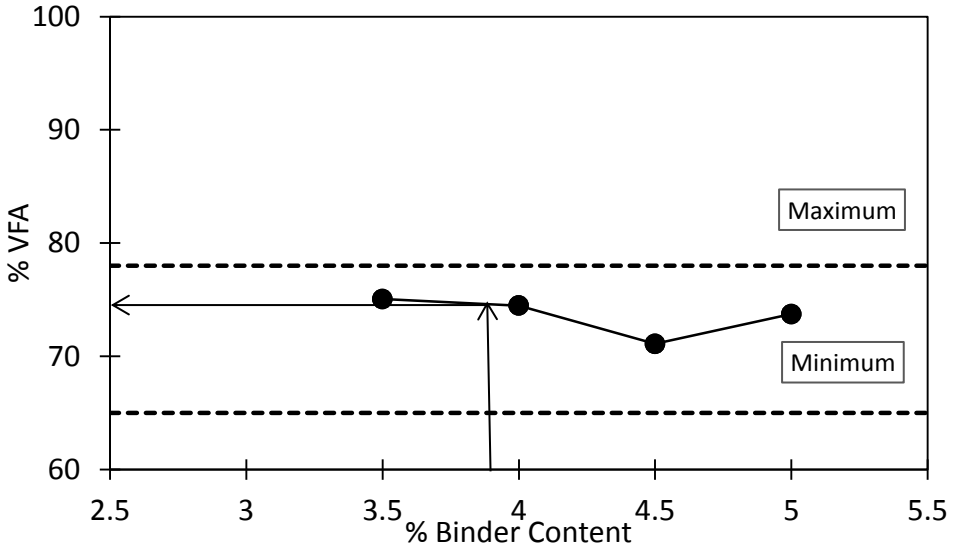


**Figure B15. VFA versus Percent Binder Content of D-6 Mixture with Graphite.**

## C. Electrical Resistivity of Conductive Asphalt Concrete

**Table C1. Electrical Resistivity of Conductive Asphalt Concrete (F516).**

| Specimen | Resistance (Ω) | Volume Resistivity (Ω. cm) |
|---|---|---|
| **Control mix** | | |
| **1** | | |
| **516–10%** | | |
| **1** | 1.30E+12 | 2.42E+12 |
| **516–15%** | | |
| **1** | 1.62E+11 | 3.02E+11 |
| **516–20%** | | |
| **1** | 2.94E+03 | 5.48E+03 |
| **2** | 4.67E+03 | 8.89E+03 |
| **3** | 6.98E+03 | 1.30E+04 |
| **516–25%** | | |
| **1** | 9.08E+02 | 1.69E+03 |
| **2** | 9.25E+02 | 1.73E+03 |
| **3** | 7.37E+02 | 1.37E+03 |
| **516–30%** | | |
| **1** | 2.32E+02 | 4.33E+02 |
| **2** | 2.02E+02 | 3.76E+02 |
| **3** | 2.92E+02 | 5.44E+02 |
| **516–35%** | | |
| **1** | 1.51E+02 | 2.81E+02 |
| **2** | 1.76E+02 | 3.28E+02 |
| **3** | 1.76E+02 | 3.27E+02 |
| **516–40%** | | |
| **1** | 8.92E+01 | 1.66E+02 |
| **2** | 7.35E+01 | 1.37E+02 |
| **3** | 7.44E+01 | 1.39E+02 |

**Table C2. Electrical Resistivity of Conductive Asphalt Concrete (F146).**

| Specimen | Resistance (Ω) | Volume Resistivity (Ω. cm) |
|---|---|---|
| **146–20%** | | |
| **1** | 9.68E+05 | 1.80E+06 |
| **2** | 1.06E+06 | 1.98E+06 |
| **3** | 1.08E+06 | 2.00E+06 |
| **146–25%** | | |
| **1** | 1.48E+04 | 2.77E+04 |
| **2** | 1.04E+04 | 1.94E+04 |
| **3** | 1.11E+04 | 2.06E+04 |
| **146–30%** | | |
| **1** | 2.09E+03 | 3.89E+03 |
| **2** | 2.64E+03 | 4.93E+03 |
| **3** | 2.13E+03 | 3.96E+03 |

**Table C3. Electrical Resistivity of Asphalt Concrete of Various Aggregate Gradation.**

| Specimen | 1st Volume Resistivity (Ω. cm) | 2nd Volume Resistivity (Ω. cm) | 3rd Volume Resistivity (Ω. cm) | Average Volume Resistivity (Ω. cm) |
|---|---|---|---|---|
| **D-3** | 2.39E+12 | 1.04E+13 | 4.01E+12 | 5.62E+12 |
| **D-5** | 4.51E+12 | 5.95E+12 | 6.26E+12 | 5.57E+12 |
| **D-6** | 4.72E+12 | 5.97E+12 | 7.02E+12 | 5.90E+12 |
| **D-3_GR** | 5.55E+05 | 4.23E+05 | 6.34E+05 | 5.37E+05 |
| **D-5_GR** | 4.58E+08 | 8.39E+08 | 4.80E+09 | 2.03E+09 |
| **D-6_GR** | 4.39E+06 | 2.50E+06 | 5.54E+06 | 4.14E+06 |
| **D-6_GR_OBC** | 1.45E+05 | 1.56E+05 | 1.33E+05 | 1.45E+05 |

## D. Indirect Tensile Strength Test Results

**Table D1. IDT Strength of Various Graphite Contents.**

| Sample | Load (lbf) | Load P (N) | $S_T$ (MPa) |
|---|---|---|---|
| | 5.64E+03 | 2.51E+04 | 1.12E+00 |
| **Cement** | 5.23E+03 | 2.32E+04 | 1.04E+00 |
| | 6.10E+03 | 2.71E+04 | 1.21E+00 |
| | 6.66E+03 | 2.96E+04 | 1.32E+00 |
| **F146—20%** | 6.72E+03 | 2.99E+04 | 1.34E+00 |
| | 6.85E+03 | 3.05E+04 | 1.36E+00 |
| | 7.85E+03 | 3.49E+04 | 1.56E+00 |
| **F146—25%** | 8.24E+03 | 3.66E+04 | 1.64E+00 |
| | 7.91E+03 | 3.52E+04 | 1.57E+00 |
| | | | |
| **F146—30%** | 6.97E+03 | 3.10E+04 | 1.38E+00 |
| | 7.82E+03 | 3.48E+04 | 1.56E+00 |
| | 6.39E+03 | 2.84E+04 | 1.27E+00 |
| **F516—20%** | 7.18E+03 | 3.19E+04 | 1.43E+00 |
| | 6.62E+03 | 2.94E+04 | 1.32E+00 |
| | 7.71E+03 | 3.43E+04 | 1.53E+00 |
| **F516—25%** | 8.69E+03 | 3.86E+04 | 1.73E+00 |
| | 7.36E+03 | 3.27E+04 | 1.46E+00 |
| | 7.55E+03 | 3.36E+04 | 1.50E+00 |
| **F516—30%** | 7.54E+03 | 3.35E+04 | 1.50E+00 |
| | 8.22E+03 | 3.66E+04 | 1.63E+00 |

1 lbf = 4.448 N

$$S_T = \frac{2 \times P}{\pi \times t \times D}$$

where t = 95 mm and D = 150 mm.

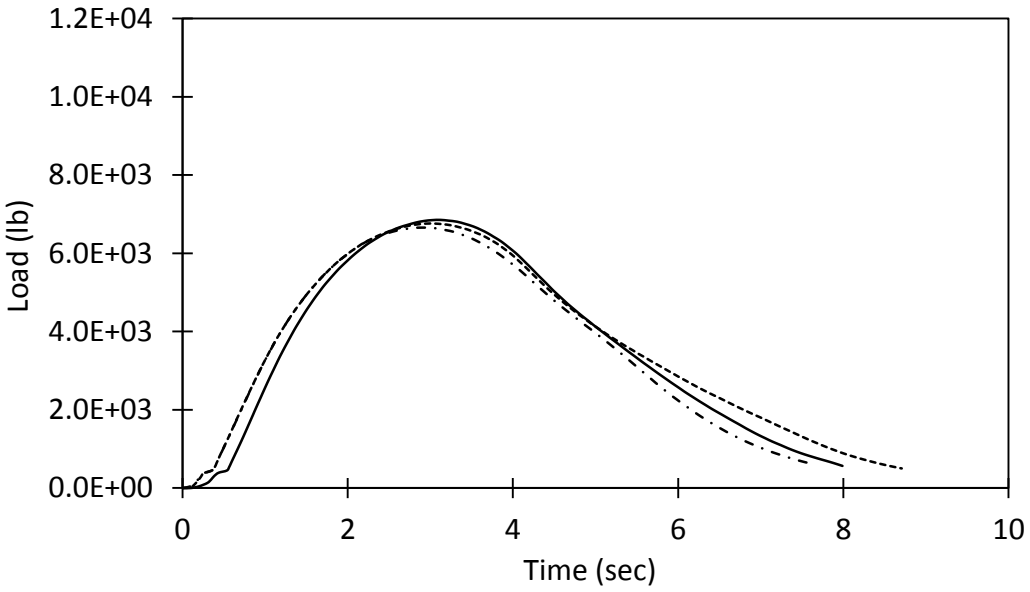


**Figure D1. IDT Strength for Asphalt Concrete with F146—20 Percent.**

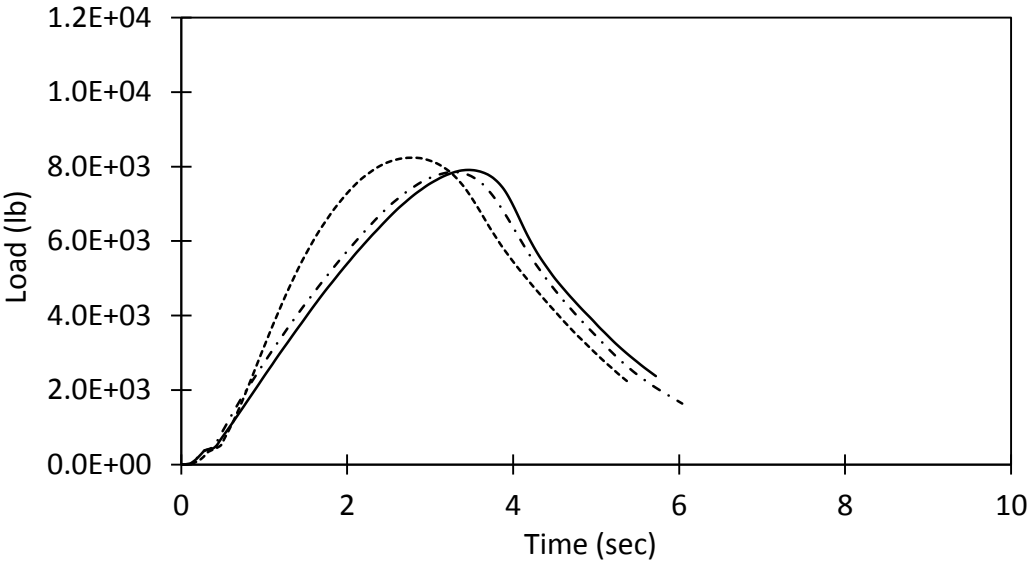


**Figure D2. IDT Strength for Asphalt Concrete with F146—25 Percent.**

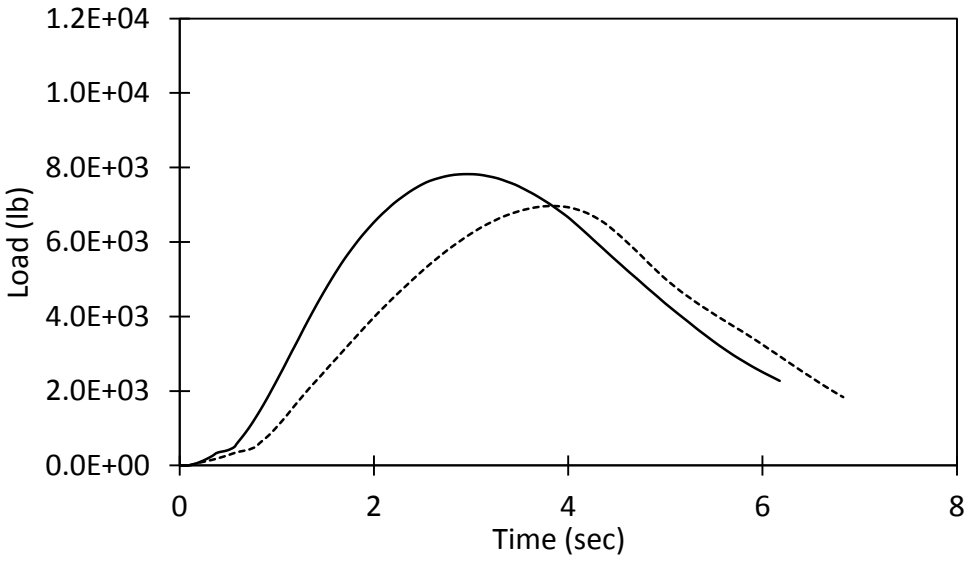


**Figure D3. IDT Strength for Asphalt Concrete with F146—30%.**

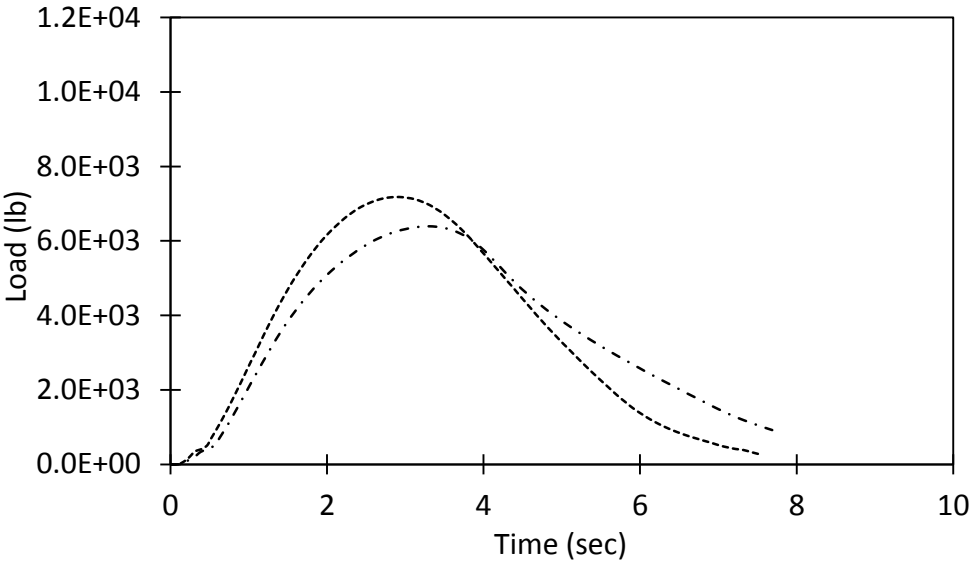


**Figure D4. IDT Strength for Asphalt Concrete with F516—20%.**

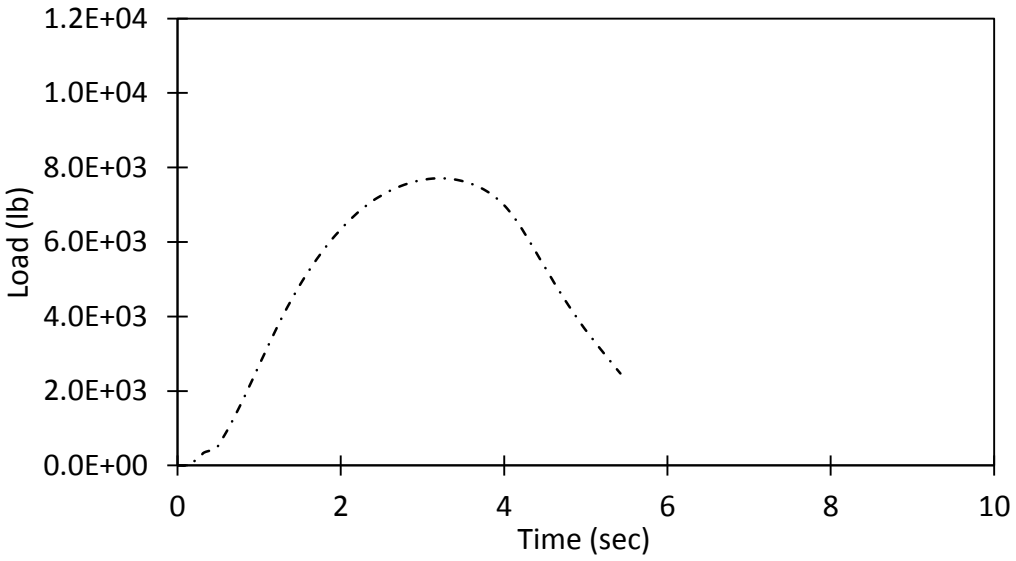


**Figure D5. IDT Strength for Asphalt Concrete with F516—25%.**

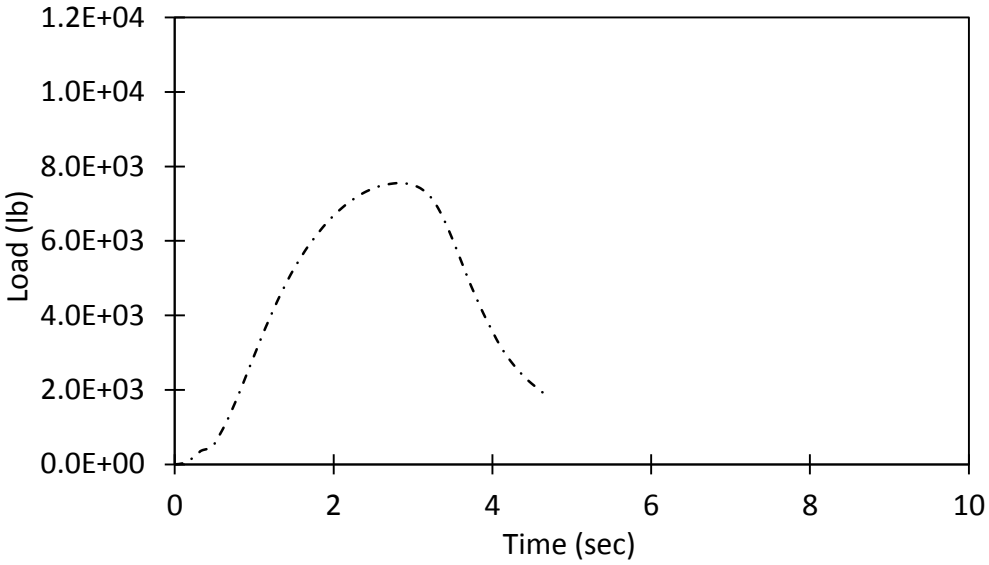


**Figure D6. IDT Strength for Asphalt Concrete with F516—30%.**

**Table D2. IDT Strength of Various Aggregate Gradations.**

| Sample | Load (lbf) | Load P (N) | $S_T$ (MPa) |
|---|---|---|---|
| | 8.59E+03 | 3.82E+04 | 1.42E+00 |
| **D-3** | 7.91E+03 | 3.52E+04 | 1.23E+00 |
| | 8.44E+03 | 3.75E+04 | 1.40E+00 |
| | - | - | - |
| **D-5** | 7.77E+03 | 3.46E+04 | 1.26E+00 |
| | 7.53E+03 | 3.35E+04 | 1.21E+00 |
| | 8.73E+03 | 3.88E+04 | 1.44E+00 |
| **D-6** | 8.91E+03 | 3.96E+04 | 1.44E+00 |
| | 1.01E+04 | 4.48E+04 | 1.64E+00 |
| | 9.00E+03 | 4.00E+04 | 1.46E+00 |
| **D-3_GR (25%)** | 9.91E+03 | 4.41E+04 | 1.58E+00 |
| | 9.92E+03 | 4.41E+04 | 1.61E+00 |
| | 9.51E+03 | 4.23E+04 | 1.55E+00 |
| **D-5_GR (25%)** | 9.65E+03 | 4.29E+04 | 1.58E+00 |
| | 9.42E+03 | 4.19E+04 | 1.53E+00 |
| | 1.11E+04 | 4.95E+04 | 1.84E+00 |
| **D-6_GR (25%)** | 1.13E+04 | 5.03E+04 | 1.87E+00 |
| | 1.08E+04 | 4.80E+04 | 1.78E+00 |
| **D-6_GR_OBC (25%)** | | | |

1 lbf = 4.448 N

$$S_T = \frac{2 \times P}{\pi \times t \times D}$$

where t = 115 mm and D = 150 mm.

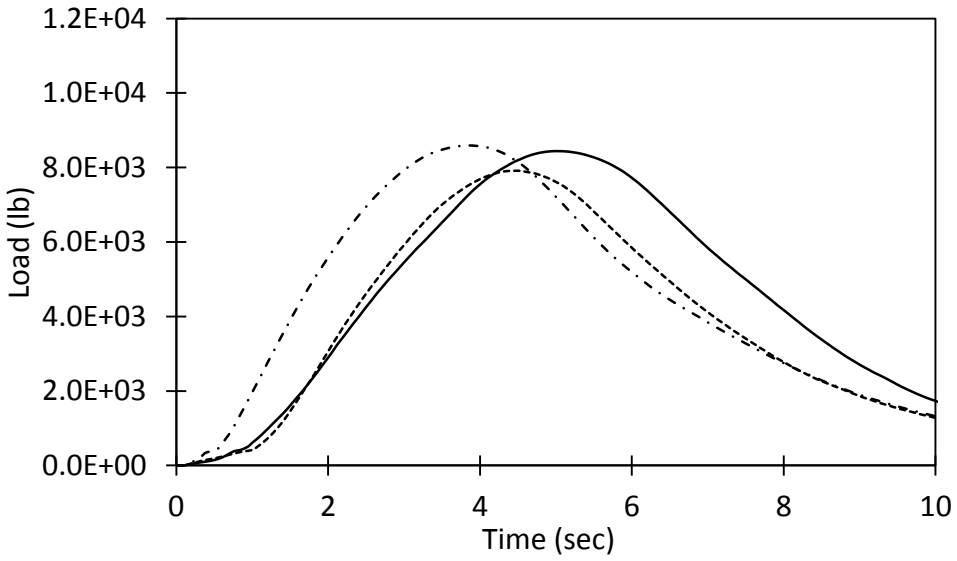


**Figure D7. IDT Strength of Asphalt Concrete of D-3 Gradation.**

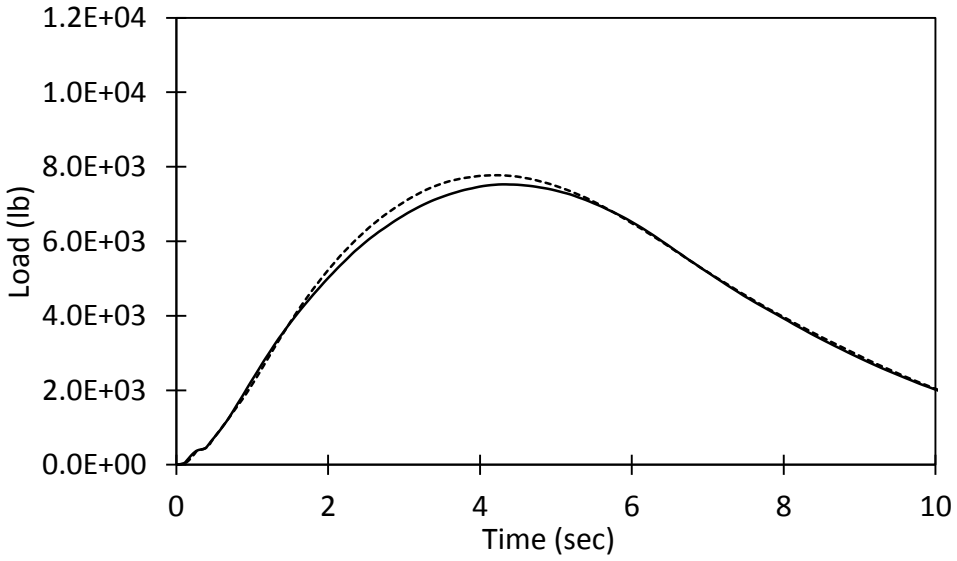


**Figure D8. IDT Strength of Asphalt Concrete of D-5 Gradation.**

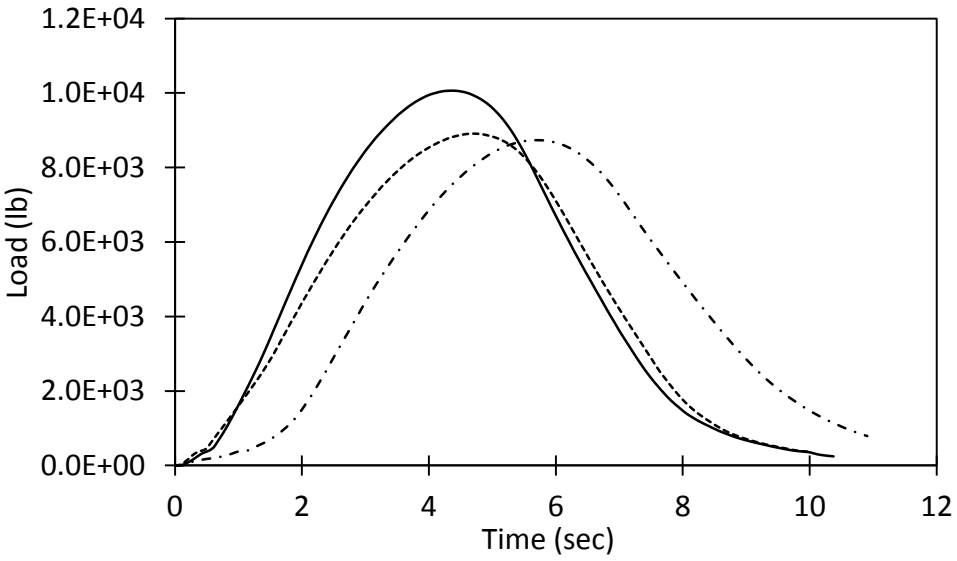


**Figure D9. IDT Strength of Asphalt Concrete of D-6 Gradation.**

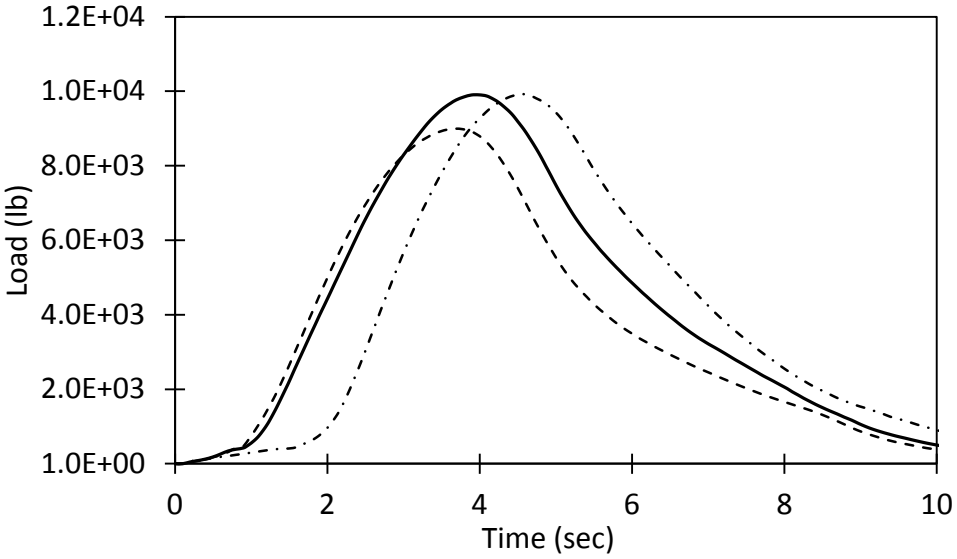


**Figure D10. IDT Strength of Asphalt Concrete of D-3 Gradation with Graphite.**

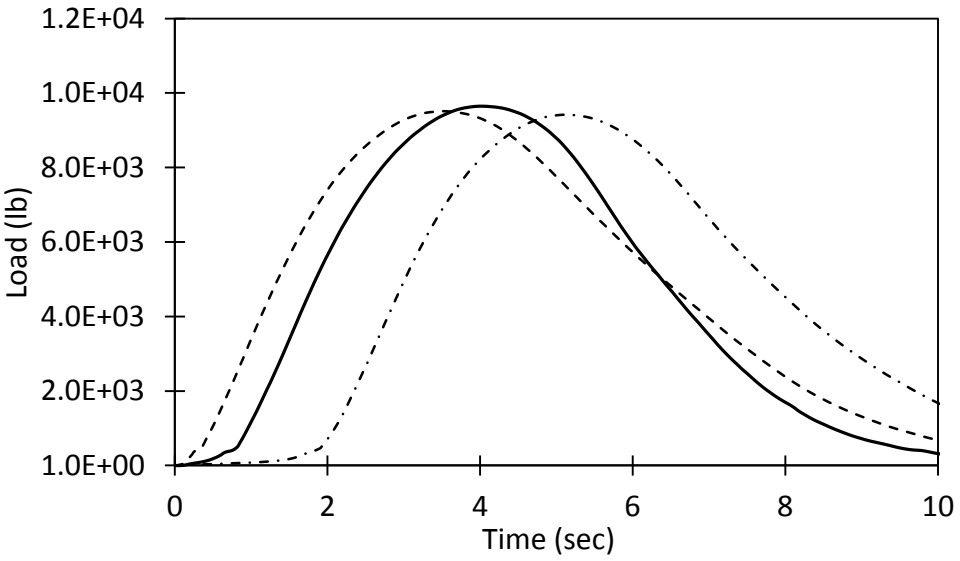


**Figure D11. IDT Strength of Asphalt Concrete of D-5 Gradation with Graphite.**

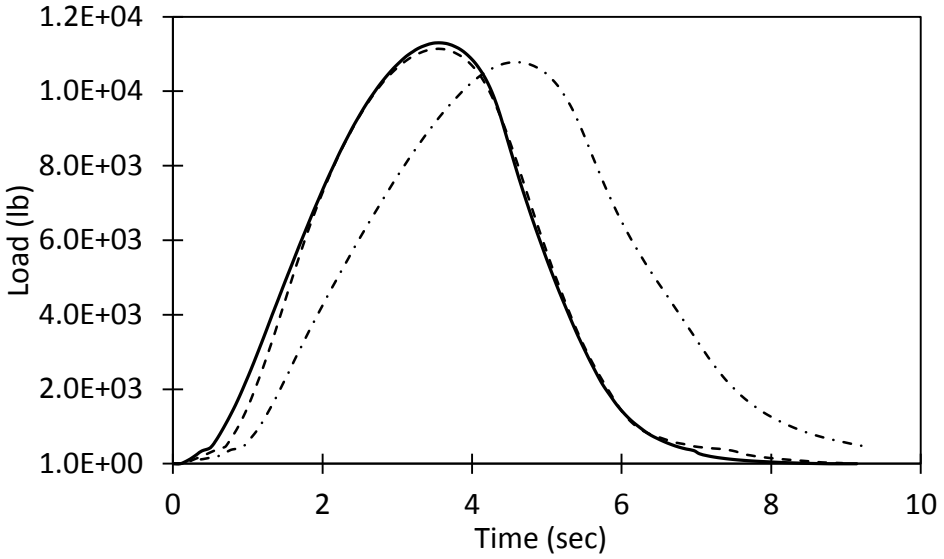


**Figure D12. IDT Strength of Asphalt Concrete of D-6 Gradation with Graphite.**